Improving integrated wildfire management in the Fynbos Biome of South Africa using information on synoptic-scale atmospheric features that promote wildfires

By

Dean Charles Harrison

Student Number HRRDEA003

UNIVERSITY OF CAPE TOWN
IYUNIVESITHI YASEKAPA • UNIVERSITEIT VAN KAAPSTAD

Minor-Dissertation

submitted in partial fulfilment of the requirements for the degree

Master of Philosophy (M.Phil)

in

Environment, Society and Sustainability

in the

Faculty of Science

at the

University of Cape Town

Supervisor: Dr Babatunde Joseph Abiodun

Co-Supervisor: Dr Pippin Anderson

August 2015

Declaration

I, Dean Charles Harrison, hereby,

1. grant the University of Cape Town free license to reproduce the above minor-dissertation in whole or in part, for the purpose of research;

2. declare that:

    i. this minor-dissertation is my own unaided work, both in concept and execution,

    ii. neither the substance nor any part of this minor-dissertation has been submitted in the past, or is being, or is to be submitted for a degree at this university or at any other university.

I am now presenting this minor-dissertation for examination for the degree of Master of Philosophy in the Faculty of Science.

_____ _____

Dean Charles Harrison Date

Abstract

Wildfire, an essential element for the Fynbos Biome of South Africa, can be a threat to property and human life if it is not well managed. Despite many studies on the dynamics and management of wildfire, the role of the atmosphere in inducing regional circulations that promote widespread wildfire is not well known. This dissertation studies the characteristics of wildfire in the Fynbos Biome, identifies synoptic-scale atmospheric features that produce favourable conditions for the wildfire, and examines possibility of using the features as indicators for wildfire occurrence. Ten years (2003 - 2012) of fire data from the MODIS “active-fires” datasets were analysed over the study domain. Daily Fire Danger Index (FDI) was calculated over Southern Africa for this period using maximum temperature (Tmax), minimum relative humidity (RHmin), and maximum wind speed (Wmax) data from the Climate Forecasting System Reanalysis datasets (CFSR) at a 0.5°x0.5° horizontal resolution. The Self Organising Maps (SOMs) technique was used to classify the FDI (anomaly) patterns on the fire days, and the atmospheric dynamics associated with each pattern were studied.

The results of the study show that occurrence of wildfire in the Fynbos Biome require that FDI ≥ 57, Tmax ≥ 21°C, RHmin ≤ 55%, and Wmax ≥ 12.7km/h. There is a strong correlation between FDI and fire occurrence (r =0.7331), but this occurs with a one-month lag. No correlation was found between FDI and fire intensity (r =0.0044). The study found that two major synoptic-scale atmospheric circulations favourable for wildfire occurrence in the Fynbos Biome are: (i) an approaching frontal system and (ii) a ridging high over the area. Both circulations induce positive FDI anomalies over the Fynbos Biome area, but while the first circulation could produce a positive FDI anomaly that extends beyond the Fynbos Biome area, the second one limits the positive FDI anomaly over the area. However, wildfire do not always occur on days when fire-conducive weather conditions are present, suggesting that the fuel and ignition wildfire ingredients are often the limiting factors of wildfire occurrence. This study suggests that incorporating the knowledge of

prevailing synoptic-scale atmospheric features into fire monitoring may improve fire management in the Fynbos Biome.

.

Table of Contents

DECLARATION I

ABSTRACT II

TABLE OF CONTENTS IV

LIST OF FIGURES VI

LIST OF TABLES X

LIST OF ABBREVIATIONS XI

CHAPTER 1. INTRODUCTION 1

1.1 INTRODUCTION TO THE FYNBOS BIOME 1

1.2 WILDFIRE IN THE FYNBOS BIOME 3

1.3 WILDFIRE MANAGEMENT IN THE FYNBOS BIOME 6

1.4 THE WILDFIRE TRIANGLE 8

1.5 AIM AND OBJECTIVES 12

CHAPTER 2. LITERATURE REVIEW AND THEORETICAL FOUNDATION 13

2.1 THE LIMITING WILDFIRE INGREDIENT 13

2.2 PREDICTING WILDFIRE RISK 14

2.2.1 Fire Danger Indices 14

2.2.2 Atmospheric features 20

2.3 LITERATURE IN SUPPORT OF DATA AND METHODS 22

2.3.1 Satellite derived fire products 22

2.3.2 Reanalysis datasets 24

2.3.3 Overview of classification techniques 26

CHAPTER 3. DATA AND METHODS 29

3.1 DATA 29

3.1.1 Fire data 29

3.1.2 Reanalysis data and calculation of the FDI 33

3.2 METHODS 35

3.2.1 Characterisation of fire occurrence and FDI over the Fynbos Biome 35

3.2.2 Classification of FDI anomaly over the Fynbos Biome 36

3.2.3 Identification of atmospheric features that produce fire-conducive conditions 37

3.2.4 Assessing the ability of atmospheric circulation features to be used as a fire forecasting tool 38

CHAPTER 4. RESULTS AND DISCUSSION 40
4.1 CLIMATOLOGY OF THE FDI AND ATMOSPHERIC VARIABLES OVER SOUTH AFRICA 40
4.2 CHARACTERISTICS OF FIRE OCCURRENCE AND FDI OVER THE FYNBOS BIOME 42
4.2.1 Seasonality and Interannual Variability 42
4.2.2 Spatial Variability 46
4.2.3 Fire occurrence thresholds 48
4.2.4 Relationship between fire intensity and FDI 49
4.3 THE CLASSIFICATION OF THE FDI PATTERN OVER SOUTH AFRICA 51
4.4 ATMOSPHERIC FEATURES THAT PRODUCE FIRE-CONDUCIVE CONDITIONS 56
4.4.1 Node (4) 65
4.4.2 Node (16) 66
4.4.3 Node (13) 67
4.4.4 Special Case - Node (1) 68
4.5 ABILITY OF ATMOSPHERIC CIRCULATION FEATURES TO BE USED AS A FIRE FORECASTING TOOL 71
CHAPTER 5. CONCLUSIONS AND RECOMMENDATIONS 82
5.1 CONCLUSIONS 82
5.2 RECOMMENDATIONS FOR FURTHER RESEARCH 86
ACKNOWLEDGEMENTS 87
REFERENCES 88
APPENDICES 98

List of Figures

Figure 1-1: The Five Mediterranean eco-regions (shaded dark green) that are located within the mid-latitudes. The Fynbos Biome is located predominantly in the Western Cape of South Africa (O'Hara, n.d) .**1**

Figure 1-2: King Protea (Protea cynaroides) – The national flower of South Africa (Harris, 2006) **2**

Figure 1-3: [Left] The Fynbos endemic Orange-breasted Sunbird (Anthobaphes violacea) sitting on a burnt protea bush (Gardner, 2015a). [Right] The critically endangered and endemic Table Mountain Ghost Frog (Heleophryne rosei) (SANBI, n.d) **2**

Figure 1-4: An ecologically-based global fire map (Pausas & Ribeiro, 2013).....**4**

Figure 1-5: [Left] Fire burning in Fynbos (Olivier, n.d). [Centre] Seeding as a post-fire reproductive strategy (Gardner, 2015b). [Right] Resprouting as a post-fire reproductive strategy (Rabie, 2015).....**5**

Figure 1-6: Photographs from the recent "Cape Fire" in March 2015, which was the most destructive fire since the year 2000. [Left] Properties under threat on the wildland-urban interface of Table Mountain National Park and the suburb of Lakeside (AndyNixPix, 2015). [Right] Geofrey Collings' home in Tokai was one of 13 houses that were either entirely or partly destroyed (DailyMail, 2015).....**5**

Figure 1-7: Preventing wildfires through public awareness campaigns and wildfire education initiatives. [Left] Today's fire danger rating signboard outside the entrance to the Table Mountain National Park (Reggie, 2010), [Centre] The "look what you have done" fire prevention campaign (Kramer, 2006), [Right] Fire education programme (City of Cape Town, n.d) **6**

Figure 1-8: Wildfire Triangle - Three ingredients required for wildfires to occur **8**

Figure 2-1: Reporting of Fire Danger for the various Fire Protection Association areas of South Africa (SAWS, 2015) **15**

Figure 2-2: Component flow of US National Fire Danger Rating System (Willis et al., 2001).....**16**

Figure 2-3: Structure of the McArthur Forest Fire Danger Index (Willis et al., 2001)**17**

Figure 2-4: Structure of the McArthur Grassland Fire Danger Index (McArthur, 1958) **17**

Figure 2-5: Nomogram used to calculate the Burning Index component of the Lowveld Fire Danger Index (Working on Fire, n.d) **18**

Figure 2-6: Rainfall Correction Factor, which is multiplied to the FDI value to get the corrected FDI value and which is determined by days since last rainfall and amount of rainfall (Working on Fire, n.d). **19**

Figure 3-1: Study Area – Spatial extant of the Fynbos Biome **31**

Figure 3-2: Histogram of fire detection confidence for the study period and study area **31**

Figure 3-3: Modified MODIS active-fires (shown in red) that occurred within the Fynbos Biome from 2003 – 2012 ..... **32**

Figure 4-1: Seasonal means of the Lowveld FDI and its constituent variables over Southern Africa for the period 2003-2012 ..... **40**

Figure 4-2: Seasonal means of the Geopotential Height and Wind Velocity at the 850mb and 500mb levels, over Southern Africa for the period 2003-2012 ..... **41**

Figure 4-3: Box-and-Whisker plots showing observed monthly distribution of the number of fire days in the Fynbos Biome from 2003-2012. The four open circles in the plot represent extreme events. The green line represents the mean monthly FDI for each of the respective calendar months **43**

Figure 4-4: Cross Correlation between the number of fire days per month (lagged) and the monthly FDI over the Western Cape. Blue stippled lines represent the confidence limit **44**

Figure 4-5: Trend in the annual number of fire days in the Fynbos Biome with positive anomalies shown in blue and negative anomalies shown in red (base period 2003-2012). The green line shows the trend in the annual FDI anomaly (base period 2003-2012). The black line represents the Oceanic Niño Index over the same period **45**

Figure 4-6: Count of fire detections in the Fynbos Biome during the study period showing spatial variability of fire occurrence **47**

Figure 4-7: Mean Fire Danger Index over all days in the study period. The highlighted window matches the map area displayed in Figure 4-6 ..... **48**

Figure 4-8: Histograms of the a) Fire Danger Index, b) Maximum surface temperature, c) Minimum surface relative humidity, and d) Maximum surface wind speed at the locations of fire detection events **49**

Figure 4-9: Scatterplots showing the relationship between Fire Intensity and the a) Fire Danger Index, b) Maximum surface temperature, c) Minimum surface relative humidity, and d) Maximum surface wind speed for all fire detection events. **50**

Figure 4-10: Resulting nodes of Self Organising Maps technique displaying spatial variation in FDI anomaly on days when fires occurred **52**

Figure 4-11: Seasonality of the resulting SOMs nodes **54**

Figure 4-12: Interannual variability in the occurrence of the resulting SOMs nodes **55**

Figure 4-13: DJF season anomalies of the Fire Danger Index on the day of fire for each node **57**

Figure 4-14: DJF season anomalies of maximum surface Temperature (°C) on the day of fire for each node **58**

Figure 4-15: DJF season anomalies of minimum surface Relative Humidity (%) on the day of fire for each node **60**

Figure 4-16: DJF season anomalies of maximum surface Wind Speed (m.s-1) on the day of fire for each node **61**

Figure 4-17: DJF season Anomalies of Geopotential Height (m) and Wind Vectors at 850mb level, on the day of fire for each node **62**

Figure 4-18: DJF season Actual Geopotential Height (m) and Wind Vectors at 850mb level, on the day of fire for each node **63**

Figure 4-19: DJF season Anomalies of Geopotential Height (m) and Wind Vectors at 500mb level, on the day of fire for each node **64**

Figure 4-20: DJF season Actual Geopotential Height (m) and Wind Vectors at 500mb level, on the day of fire for each node **65**

Figure 4-21: The Anomalies and Actual values of Geopotential Height (m) and Wind Vectors for Node (1) for the DJF, MAM, JJA and SON seasons at both the 850mb and 500mb levels **70**

Figure 4-22: The FDI anomalies on the days of fire events for Node (1) for the DJF, MAM, JJA and SON seasons **70**

Figure 4-23: Comparison between: The actual number of fire days that occurred in the DJF season [Column 1] and the number of days the DJF FDI composite [Column 2], the DJF geopotential height anomaly at the 850mb level composite [Column 3], and the DJF geopotential height anomaly at the 500mb level composite [Column 4] occurred during the entire study period, for each of the resulting SOMs nodes **72**

Figure 4-24: Comparison between: The actual number of fire days that occurred in the MAM season [Column 1] and the number of days the MAM FDI composite [Column 2], the MAM geopotential height anomaly at the 850mb level composite [Column 3], and the MAM geopotential height anomaly at the 500mb level composite [Column 4] occurred during the entire study period, for each of the resulting SOMs nodes **78**

Figure 4-25: Comparison between: The actual number of fire days that occurred in the SON season [Column 1] and the number of days the SON FDI composite [Column 2], the SON geopotential height anomaly at the 850mb level composite [Column 3], and the SON geopotential height anomaly at the 500mb level composite [Column 4] occurred during the entire study period, for each of the resulting SOMs nodes **79**

Figure 4-26: Comparison between: The actual number of fire days that occurred in the JJA season [Column 1] and the number of days the JJA FDI composite [Column 2], the JJA geopotential height anomaly at the 850mb level composite [Column 3], and the JJA geopotential height anomaly at the 500mb level composite [Column 4] occurred during the entire study period, for each of the resulting SOMs nodes **81**

List of Tables

Table 1-1: Fuel characteristics that allow for wildfire occurrence and spread **10**

Table 1-2: Weather characteristics that allow for wildfire occurrence and spread....**11**

Table 2-1: Wind speed correction factor for the Burning Index of the Lowveld Fire Danger Index **19**

Table 3-1: Example of parameters provided for a fire detection by the active-fires product **30**

Table 3-2: Metadata for CFSR variables **34**

Table 3-3: User specified parameters chosen for SOM_PAK **37**

Table 4-1: Correlations between the DJF FDI anomaly nodes and the respective DJF nodes of each of the FDI constituent variables.....**59**

Table 4-2: The percentage of days that fires occurred relative to the number of days the DJF FDI composite occurred during the study period, for each of the resulting SOMs nodes.....**73**

Table 4-3: The percentage of days that the DJF FDI composite occurred, relative to the number of days the DJF geopotential height (850mb level) anomaly composite occurred, for each of the resulting SOMs nodes. **75**

List of Abbreviations

BI	Burning Index
CFSR	Climate Forecasting System Reanalysis
CISL	Computational & Information Systems Lab
DJF	December, January, February
ENSO	El Ninõ Southern Oscillation
EOS	Earth Observing System
FDI	Fire Danger Index
FFDI	Forest Fire Danger Index (McArthur)
FIRMS	Fire Information for Resource Management System
GCM	Global Circulation Model / Global Climate Model
GFDI	Grassland Fire Danger Index (McArthur)
GIS	Graphical Information System
ITCZ	Inter Tropical Convergence Zone
JJA	June, July, August
KBDI	Keetch-Byram Drought Index
LANCE	Land, Atmosphere Near real-time Capability for EOS
MAM	March, April, May
MODIS	Moderate Resolution Imaging Spectroradiometer
NASA	National Aeronautics and Space Administration
NCAR	National Centre for Atmospheric Research
NCEP	National Centres for Environmental Prediction
NFDRS	National Fire Danger Rating System
NGO	Non-Governmental Organisation
ONI	Oceanic Ninõ Index
PCA	Principal Component Analysis
SANBI	South African National Biodiversity Institute
SAWS	South African Weather Service
SOMs	Self Organising Maps
SON	September, October, November

Chapter 1. Introduction

1.1 Introduction to the Fynbos Biome

The Fynbos Biome, commonly referred to as the Cape Floristic Region, is one of the world's five Mediterranean eco-regions that typically occur on the west coast of continents in the mid-latitudes (Figure 1-1). Located predominantly in the Western Cape province of South Africa, the Fynbos Biome is also one of the world's few biodiversity hotspots. The Fynbos Biome only covers an area of approximately 90 000 square kilometres and yet it contains over 9 000 floral species, of which a phenomenal 69% are endemic to the region (Cowling *et al*., 1996; Goldblatt & Manning, 2002). The Fynbos vegetation is so taxonomically diverse and distinctive that phytogeographers often classify Fynbos as a separate floral kingdom (Cody, 1986). Further illustrating the iconic status of Fynbos is the King Protea, a distinctive, large flower occurring in the region, which is the national flower of South Africa (Figure 1-2).

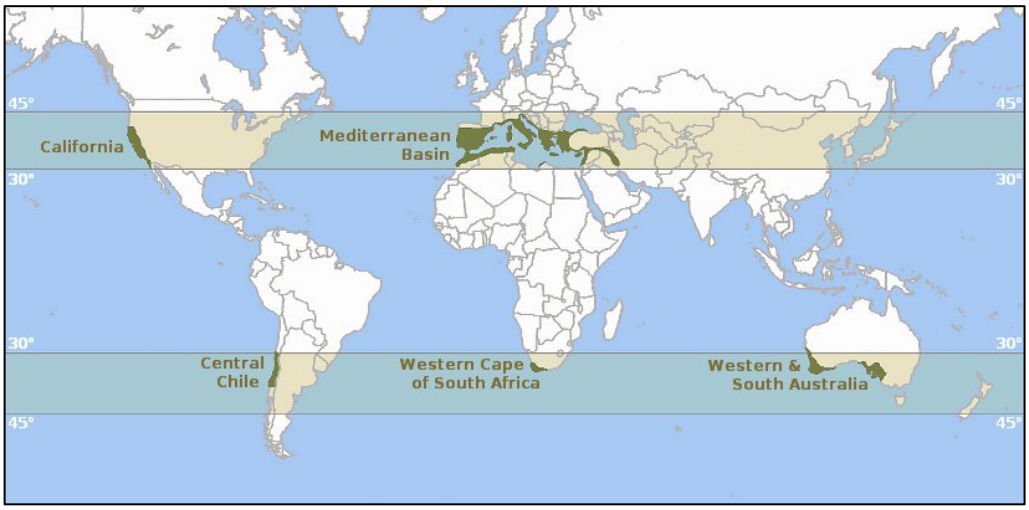

Figure 1-1: The Five Mediterranean eco-regions (shaded dark green) that are located within the mid-latitudes. The Fynbos Biome is located predominantly in the Western Cape of South Africa (O'Hara, n.d).

Figure 1-2: King Protea (*Protea cynaroides*) – The national flower of South Africa (Harris, 2006).

Due to the high biodiversity and endemism of Fynbos, it is not surprising that the same is true of the fauna in the region, which rely on the Fynbos for survival. The Orange-breasted Sunbird (*Anthobaphes violacea*) – one of six endemic birds – and the Table Mountain Ghost Frog (*Heleophryne rosei*) are among these (Figure 1-3). In fact, some fauna and flora species are so highly specialised that they are only found in a single valley or on a single slope. The Table Mountain Ghost Frog – a critically endangered species – is restricted to a total range of less than 10km^2 and is only found on the southern and south-eastern slopes of Table Mountain (CapeNature, 2013).

Figure 1-3: [Left] The Fynbos endemic Orange-breasted Sunbird (*Anthobaphes violacea*) sitting on a burnt protea bush (Gardner, 2015a). [Right] The critically endangered and endemic Table Mountain Ghost Frog (*Heleophryne rosei*) (SANBI, n.d).

Numerous conservation areas have been established within the Fynbos Biome in order to meet the globally informed species conservation agenda. However, protecting and managing the Fynbos region is not only important in terms of protecting the many unique species which live in it, but also in order to foster the social benefits it provides. Turpie *et al*. (2003) performed an ecosystem services valuation for the rich biodiversity of the Cape Floristic Region and revealed that the total economic value for the terrestrial and marine biodiversity is likely in excess of R10 000 million Rand (value in year 2000) per year. This equates to over 10% of the economy in the region. Therefore the need for increased conservation efforts cannot be understated.

1.2 Wildfire in the Fynbos Biome

Fire is an ecological feature that has evolved into many of the world's eco-regions (Shlisky, 2007), as observed in Figure 1-4. Each eco-region has a natural fire regime that is characterised by the seasonality, intensity and fire-return-interval of fire occurrence. Fires in the natural landscape are referred to by many different names – often determined by global location and the natural vegetation type – such as: veld fires, wildland fires, bushfires, and rangeland fires. These umbrella terms refer to all fires within natural vegetation, regardless of how or why the fire started. For the purposes of this minor-dissertation, wildfires are defined as veld fires that occur without the planned intent of the presiding fire manager. Therefore, a prescribed burn initiated by a fire manager in natural vegetation is still considered to be a veld fire, but is not considered as a wildfire.

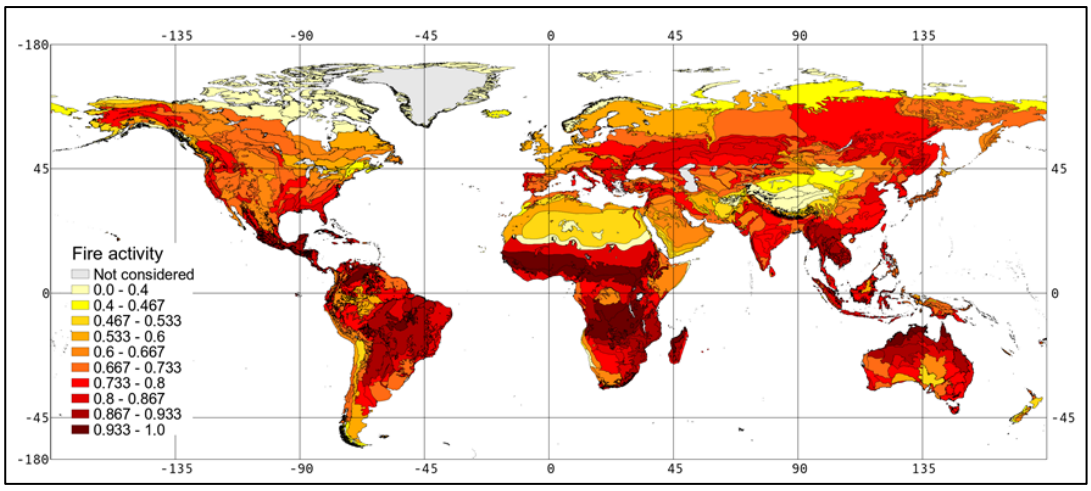

Figure 1-4: An ecologically based global fire map (Pausas & Ribeiro, 2013).

Due to the Mediterranean climate of the Fynbos Biome, which is characterised by hot and dry summers and cool and wet winters (Köppen, 1931; Wilson *et al.*, 2010), fires are a natural and prevalent phenomenon in the landscape. These climatic conditions result in a dominant austral summer wildfire regime in the region, although some fires do occur during the winter season (Van Wilgen *et al.,* 2010). Because of the historical prevalence of fires in the region, many of the floral species in the Fynbos Biome have evolved to become pyrophytes. These fire-adapted species have become dependent on fire for reproduction (Figure 1-5), the recycling of nutrients, and the removal of dead/senescent vegetation (Bond *et al.*, 2003). Fire is therefore an essential natural ecological process, central to the continued ecological functioning of Fynbos ecology and the conservation of its extraordinary biodiversity. Changes to the natural fire regime of the Fynbos Biome, whether through natural or anthropogenic processes, can severely threaten this ecological function (Kruger *et al.*, 2006).

Figure 1-5: [Left] Fire burning in Fynbos (Olivier, n.d). [Centre] Seeding as a post-fire reproductive strategy (Gardner, 2015b). [Right] Resprouting as a post-fire reproductive strategy (Rabie, 2015).

Although fires are an essential component for the Fynbos Biome, they can have severe negative impacts on humans, specifically those who reside on the wildland-urban interface (Gill and Stephens, 2009) (Figure 1-6). Generally all wildfires require human suppression activities to prevent destruction of property. The financial costs associated with these suppression efforts can be immense (of the order of hundreds-of-thousand to tens-of-millions of South African Rand). Despite suppression efforts, wildfires often result in the destruction of houses and farms (Kruger *et al.*, 2006), which dramatically escalates the financial costs. The threat to human life must also not be underestimated, with fatalities – especially among fire fighters – being a reality (de Ronde, 2002, Teie *et al.*, 2010).

Figure 1-6: Photographs from the recent “Cape Fire” in March 2015, which was the most destructive fire since the year 2000. [Left] Properties under threat on the wildland-urban interface of Table Mountain National Park and the suburb of Lakeside (AndyNixPix, 2015). [Right] Geofrey Collings' home in Tokai was one of 13 houses that were either entirely or partly destroyed (DailyMail, 2015).

1.3 Wildfire Management in the Fynbos Biome

Traditionally, wildfire management focused on reactive wildfire suppression when a wildfire occurred. This led to many unintended and negative ecological and social consequences. However, there has been a recent global paradigm shift to a more proactive integrated management approach in the field of resource management. Both globally and within the Fynbos Biome, this integrated management approach is being continually adopted into fire management theory and practice (Hann & Bunnell, 2001; Silva *et al.*, 2010). Provincial Government and private landowners have taken massive strides to incorporate and improve integrated fire management practices within the domain of the Fynbos Biome. Three core principals that embody integrated fire management are *Prevention*, *Preparation* and *Prediction* (Gill & Stephens, 2009).

The focus of wildfire prevention within the Fynbos Biome has been on the reduction of anthropogenic ignitions through public awareness campaigns and wildfire education initiatives. Examples include displaying the daily FDI at the entrance to conservation areas, billboard awareness campaigns and fire education programmes, particularly at schools and informal settlements (Figure 1-7).

Figure 1-7: Preventing wildfires through public awareness campaigns and wildfire education initiatives. [Left] Today's fire danger rating signboard outside the entrance to the Table Mountain National Park (Reggie, 2010), [Centre] The "look what you have done" fire prevention campaign (Kramer, 2006), [Right] Fire education programme (City of Cape Town, n.d).

Despite the increased efforts in wildfire prevention, unintentional wildfires are part of the ecological system of the Fynbos Biome and will continue to occur. There have been numerous advances in the preparation for wildfires and some examples include: fire suppression agencies are receiving better funding which improves training and access to specialised and advanced fire fighting equipment; strategic firebreaks are constructed and maintained to reduce the potential spread of wildfire and to assist with the effectiveness of wildfire suppression (Teie, 2009); State landowners and municipalities are now required by law to be members of Fire Protection Associations, which stipulate minimum fuel preparation and suppression resource requirements. Lastly, and most importantly, prescribed burning operations and alien vegetation clearing help to reduce fuel loads. While prescribed burning operations are useful in this regard, the natural fire-return-interval needs to be considered. Within the Fynbos Biome the general policy is to burn vegetation from around March to April at 12-15 year intervals (Van Wilgen *et al*., 1992). However in practice, numerous factors make it difficult for fire managers to conduct prescribed burns over sufficient areas (Van Wilgen *et al.*, 2010). Consequently excessive fuel loads persist in some areas.

The third core principal of wildfire management – prediction – is primarily achieved through the use of fire danger indices (Southey, 2009). In November 2013, the South African Department of Agriculture, Forestry and Fisheries declared the Lowveld Fire Danger Index (FDI) as the official fire danger rating system for South Africa (Staatskoerant, 2013). Although the Lowveld FDI provides a reasonably good measure of short-term wildfire risk, its longer-term performance is hindered by the decreasing reliability of the numerical weather forecasting model outputs for longer-term forecasts (Banitz, 2001). The literature has recently started investigating atmospheric circulation features and how they relate to wildfire danger (Millán *et al*. 1998; Papadopoulos *et al*., 2013; Wilson *et al*., 2010). Although this line of research is still in its infancy, it is already showing potential for improving the predictability of wildfires. Furthermore, the goals of fire management would be achieved with greater success if the predictability of wildfires were improved.

1.4 The Wildfire Triangle

Fire is a prevalent ecological feature in some vegetation types but is absent in others. In order for wildfires to occur, three essential ingredients are required. These are *ignition sources*, *fuel* and fire favourable *weather/climate*, which can be portrayed as a Wildfire Triangle as in Figure 1-8. For any given space and time, one of these three components acts as the limit for the occurrence of wildfires (Archibald *et al.,* 2010).

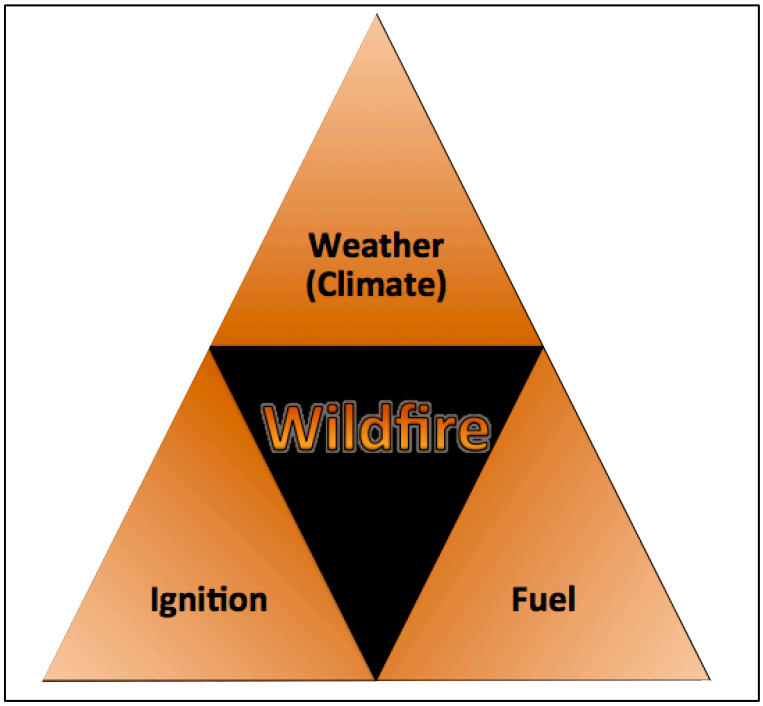

Figure 1-8: Wildfire Triangle - Three ingredients required for wildfires to occur.

Ignition sources of wildfire can broadly be classified as either natural or anthropogenic. Natural ignitions are usually a result of lightning strikes and, less commonly, rock falls (Cowling *et al.,* 2004). Anthropogenic ignitions can further be classified as intentional or unintentional (Teie, 2009). Intentional ignitions include arson activities and prescribed burn activities, while there are numerous unintentional anthropogenic ignition sources. These include, but are not limited to, vagrant and recreational cooking fires, non-extinguished cigarette disposals, electricity transmission line accidents, motor vehicle accidents and irresponsible use of sea rescue flares and Chinese-

lanterns (Erasmus, 2013). The ratio of fire ignitions attributed to anthropogenic activities relative to natural activities has been increasing dramatically around the world (Goldammer & Crutzen, 1993). Wildfires in the eastern half of the Fynbos Biome seem to be caused mainly by lightning strikes, but anthropogenic ignitions have become the dominant cause of wildfires in the western half of the Fynbos Biome (Southey, 2009; Van Wilgen, 1984). The relative increase in anthropogenic ignitions has resulted in severe ecological and social impacts, which are expected to intensify with the increase in population growth rates (Van Wilgen *et al.*, 2010).

In the case of wildfires, the general fuel under consideration is the vegetation (both indigenous and alien). There are numerous factors which determine whether a wildfire will burn in vegetation, as well as the rate of spread and the intensity (Teie, 2009). Some of these factors are shown in Table 1-1. It is also important to consider anthropogenic fuels, particularly on the urban-wildland interface. Houses, outdoor-furniture, woodpiles and overgrown gardens provide combustible materials that will contribute to the dynamics and spread of a fire.

Table 1-1: Fuel characteristics that allow for wildfire occurrence and spread.

Factor	Effect
Size and Shape	Less heat is required for light fuels to ignite but these fuels burn away quickly and are easier to put out. Heavy fuels, require a greater fire-intensity to ignite but can burn for days once ignited.
Chemical Composition	Certain plant types have a higher propensity to burn due to their chemical content. Fynbos vegetation generally has high oil content, which increases with the age of the plants. The higher oil content leads to increased combustibility.
Fuel Age	This is a complex factor that affects many others. An increase in the age of vegetation increases oil content as well as vertical and horizontal continuity and will eventually lead to a reduction in fuel moisture (senescence).
Fuel Moisture	The higher the fuel moisture content, the lower the propensity of the vegetation to burn. This is affected by climate/weather as well as approaching fire.
Fuel Temperature	The higher the fuel temperature, the higher its propensity to burn. This is affected by climate/weather as well as approaching fire.
Vertical and Horizontal continuity	In order for a fire to spread, unburnt fuel needs to be close enough to radiant heat from nearby flames before combustion will occur. For example, rocky areas with scattered vegetation may impede the spread of wildfire.

The climate of a particular region is one of the strongest controls of the fire regime (Teie, *2009*). In areas with Mediterranean climates like the Fynbos Biome, there is a summer fire regime due to the hot and dry conditions. These climatic conditions lead to an increase in fuel temperature and a reduction in fuel moisture. The South African Highveld, in contrast, has a winter fire regime in its grassland biome because it experiences convective

summer rainfall and very little precipitation in winter (Tyson, 2000). This leads to high grass curing (reduction of moisture in grasses), which sees the majority of wildfires in that region occurring in winter. Weather on a particular day, as well as the preceding few days, determine the probability of an ignition source leading to an actual wildfire ignition as well as the fire behaviour. The main weather characteristics that affect wildfires (Teie, 2009) are shown in Table 1-2. The weather on days preceding a particular day has a cumulative, lagged effect on wildfire potential and should be considered when trying to forecast fire risk (Teie *et al*., 2010). For example, if there were a number of hot and dry days leading up to a particular day, the cumulative reduction in fuel moisture over the successive days will increase the wildfire potential for that day.

Table 1-2: Weather characteristics that allow for wildfire occurrence and spread.

Factor	**Effect**
Air temperature	An increase in air temperature will result in an increase in the fuel temperature, but will also lead to a reduction in the relative humidity of the given air mass.
Relative Humidity	A reduction in relative humidity will result in a decrease in the fuel moisture and will increase the air's potential to facilitate combustion.
Atmospheric Stability	Wind speed and direction play a very important role in the intensity and spread of an existing wildfire, but they have relatively little influence on creating a wildfire-conducive environment.
Precipitation	The fire regimes in Southern Africa are bound to the summer and winter rainfall areas. Precipitation leads to an increase in fuel and soil moisture, which reduces the potential for vegetation to burn. However, due to the high oil content of Fynbos wildfires can still occur and spread during light precipitation and even soon after heavy rain.

1.5 Aim and Objectives

The aim of this minor-dissertation is to examine the synoptic-scale atmospheric features that induce favourable conditions for wildfire in the Fynbos Biome, potentially improving wildfire predictability. The knowledge may then lead to better-informed decisions taken by policy-makers, fire managers and the general public. The main objectives to achieve this aim are to:

- Investigate the characteristics of fire occurrence in the Fynbos Biome.
- Identify the dominant synoptic-scale atmospheric circulation features that are associated with wildfire.
- Assess how often these identified synoptic-scale atmospheric features lead to actual fire events.

This minor-dissertation is divided into five main chapters. Following the introductory chapter, Chapter 2 provides a review of the relevant fire management literature but also provides some context for using the selected data and analysis techniques. Chapter 3 details the fire and atmospheric data used in this study, how the data were sourced and the pre-processing that was applied to the data. Subsequently, the analyses performed on the data are described. The results of the analyses are then presented and discussed in Chapter 4. Finally, Chapter 5 states the main conclusions for the study and suggests a few recommendations for further research. The Acknowledgements, References and Appendices then follow the five main chapters successively.

Chapter 2. Literature Review and Theoretical Foundation

2.1 The limiting wildfire ingredient

A major concern of wildfire literature in South Africa is that studies are generally limited to research conducted from within a few national parks or conservation areas (Parr & Chown, 2003; Southey, 2009; Van Wilgen, 2010). The results of those studies are then often presumed to be applicable for an entire region and are presented as such. However, the wildfire ingredients that are available in conservation areas will be different to those in non-conserved areas. This research bias needs to be considered when investigating the limiting wildfire ingredient in the Fynbos Biome.

A fire favourable weather/climate study attempting to improve the predictability of wildfire necessitates the assumption that fire favourable weather/climate can act as the limit to wildfire occurrence. At the present time, there is still no strong consensus in the literature about whether fire favourable weather/climate acts as the limit. Archibald *et al.* (2010), whose research was among the first to investigate the climate interactions in Southern Africa, found a difference in the limiting ingredient to fire occurrence within protected/conserved areas and outside of protected areas. The authors concluded that human impact (ignitions and fuel) is more important than the effect of climate variability on wildfire occurrence outside of protected areas. However within protected areas variation in accumulated rainfall and the length of the dry season are the dominant drivers. Van Wilgen *et al.* (2010) performed a case study of fire management across ten protected areas within the Fynbos Biome and came to two relevant conclusions regarding the limit to wildfire occurrence: Firstly, their results suggested that post-fire age, which is a proxy for fuel accumulation, did not limit the occurrence of wildfires (except

in the first couple of years directly post-fire). A consequence of this result for fire management is that while prescribed burn operations may reduce the fuel load to aid in the suppression of wildfires, there is little evidence to suggest that they will actually reduce the risk of wildfire occurring. Secondly, their results show that even though inland regions experience generally higher fire danger conditions, there was little difference in the fire-return-intervals between inland and coastal zones. The implication of these two conclusions is that it is the potential sources of ignition – and not fuel or fire favourable/weather – that act as the limit to wildfire occurrence within the protected areas. This contradicts the study by Archibald *et al.* (2010) and therefore it remains unclear whether fire weather/climate can act as the limit to wildfire occurrence. Southey's (2009) study of four protected areas adds further uncertainty as the results show that ignitions in the western part of the Fynbos Biome are limited by ignitions, but fuel and weather restrict fires in the eastern part of the Fynbos Biome. The justification for undertaking the research in this minor-dissertation relies on the premise that fire weather/climate can act as the limit to wildfire. The results of this study could add further insight into this premise.

2.2 Predicting Wildfire Risk

2.2.1 Fire Danger Indices

Fire Danger Indices are the most commonly used metric for assessing wildfire potential in both the academic literature and in fire management practice. It should be noted that there is an important distinction between fire danger and fire behaviour, even though many of the same variables are used in the calculations of each of these concepts. Fire Danger is defined as a broad area description of the potential for wildfire ignition, an estimate of wildfire rate of spread and the requirements for potential wildfire suppression. In South Africa, the maximum forecasted fire danger is published daily (example shown in Figure 2-1) for each of the Fire Protection Association jurisdictions. The fire danger values published by the South African Weather

Service (SAWS) have important legal consequences since different value ranges have associated fire bans and minimum fire suppression resource requirements (Staatskoerant, 2015). Fire danger values are also used in wildfire suppression activities to quickly assess potential and expected wildfire behaviour. Fire behaviour is defined as the site-specific dynamics of a fire that describe its movement, intensity and rate of combustion (Everson *et al.*, 1988). A separate academic field is dedicated to the study of fire behaviour dynamics and the computational modelling of fire behaviour.

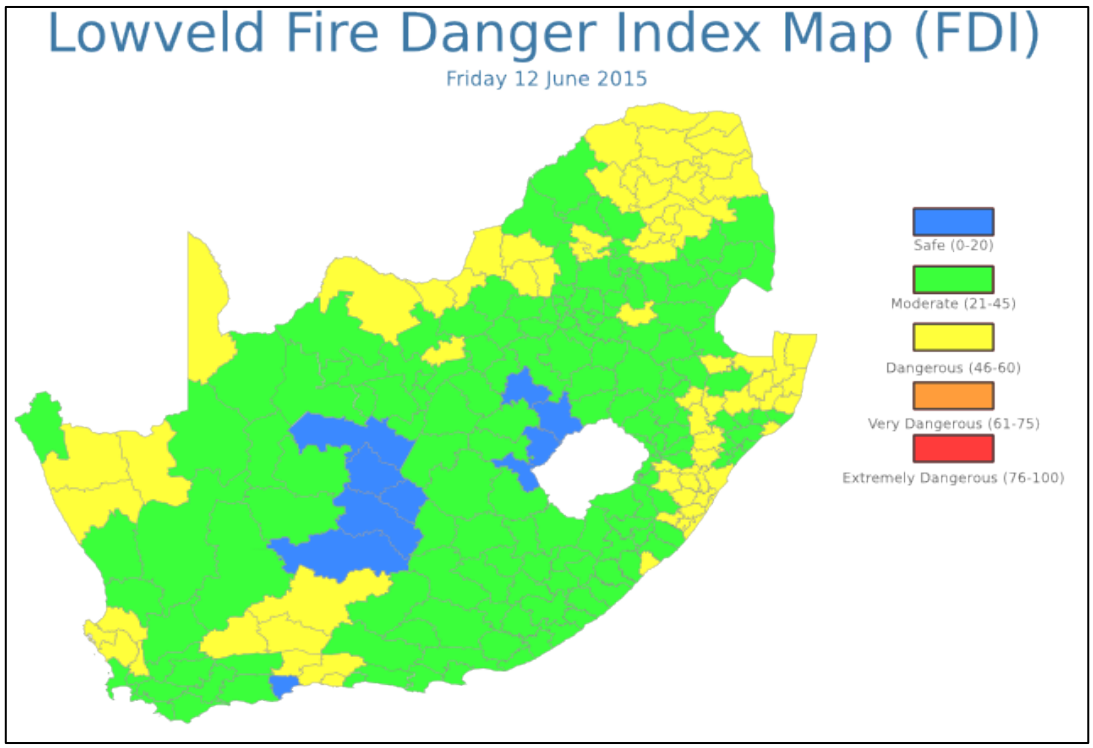

Figure 2-1: Reporting of Fire Danger for the various Fire Protection Association areas of South Africa (SAWS, 2015).

Numerous indices have been developed over the past five decades that vary in complexity and also in the type of weather variable and fuel variable inputs. The three most widely used indices are the United States National Fire Danger Rating Systems (NFDRS), the McArthur Forest Fire Danger Index (FFDI) and the McArthur Grassland Fire Danger Index (GFDI).

The NFDRS is the most complex of the fire danger rating systems and was developed particularly for forest fires in the US. It incorporates a wide variety

of complex inputs that are not always available. A large portion of the complexity can be attributed to the calculation of fire behaviour, which is based on Rothermal's (1972) fire behaviour model. The final output is a Fire Severity Index, which is composed of a Spread Component, Burning Index, Energy Release Component and an Ignition Component (Willis *et al.,* 2001). A flow diagram of the NFDRS is shown in Figure 2-2. The NFDRS is the only fire danger rating system that takes into account all three of the wildfire ingredients seen in Figure 1-8.

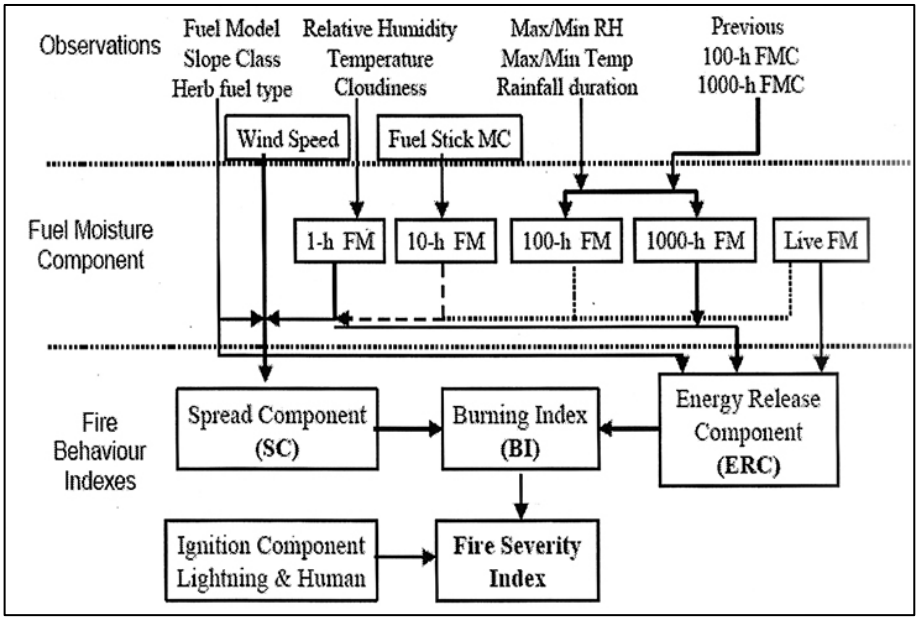

Figure 2-2: Component flow of US National Fire Danger Rating System (Willis *et al.*, 2001).

The McArthur FFDI, developed using an empirical model of forest fires in Australia, is a much simpler system than the NFDRS systems and applies to all forest and scrubland vegetation types (McArthur, 1958). The Keetch-Byram Drought Index (KBDI) (Keetch and Byram, 1968), rainfall amount and time since last rainfall are the only inputs required in addition to air temperature, relative humidity and wind speed (Willis *et al.,* 2001). These six inputs are used in various sub-models to ultimately calculate the Forest Fire Danger Index value. The McArthur FFDI structure is shown in Figure 2-3.

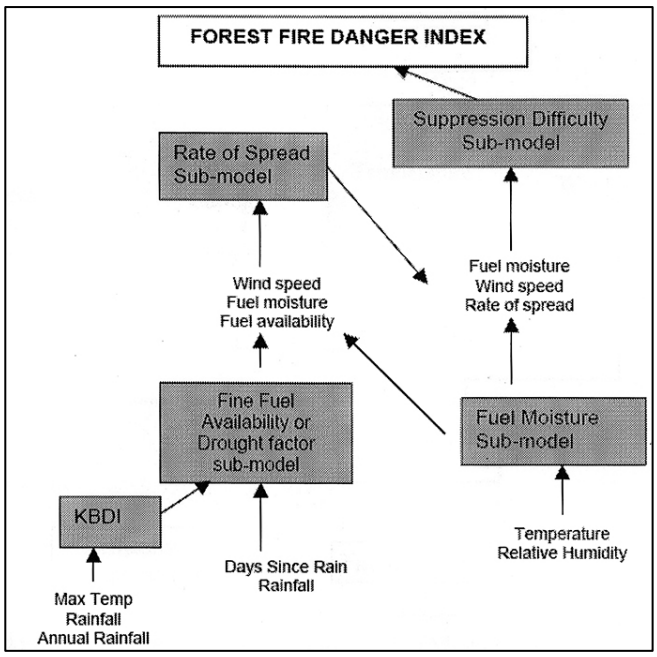

Figure 2-3: Structure of the McArthur Forest Fire Danger Index (Willis *et al.*, 2001).

The McArthur GFDI, also known as the MK 4 model, is very similar to the McArthur FFDI with the main difference being that grass curing is used instead of the KBDI to define the fine-fuel moisture content in grassland vegetation biomes. The components and structure of the McArthur GFDI is shown in Figure 2-4.

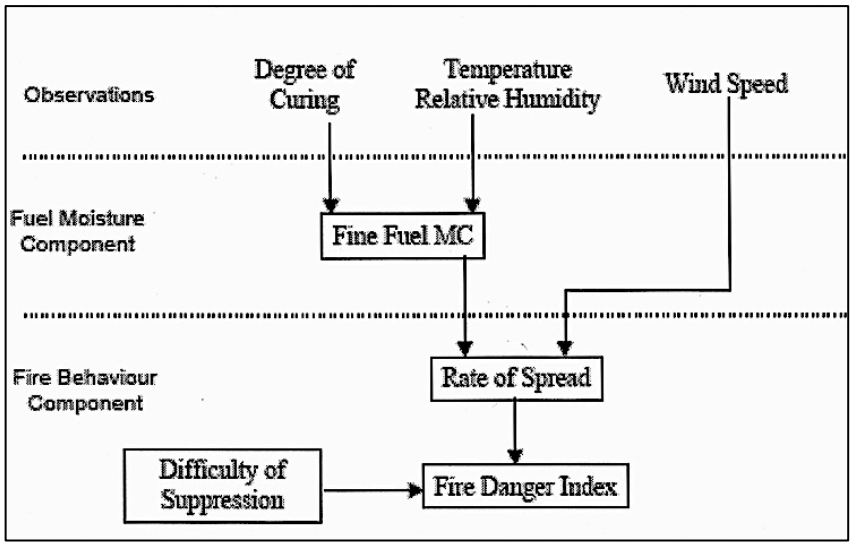

Figure 2-4: Structure of the McArthur Grassland Fire Danger Index (McArthur, 1958).

In South Africa, a modified version of the Fire Hazard Index – a system developed in Zimbabwe – has been used unofficially for many decades, particularly for grassland fires in the Lowveld. This rating system has therefore become commonly referred to as the Lowveld Fire Danger Index. It uses similar inputs to the McArthur models but scaled into a simple model, which does not require complex calculations. The ease of calculation of the Lowveld Fire Danger Index means that fire managers and fire fighters can easily calculate it in the field, with relatively cheap handheld equipment. The Lowveld Fire Danger Index consists of a Burning Index (BI) which is derived from the surface air temperature (°C) and relative humidity (%). The nomogram shown in Figure 2-5 has been developed to make it even easier to determine the BI, which can then be modified with a simplified wind correction factor table (Table 2-1). The final correction made to the FDI in the Lowveld Fire Danger Index is to multiply the BI – after the wind correction – by the rainfall correction factor (Figure 2-6).

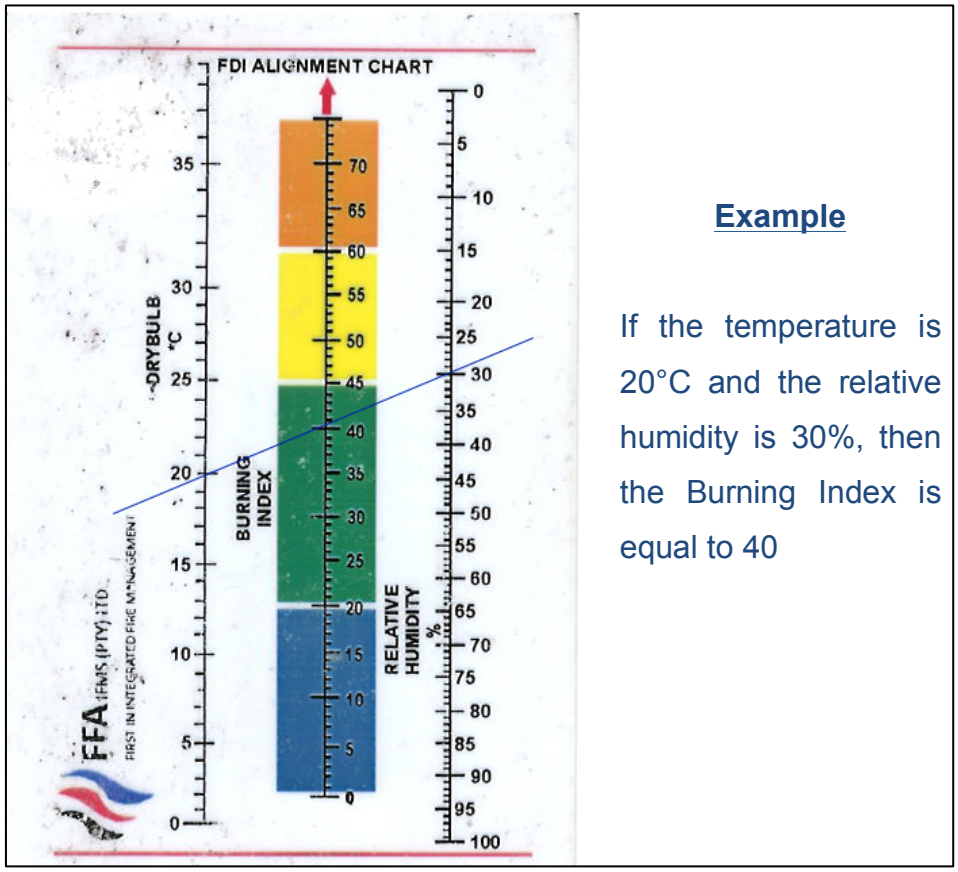

Figure 2-5: Nomogram used to calculate the Burning Index component of the Lowveld Fire Danger Index (Working on Fire, n.d).

Table 2-1: Wind speed correction factor for the Burning Index of the Lowveld Fire Danger Index.

Wind speed (km/h)	Add to initial Burning Index
0-2	+ Nil
3-8	+05
9-16	+10
17-25	+15
26-32	+20
33-36	+25
37-41	+30
42-45	+35
46+	+40

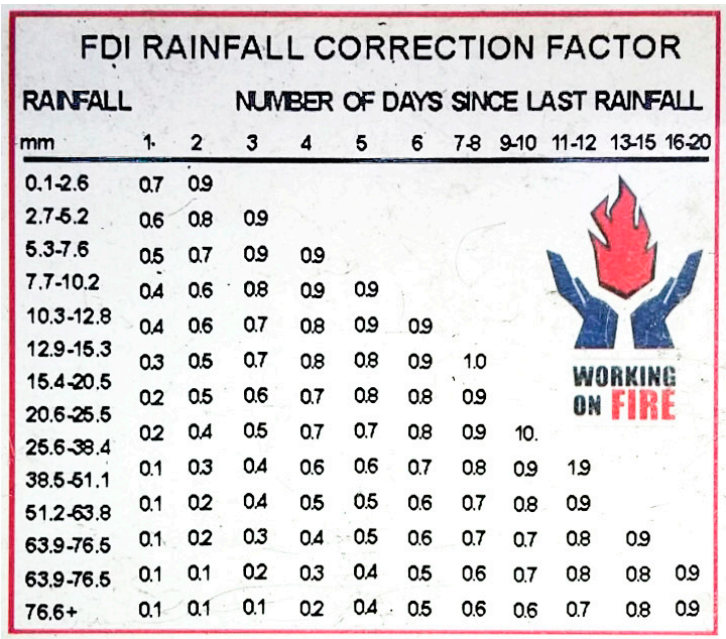

Figure 2-6: Rainfall Correction Factor, which is multiplied to the FDI value to get the corrected FDI value and which is determined by days since last rainfall and amount of rainfall (Working on Fire, n.d).

Since the unofficial inception of the Lowveld Fire Danger Index, there have been various modifications to the calculation. The most common modifications include the additions of wind, grass curing and rainfall factors respectively. During this time there was a general consensus amongst fire managers within the Fynbos Biome that the Lowveld Fire Danger Index

should be calculated through first determining the BI and then adding a corrective factor for wind speed (higher wind speeds being associated with increased fire danger). The rainfall factor was excluded for Fynbos vegetation because the physical and chemical composition of the pyrophytes was believed to offset the fire retardant effect of rain droplets soon after it stopped raining. There is however no academic precedent for excluding the rainfall factor in Fynbos vegetation. Furthermore, the curing factor – the proportion of dead grass to live grass – was also excluded because the process is far less pronounced in Fynbos vegetation.

2.2.2 Atmospheric features

Even though the effect of weather/climate variability on the occurrence of wildfires remains largely unresolved in the literature, atmospheric features and processes at varying size and temporal scales have been linked to fire danger. Geldenhuys (1994) identified that föhn-like berg-winds increase the propensity for wildfires when the author was investigating the spatial location of forests within the Fynbos Biome. Berg-winds bring warm and dry continental air over the Fynbos Biome and are caused at the smallest synoptic scale by a coastal low-pressure system that precedes an approaching mid-latitude cold front (Tyson, 2000). At the other extreme, Wilson *et al*. (2010) revealed that there are teleconnections (atmospheric forcings resulting from distant atmospheric features) to global circulation patterns that also influence seasonal fire risk. The authors found that positive phases in the Antarctic Ocean Circulation lead to a reduction in low-level moisture in the Fynbos Biome, which corresponds to increased fire risk. There is also an abundance of studies (Linn *et* al., 2007; San José *et al.*, 2014; Zhou *et al.,* 2015) that show how micro-scale and meso-scale atmospheric features are highly influential factors for determining fire behaviour and dynamics. However these factors are too small and localised to be considered for the broader-scale definition of fire danger (Everson *et al.*, 1988). Therefore, when studying fire weather/climate, it is vitally important to consider the spatial scope and resolution of the study and understand how

the spatial and temporal resolution of the data and methods employed by the researcher limit the possible outcomes.

The majority of fire weather-related studies investigate the meteorological conditions at the time of fire events (Kipfmueller & Swetnam, 2000). However, Papadopoulos *et al.* (2013) used back-trajectories to study the relationship between wildfires in Greece and antecedent synoptic states. The main result of their study showed that large wildfires in Greece are derived from a particular synoptic feature with an extended duration, followed by another particular synoptic feature that occurs one week directly prior to ignition. This study presents a strong argument that by furthering the knowledge of the atmospheric features that precede fire events, and incorporating it into the wildfire forecasting metrics, the overall predictability of wildfires may be improved.

Southey (2009) takes a novel approach to analysing the relationship between fire events and weather conditions, using the Self Organising Maps (SOMs) technique on atmospheric pressure at mean sea level. The author concludes that there is a significant relationship between synoptic atmospheric states and fire events for the Fynbos Biome. This minor-dissertation builds on the work of Southey in a number of innovative ways. Firstly, while Southey only makes use of fire data obtained from four conservation areas within the Fynbos Biome, this study uses the satellite derived active-fires product to acquire fire data for the entire biome. The results from this minor-dissertation would therefore be more representative of the entire region. Secondly, while Southey makes use of NCEP-NCAR reanalysis data at a 2.5° horizontal resolution, this study uses CFSR reanalysis data at a 0.5° horizontal resolution. CFSR has been shown to be better at reproducing observed values due to its higher horizontal and spatial resolution combined with its newly developed coupled ocean-sea ice model (Saha *et al*., 2010; Zhang *et al.*, 2012). The higher higher resolution of the CFSR reanalysis data also means that it will be able to resolve smaller-scale atmospheric features that may be important in producing fire-conducive conditions. Finally, Southey performs the SOMs technique over all days in the study period and then

matches the fire days to the resulting nodes. Therefore the resulting nodes reflect the dominant synoptic states in the entire period and not those that produce wildfire-conducive conditions. This study performs the SOMs technique only over days that fires occurred, which would facilitate the identification of very important fire producing synoptic states that do no occur regularly.

2.3 Literature in support of data and methods

2.3.1 Satellite derived fire products

The advent of the satellite era has seen the proliferation of a number of useful remote sensing applications. Through these remote sensing products, it is possible to obtain a plethora of different types of data over a large geographical area, including practically inaccessible areas. This greatly enhances the data availability to researchers for use in diverse disciplines. In contrast, land owners/managers on the ground may not record events, or may do so with varying degrees of accuracy and detail. It can also be difficult to obtain and process data from many individual sources. The data provided by satellite products are generally freely available for download by the public, are indiscriminate of land ownership/use, and are in a uniform format.

Satellite remote sensing products do have their own set of limitations. Firstly, they have a limited horizontal resolution, making small-scale events difficult to detect (Roy *et al.*, 2002). Secondly, the available data products are derived using algorithms that interpret the electro-magnetic spectrum received by the satellite sensors. This can lead to a problem of threshold values used in the algorithm that are not suitable for a specific area (Csiszar *et al.*, 2003; Li *et al.*, 2003). Thirdly, satellites that are not geostationary have a temporal resolution which means that that they may miss short events if they are not overhead when the event occurs (de Klerk, 2008). Lastly, other factors such as cloud cover can mask surface processes occurring at the time of satellite overpass (Li *et al.*, 2003).

The Moderate Resolution Imaging Spectroradiometer (MODIS) instrument is a key instrument on-board the Terra and Aqua Earth Observing System satellites. Each of these satellites covers the entire globe every 1 to 2 days, but the timing of their orbits are staggered, effectively halving the temporal resolution obtainable. The MODIS sensor acquires data in 36 spectral bands. Algorithms applied to these spectral bands can then be used to derive fire products.

There are currently two fire-related satellite products available. The first is the burnt area product, which determines the approximate date and area extent of fires by contrasting differences in pre-fire and post-fire surface reflectance at a 500m resolution. The algorithm used to determine burnt areas is described by Roy *et al.* (2005a). It appears that this data has only been freely available to the public from the beginning of 2008. The second product is the active-fires product that detects fires in 1km pixels, burning at the time of satellite overpass under relatively cloud-free conditions. The algorithm used to determine active-fires is described by Giglio *et al.* (2003) and involves first determining middle-infrared and thermal infrared brightness at threshold values and then rejects false detections by incorporating the brightness temperature relative to nearby pixels. This data has been freely available to the public since 2000, but it should be noted that the MODIS Aqua satellite was only put into operation in 2002.

Although the use of these two fire products has been thoroughly explored in the grasslands, savannah and woodlands of South Africa (see Roy *et al.*, 2005a; Trigg & Flasse, 2001), very few studies have been undertaken in the Fynbos Biome (de Klerk, 2008). In 2008, when the burnt area product was not yet available to the public, de Klerk (2008) performed a validation study of the active-fires product in the Fynbos Biome to see if it could be used to obtain a fire history for the region. However, de Klerk found that the active-fires product was unsuitable for creating a fire history because it only revealed about 60% of the fire area extent that was mapped by reserve managers. However, de Klerk claims that the active-fires product was

suitable for determining both the occurrence and location of fire, which fulfils the needs of this minor-dissertation.

There are a number of other foreseeable limitations to the active-fires product in the Fynbos Biome: The Fynbos Biome is a region that is mountainous and is adjacent to the west coast of South Africa (Goldblatt & Manning, 2002). The mountains can cause topographic shadows, which may lead to fires being undetected (Roy *et al*., 2005b). Sun-glint along coastlines also makes it difficult for the active-fires algorithm to detect fires near the ocean (Giglio *et al*. 2003). Additionally, heavy cloud cover – particularly in the winter season – may mask fire events (Li *et al.*, 2003). Taking these limitations into account, it can therefore be assumed that the active-fires product will not detect all fires in the region. This is in addition to the fires missed by the satellites that are not passing overhead at the time of fire occurrence, as well as small-scale fire events not being resolved by the satellites' spatial resolution. Despite these limitations, the MODIS active-fires data was used in this study because the benefits accrued, by having a uniform and biome-wide dataset, vastly outweighs the restrictions.

2.3.2 Reanalysis datasets

Reanalysis weather data provides a close equivalent to observed weather data, but is not limited by the number and location of weather recording stations in an area. It is the data assimilation of Global Circulation Models (GCM) constrained by observation data (Zhang *et al.*, 2012). The result is a grid of values for each weather variable at a certain spatial and temporal resolution over the entire globe. During the temporal coverage of reanalysis datasets, the GCM physics and parameterisations are not changed to ensure consistent and comparable output (Zhang *et al.*, 2012). Reanalysis models have their own set of limitations, which are a function of the limitations inherent in GCMs.

It is important to note that there are prognostic and diagnostic weather variables in a reanalysis dataset. The prognostic variables are based on the

fundamental physics equations inherent within the GCMs and all reanalysis models capture these variables with a relatively high degree of accuracy (Hewitson, 2013). An example of a prognostic variable is wind velocities at different pressure levels in the atmosphere. Diagnostic variables are derived variables that the GCMs do not assimilate. An example of a derived variable is precipitation, which is derived as a function of the flow of moisture and convergence/uplift (Zhang *et al.*, 2012). Therefore there can be a large discrepancy amongst reanalysis models with regards to derived variables, which should consequently be interpreted with caution.

A number of studies have been undertaken to assess the relative performance of various reanalysis models in deriving precipitation (see Bett *et al*., 2006; Bosilovich *et al*., 2008; Bromwich *et al*., 2011). These studies show that different reanalysis models can produce significantly different results. Zhang *et al.* (2012) compared the performance of eight global reanalysis models in deriving precipitation in the Southern Africa region. They found that the Climate Forecast System Reanalysis (CFSR) (Saha *et* al., 2010) provided results that matched closest to observation and attributed this performance to the model's high horizontal and vertical spatial resolution, as well as its newly developed coupled ocean-sea ice model. Although other derived variables have not been adequately tested, similarly to precipitation, it could be suggested that CFSR may perform equally well with these variables due to this model's advancements and high resolution. However, these variables should still be interpreted with caution.

The CFSR is initialised by observation 6 hourly (00Z, 06Z, 12Z, and 18Z) with horizontal resolution products at 0.3°, 0.5° 1.0° and 2.5° (Saha *et al*., 2010). Therefore CFSR provides reanalysis data four times a day. However, it is possible to obtain hourly time-series data from CFRS. These are hourly forecasted values between the four reanalysis initialisations. Although these forecasts improve the temporal resolution of weather variables, the model is not constrained by observations when determining these interim values. Therefore, these forecasts should be used with greater caution and are not

considered as reanalysis data. Given the higher available resolution and seemingly superior performance of CFSR the model, the CFSR reanalysis datasets were selected for this study.

2.3.3 Overview of classification techniques

There are numerous multivariate statistical techniques available, executed in order to classify information into useful categories (Everitt *et al*., 2011). The cluster analysis technique is so widely used in the literature that the technique itself has evolved differently in diverse research disciplines (Punj & Stewart, 1983). There are different strengths and weaknesses inherent within each of these cluster analysis versions/methods and consequently, dissimilar results are produced by the respective methods. Gower (1967) claims that no particular method is incorrect and suggests that the disparities are due to the absence of a clear definition of a cluster in the literature. Therefore, the inherent strengths and weaknesses of different cluster analysis methods should be considered when selecting the most appropriate one for a particular research study. Researchers will often use more than one method to verify their results (Gower, 1967).

Principal Component Analysis (PCA), also known as Eigenvector Analysis or Empirical Orthogonal Functions, is a discriminant analysis technique used to reduce the dimensionality of data (Rao, 1964). The main difference between cluster analysis – which most often uses Euclidian distance as the dissimilarity metric – and PCA is that the clusters do not obey a predetermined domain structure (Jolliffe, 2002). Therefore PCA gives all properties inherent within variables equal weighting when determining clusters, while cluster analysis gives more weight to properties of variables that are dependent on one another. Jolliffe (2002) claims that there is no benefit to using PCA over cluster analysis unless the equal weighting of properties inherent within variables is desired by the researcher.

The Self Organising Maps (SOMs) technique is a graphical spatial analysis tool that is applied in diverse research disciplines (Liu *et al.*, 2006). It is a tool

that analyses a continuous system based on descriptions of discrete states in the system called nodes (Kohonen, 1997). SOMs also determines the frequency of each discrete state in the progression of the continuous system.

Unlike Principal Component Analysis (PCA), SOMs does not attempt to cluster data, but rather attempts to visually display patterns in space where data points close to each other have similar values (Southey, 2009). Therefore SOMs shows spatial patterns of the variable, where it has high to low values, as the system evolves. The number of nodes or discrete states that SOMs produces is chosen by the analyst and depends on the level of generalisation that the analyst desires (Kohonen, 1997). More nodes will show a greater number of discrete states in the system, but there will be less noticeable distinctions between these states.

SOMs presents the results in a 2-dimensional array of nodes such that the four corner nodes show the most extreme states of the system and diagonally opposite corners are the most opposite states from one another (Hewitson & Crane, 2002). The nodes between these four corners represent a smooth transition between the extreme states. It should be noted that successive nodes do not necessarily represent a temporal progression of system states (Southey, 2009). Hewitson and Crane (2002) and Kohonen (1997) provide a useful description of the SOMs process and how to analyse the results.

Although PCA is a well-established method in climatological and meteorological research (Reusch *et al.*, 2005), the relatively new SOMs technique is now being used in similar applications in the atmospheric disciplines (Abiodun *et al., 2015;* Hewitson & Crane, 2002). Reusch *et al.* (2005) tested the performance of PCA relative to SOMs using known data patterns. They found that PCA, even with rotated components, could not adequately extricate spatial patterns, splits patterns into smaller individual components and fails to assign the variance correctly between the principal components. The authors also found that when using PCA it is almost impossible to determine mixing of spatial patterns without knowing the real pattern mixing processes. These authors claim further that SOMs is able to

successfully extract robust and generalised spatial patterns, while attributing the correct variance to each node. Liu *et al.* (2006) conducted a similar study and made comparable conclusions. Another benefit of using SOMs over PCA is that it is a non-linear alternative, with the latter being constrained to orthogonal linear functions (Southey, 2009). Therefore the present study uses SOMs as the classification technique.

Chapter 3. Data and Methods

3.1 Data

The two main sets of data used in this study are fire data and atmospheric reanalysis data that both span a ten-year period from the beginning of January 2003 until the end of December 2012. This was the maximum study period possible, given the availability of the different datasets at the time of data collection. Due to the complexity of the data analysis in this study, it was not feasible to extend the study period to include the data that subsequently became available.

3.1.1 Fire data

The fire data used for this study is the collection 5.1 version of the active-fires product (MCD14ML) derived from the two MODIS sensor satellites. This version is processed at the University of Maryland and has a three-month lag compared to the version 5.0 near-real time product (MCD14DL) processed by LANCE FIRMS. The MCD14ML product used in this study is the standard/science quality data distributed by NASA-FIRMS (2011).

The possible study period is bound by the launch of the second MODIS sensor satellite (Aqua) in July of 2002. Prior to this launch, the first MODIS sensor satellite (Terra) would only pass over South Africa twice a day. Aqua's staggered orbit relative to Terra, doubles the number of daily satellite passes over the region. Furthermore, the timing of Aqua's overpass coincides with the time of the day (afternoon) when most fires occur in the Fynbos Biome.

The collection 5 active-fires product has the following parameters for each fire detection: Location, satellite trajectory information, detection date and time, satellite ID (A=Aqua and T=Terra), Confidence factor (%), the brightness

temperature (K) and the Fire Radiative Power (MW). Table 3-1 provides an example of the detection parameters. Detailed descriptions of each parameter can be found at NASA-FIRMS (2011).

Table 3-1: Example of parameters provided for a fire detection by the active-fires product.

Active-fires Parameter	**Example Value**
Latitude	-34.034 °S
Longitude	19.496 °E
Brightness	437.5 K
Scan	1.3
Track	1.1
ACQ_Date	04/01/18
ACQ_Time	12h53
Satellite	A
Confidence	100 %
Version	5.1
Bright_T31	318.7 K
FRP	833.7 MW

The MCD14ML dataset obtained was modified using GIS software as follows: Firstly, only fire detection data pertaining to fires that occurred within the study area of the Fynbos Biome, as defined by Mucina and Rutherford (2006) (Figure 3-1), were retained. The digital GIS shapefile used for the Fynbos Biome is obtainable from SANBI (2006). Secondly, fires that were detected within the urban environment were excluded from the dataset because anthropogenic ignition sources in urban areas greatly outweigh the importance of fire favourable weather. Lastly, only fire detections that had a 100% confidence were considered for this study. Figure 3-2 shows the confidence distribution of the fire detections prior to this third and final step being performed. The resulting active-fires dataset after all modifications is represented in Figure 3-3.

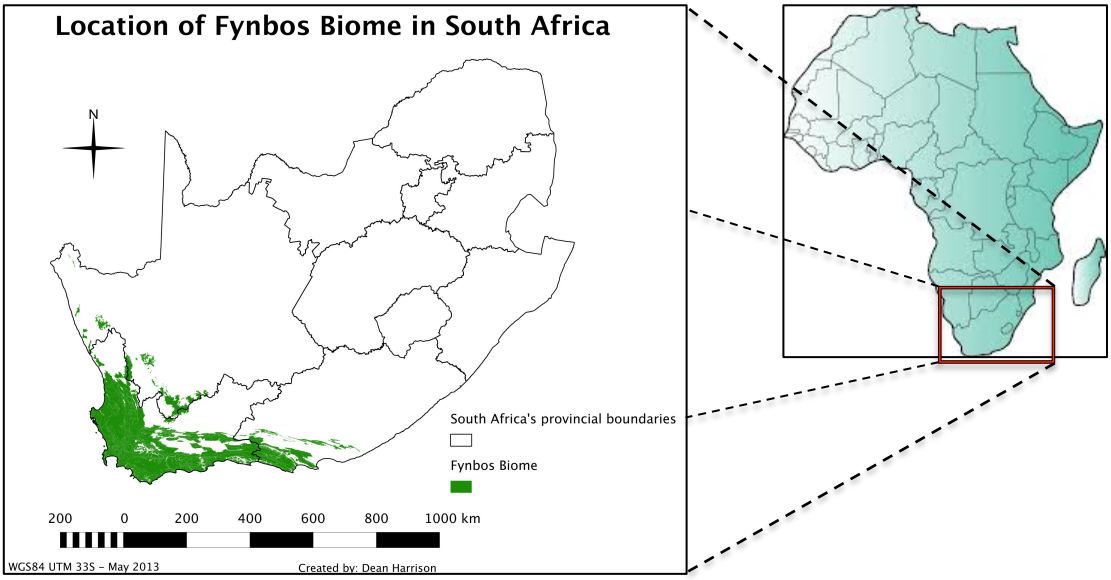

Figure 3-1: Study Area – Spatial extent of the Fynbos Biome.

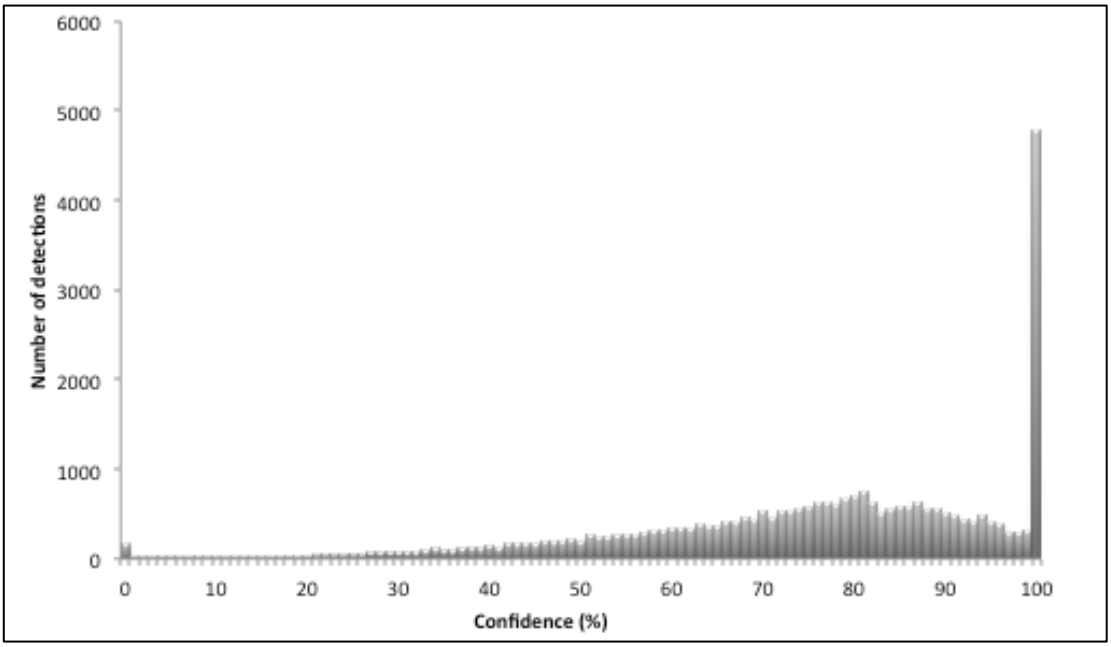

Figure 3-2: Histogram of fire detection confidence for the study period and study area.

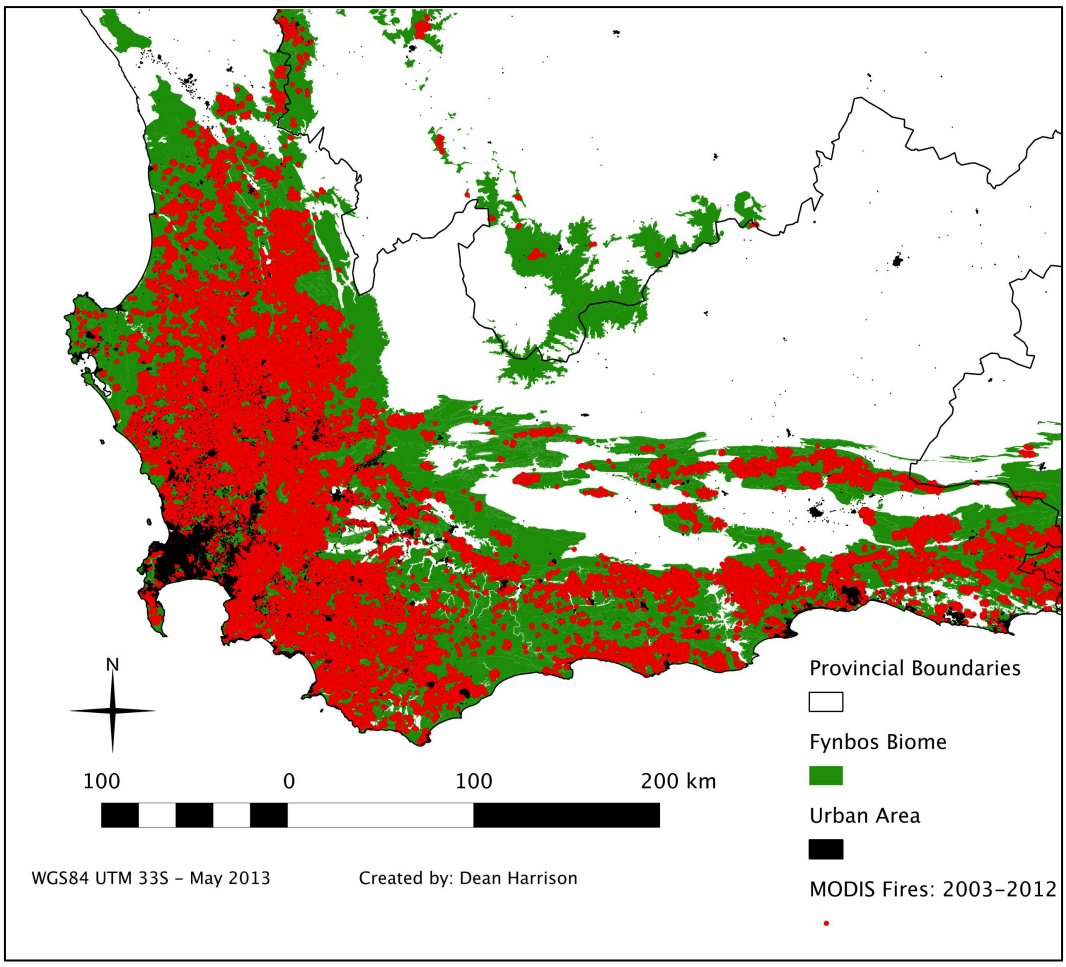

Figure 3-3: Modified MODIS active-fires (shown in red) that occurred within the Fynbos Biome from 2003 – 2012.

There are two important limitations to the fire data used in this study: Firstly, the use of the MODIS active-fires product only allowed for a maximum study period of 10 years due to the availability of these data. While a study period of this length does provide reasonable insight into the seasonality of fires, the study period is not sufficient to investigate the longer-term temporal climate variability and its relationship to the occurrence of wildfires. Secondly, since the MODIS active-fires product cannot discern between wildfires and prescribed burns, these planned fires were not excluded from the fire dataset. Prescribed burns are conducted by fire managers on selected days where the fire danger is not too high, in order to minimise the chances of a fire getting out of control. However, the fire danger must also not be too low, since there are minimum fire intensity requirements in order for the fire to optimally perform its ecological functions. Therefore, the inability to remove prescribed

burns from the dataset will weaken the associations between atmospheric features and wildfires identified in this study. The data for prescribed burns do exist, making it possible to exclude these fires in future studies. However, all efforts by the author to obtain access to these data from the respective authorities failed.

3.1.2 Reanalysis data and calculation of the FDI

Atmospheric data for the study period were obtained from two NCEP CFSR Selected Hourly Time-Series Products acquired from the CISL Research Data Archive (2013). The CFSR version one dataset (ds093.1) spans the period from January 1979 to December 2010. The Climate Forecast System Version 2 (CFSv2) (ds094.1) spans from January 2011 to the present and is archived as an extension to CFSR with no changes to the model dynamics and parameterisation schemes. At the time of data collection, CFSv2 data was only available until the end of 2012. Therefore using the CFSR and CFSv2 datasets, a homogenous and complete dataset can be obtained for the study period January 2003 to December 2012.

Three sets of CFSR variables, at a 0.5°x0.5° horizontal spatial resolution, were obtained for this study from the CISL Research Data Archive (2013): surface atmospheric variables, upper level atmospheric variables at the 850mb pressure level and upper level atmospheric variables at the 500mb pressure level. The relevant metadata of the CFSR variables used in this study are shown in Table 3-2 below. The maximum temperature variable was only available at a higher resolution and therefore this variable had to be re-gridded post-collection to 0.5°x0.5°. Using the u-component and v-component of wind, the wind speed and wind direction was calculated for each of the three levels.

Table 3-2: Metadata for CFSR variables.

Variable	Unit	Variable Type	Level	Horizontal Resolution
Maximum Temperature	K	Surface	2m above ground	0.313°x0.312° (ds093.1) and 0.205°x0.204° (ds094.1)
Relative Humidity	%	Surface	2m above ground	0.5°x0.5°
u-component of wind	$m.s^{-1}$	Surface	10m above ground	0.5°x0.5°
v-component of wind	$m.s^{-1}$	Surface	10m above ground	0.5°x0.5°
Geopotential Height	m	Upper Level	850mb pressure level	0.5°x0.5°
u-component of wind	$m.s^{-1}$	Upper Level	850mb pressure level	0.5°x0.5°
v-component of wind	$m.s^{-1}$	Upper Level	850mb pressure level	0.5°x0.5°
Geopotential Height	m	Upper Level	500mb pressure level	0.5°x0.5°
u-component of wind	$m.s^{-1}$	Upper Level	500mb pressure level	0.5°x0.5°
v-component of wind	$m.s^{-1}$	Upper Level	500mb pressure level	0.5°x0.5°

All the data for the variables listed were then converted into daily data. This was calculated as the average of the variable values within a particular day for the upper level atmospheric variables. However, for the surface level variables the daily value was calculated as a minimum or maximum value for that particular day. The resulting daily surface variables included maximum temperature, minimum relative humidity and maximum wind speed.

The daily Lowveld Fire Danger Index (FDI) was then calculated at a 0.5°x0.5° resolution using the surface reanalysis variables according to the following equation:

$$FDI = (32.8937 + 1.07188 \times T_{max} - 0.394077 \times RH_{min}) + (1.1782 + 0.7212 \times WS_{max})$$

where:

- FDI = Lowveld Fire Danger Index
- T_{max} = Maximum Temperature (°C)
- RH_{min} = Minimum Relative Humidity (%)
- WS_{max} = Maximum Wind Speed (km/h)

The FDI anomaly for each day was then calculated where the deviation was determined from the monthly mean of the FDI, with the study period being the base period over which the mean was calculated.

It should be noted that the calculation of the Lowveld FDI performed in this study differs slightly from the new official calculation, which was instated by the Department of Agriculture, Forestry and Fisheries during this study.

3.2 Methods

3.2.1 Characterisation of fire occurrence and FDI over the Fynbos Biome

1) A box-and-whisker plot was used to show the seasonality of fire occurrence in the Fynbos Biome, based on the total number of fire days per month for each of the years in the study period. For the purposes of this minor-dissertation, a fire day is defined as a day on which one or more fire detections occurred. A cross-correlation analysis was performed between the number of fire days per month and the monthly FDI over the Western Cape, using the software by Wessa (2012). The interannual variability of fire occurrence was then assessed by looking at the trend in the anomaly of the annual number of fire days (the study period was used as the base for

calculating the anomaly). The interannual variability of fire occurrence was then compared to the interannual variability in the annual mean FDI anomaly over the Western Cape as well as the Oceanic Niño Index (ONI) – a commonly used index for determining the state of the El Niño Southern Oscillation (ENSO). The monthly ONI data was obtained from NOAA (2015).

2) The spatial variability of fires that occurred during the study period was determined with the aid of GIS software. The Fynbos Biome shapefile was overlain by a grid with 0.2°x0.2° cells and the number of fire detections per cell were counted. This was then compared to the spatial variability in the average FDI during all days in the study period.

3) Histograms were created to assess the distributions of the FDI and its three constituent variables. Threshold values for fire occurrence within the Fynbos Biome could subsequently be determined.

4) The relationship between fire intensity and the Fire Danger Index was assessed: i) graphically by using a scatterplot and ii) by calculating the correlation factor between the two variables for all fire events. The same methods were then replicated to assess the relationship between fire intensity and each of the three FDI constituent variables respectively. Fire Radiative Power, obtained from the MODIS active-fires dataset, was used as the measure of fire intensity.

3.2.2 Classification of FDI anomaly over the Fynbos Biome

The Self Organising Maps (SOMs) software package SOM_PAK (Kohonen *et al.*, 1995) was used to perform the SOMs analysis technique. The FDI anomaly on days when fires occurred was classified into 16 distinct nodes (4x4). On fire days with multiple fire detections, the FDI anomaly on the given day was input into the SOMs analysis technique for each fire detection to give more weight to days with larger or multiple fires. Table 3-3 shows the user-specified parameters chosen for this SOMs clustering process. The spatial

domain over which the technique was performed was between 28°S-36°S and 17°E-27°E which incorporates the domain of the Fynbos Biome.

Table 3-3: User-specified parameters chosen for SOM_PAK.

Initialising Data	
Topology	Rectangular
Neighbouring Function	Bubble
x-dimensions	4
y-dimensions	4
Training Phase	
Iterations	50000
Alpha	0.1
Radius	3”
Second Phase	
Iterations	645000
Alpha	0.01
Radius	1”

The fire days clustered in each node respectively were then analysed to determine the seasonality and interannual variability of each node.

3.2.3 Identification of atmospheric features that produce fire-conducive conditions

All further analyses in this study were based on the 16 nodes determined by the SOMs technique, but categorised into their four seasonal components. Different composites were created by averaging the two-dimensional matrices – for a number of variables – on all the fire days pertaining to a particular node. This was replicated for all 16 nodes in each season. The DJF composites (dominant fire season) and the relationships between them are identified and described. The composite results pertaining to the other three seasons can be found in the appendices. Composites were obtained for the following variables:

- Maximum surface temperature anomalies.
- Minimum surface relative humidity anomalies.
- Maximum surface wind speed anomalies.
- Actual Fire Danger Index.
- Fire Danger Index anomalies.
- Actual geopotential height and associated wind vectors at the 850mb level.
- Anomalies of geopotential height and associated wind vectors at the 850mb level.
- Actual geopotential height and associated wind vectors at the 500mb level.
- Anomalies of geopotential height and associated wind vectors at the 500mb level.

Furthermore, two-dimensional spatial correlation was used to assess how important the FDI constituent variables are in producing the resultant spatial pattern of the FDI.

3.2.4 Assessing the ability of atmospheric circulation features to be used as a fire forecasting tool

The composite of the actual Fire Danger Index on fire days, for each node and for each season, was compared to the Fire Danger Index for every day in the study period in order to determine how many days that composite occurred. The comparison was made using two-dimensional spatial correlation of the two-dimensional matrices. Any comparison with a correlation factor greater than or equal to the user-defined value of 0.7 was deemed to be a matching day. There is no literature to support what the user-defined value should be. The spatial domain over which the two-dimensional spatial correlation was performed was between 28°S-36°S and 17°E-27°E.

This procedure was replicated for the composite of the geopotential height anomaly at the 850mb level and again for the composite of the geopotential height anomaly at the 500mb level. However, the spatial domain over which the two-dimensional spatial correlation was performed for these two variables

was between 10°S-45°S and 5°E-50°E. This larger domain is required to take into account the synoptic-scale atmospheric features.

Chapter 4. Results and Discussion

4.1 Climatology of the FDI and atmospheric variables over South Africa

The seasonal means of the Lowveld Fire Danger Index (FDI) and its constituent variables are shown in Figure 4-1. The seasonal means of the geopotential height and associated wind vectors that control the climate over Southern Africa are shown in Figure 4-2.

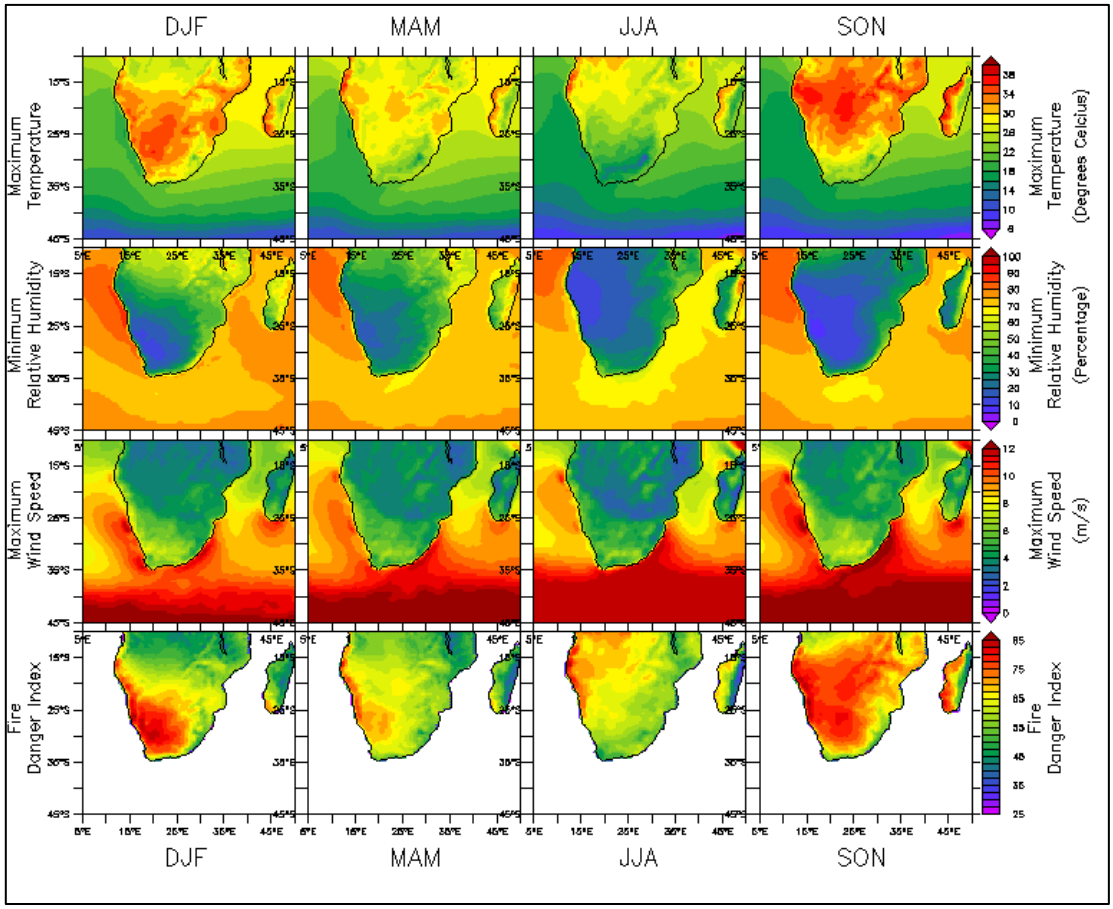

Figure 4-1: Seasonal means of the Lowveld FDI and its constituent variables over Southern Africa for the period 2003-2012.

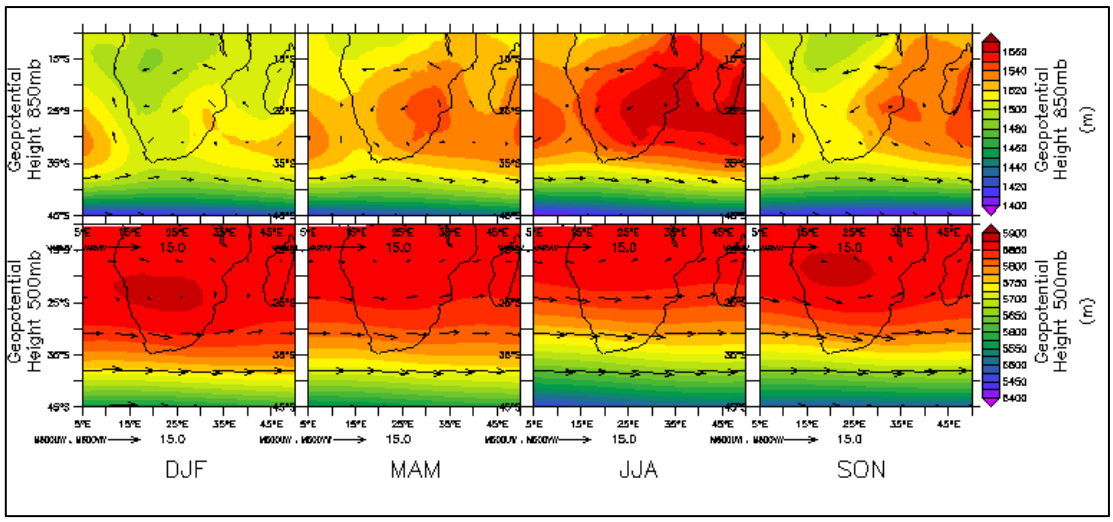

Figure 4-2: Seasonal means of the Geopotential Height and Wind Velocity at the 850mb and 500mb levels over Southern Africa for the period 2003-2012. Geopotential Height (m) shown by colour scale and Wind Velocity (m/s) shown by arrow vectors.

The FDI is highest in the Fynbos Biome during the December/January/February (DJF) season, which is consistent with the associated summer fire regime described in the literature (Van Wilgen *et al.* 2010). This summer fire regime in the Fynbos Biome is characterised by high maximum temperatures and low relative humidity, which lead to a high burning index. The strong prevailing southeast wind in the summer period, caused by the ridging Atlantic anti-cyclone and the low-pressure cell in Southern Africa's interior, further increases the FDI along the west coast of the Fynbos Biome.

It is interesting to note that in the September/October/November (SON) season, the greater area of Southern Africa has a cumulatively higher FDI than the DJF season. However, the FDI over the Fynbos Biome is on average still less than that of the DJF season. This pattern in the FDI over the greater area of Southern Africa can be attributed to two factors. Firstly, the southward movement of the Inter Tropical Convergence Zone (ITCZ), which leads to increased temperatures in the region. The second explanation that accounts for the higher FDI is the low relative humidity experienced prior to the start of the seasonal rains in the summer rainfall region.

The FDI is lowest in the June/July/August (JJA) season when winter rainfall is at its peak in the study area. The northward movement of the ITCZ in the austral summer exposes the Fynbos Biome to mid-latitude cyclones, bringing cooler temperatures and frontal rain. Although not incorporated into the FDI, the winter rainfall leads to increased soil and vegetation moisture that also reduces burning potential.

4.2 Characteristics of fire occurrence and FDI over the Fynbos Biome

4.2.1 Seasonality and Interannual Variability

An analysis of the satellite-derived fire detection data used in this study shows the expected summer fire regime in the Fynbos Biome, as can be seen in Figure 4-3. In the summer months, fires occur on more than a third of the days in each month. However, while the Fynbos Biome does have a summer fire regime, it should be noted that fire days do still occur in the winter period, albeit at a reduced frequency. This is consistent with the fire seasonality found by Van Wilgen *et al.* (2010), who further attribute the majority of winter fires to the eastern coastal zone of the Fynbos Biome. For each particular month during the ten-year study period, there appears to be a fair amount of annual variability. For the summer months, the number of fire days per month can vary by 15 days or more. There is also annual variability between the winter months, although it is less pronounced than that found in summer months. It can also be observed that during some years, extreme numbers of fire days occur. For example, in the year 2008 there were 14 fire days for the month of September, compared to the September mean of 4 fire days. Similarly there were extreme numbers of fire days for April 2009, May 2004 and October 2005. These extreme events all occurred within different years of the study period, which does suggest that the factors leading to the extreme events had short durations with no apparent lag.

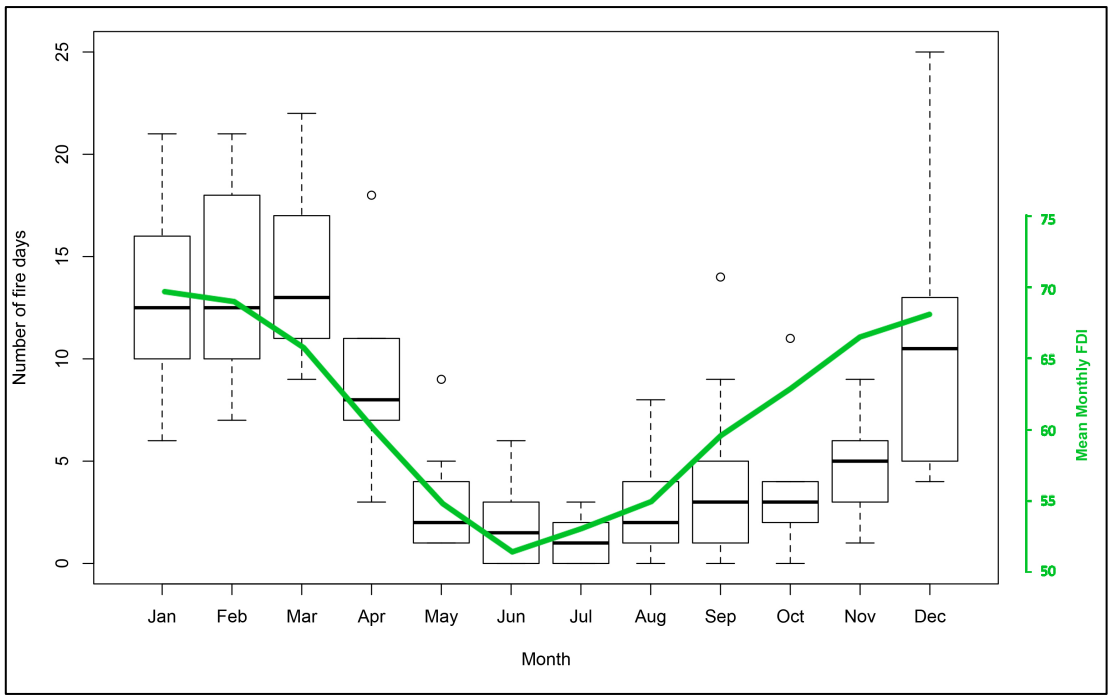

Figure 4-3: Box-and-Whisker plots showing observed monthly distribution of the number of fire days in the Fynbos Biome from 2003-2012. The four open circles in the plot represent extreme events. The green line represents the mean monthly FDI for each of the respective calendar months.

The seasonality of the mean monthly FDI, also shown in Figure 4-3, is higher in summer and lower in winter. January has the highest average FDI of 69.87 while June has the lowest average FDI of 50.76. When compared to the seasonality of fire occurrence, the same annual cycle is evident, suggesting that the seasonal climate plays an important role in influencing the occurrence of wildfires. However, it is interesting to note that there is a slight lag in the annual cycle between the mean number of fire days per month and the monthly FDI, with the former having its peak in March and trough in July. The lag can probably be attributed to the cumulative influence of preceding atmospheric conditions on the state of the fuel, leading up to the occurrence of a fire. This might imply that it is not sufficient to consider the relationship between the fire occurrence and the FDI only on the days that fires occurred.

In order to confirm the observed lag between the number of fire days per month and the monthly FDI, a cross correlation analysis was performed. As evidenced by Figure 4-4, the highest correlation of 0.7331 occurred when the number of fire days lagged the monthly FDI by one month. This result

provides further evidence that weather-related fire studies should not rely on the FDI at the time of fire occurrence exclusively.

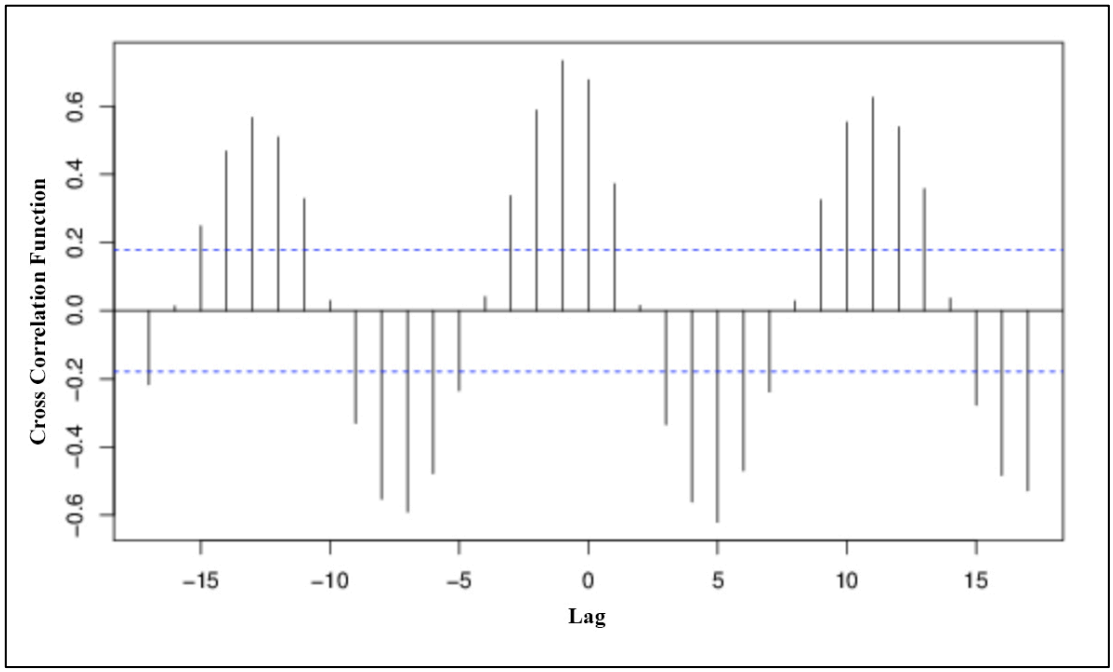

Figure 4-4: Cross Correlation between the number of fire days per month (lagged) and the mean monthly FDI over the Western Cape. Blue stippled lines represent the confidence limit.

There is also some degree of interannual variability in the cumulative number of fire days. For the study period, there was a mean of 80.4 ± 11.5 fire days per year. The anomalies of the number of fire days per year are shown in Figure 4-5 and the results suggest an overall negative trend in the number of fire days per year. However, this result could portray a short negative fluctuation in a dominant longer-term temporal cycle (Kalabokidis *et al.*, 2015). Although beyond the study period, the 2014-2015 fire season returned to peak intensity, equivalent to the year 2000.

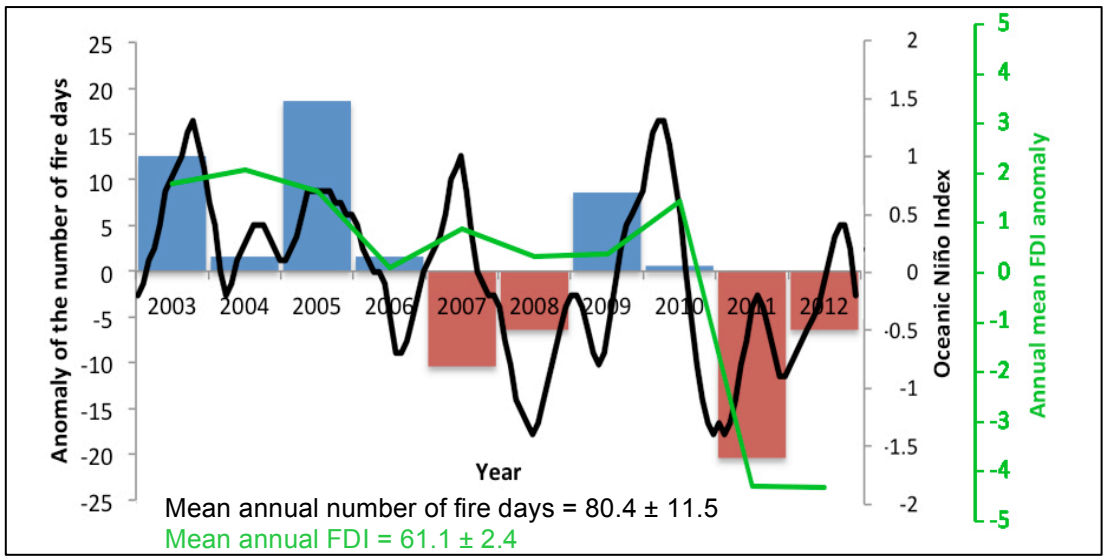

Figure 4-5: Trend in the annual number of fire days in the Fynbos Biome with positive anomalies shown in blue and negative anomalies shown in red (base period 2003-2012). The green line shows the trend in the annual mean FDI anomaly over the Western Cape (base period 2003-2012). The black line represents the Oceanic Niño Index over the same period.

Despite the relatively low interannual variability in the annual mean FDI over the Western Cape (mean of 61.1 ± 2.4), there is also a decreasing trend evident during the study period (Figure 4-5). Although the correlation between the annual FDI and the annual number of fire days seems moderate at best, it does provide additional evidence that the climate has some role in moderating fire occurrence. To test this assertion further, the trend in the annual number of fire days is compared to the Oceanic Niño Index.

The Oceanic Niño Index has become the standard ENSO index used by NOAA for determining El Niño (positive ONI) and La Niña (negative ONI) events (NOAA, 2015). The state of ENSO has been shown to affect the amount of rainfall experienced by the Fynbos Biome by impacting the intensity, track and frequency of mid-latitude frontal systems (Allan, 2000; Reason & Rouault, 2002). A time series of the monthly ONI, during the study period, is superimposed in Figure 4-5 to determine whether a relationship exists between ENSO and the number of fire days per year. In most cases a positive anomaly in the number of fire days per year corresponds to a positive ONI (El Niño event), while a negative anomaly corresponds to a negative ONI

(La Niña event). The reverse seems true only in the years 2006-2007. Therefore there is some evidence that a relationship does exist between the state of ENSO and the number of fire events per year. This is in agreement with the relationship identified by Cowling *et al*. (2004) but due to the short study period, a robust measure of the correlation between the number of fire days and the ONI cannot be determined. However, if a direct relationship was found in future studies, it would provide some further evidence that climate variability can be a limit to the occurrence of wildfires in support of the claim by Archibald *et al.* (2010) (although no distinction is made in this study between conserved and non-conserved land).

4.2.2 Spatial Variability

The spatial variability of fires that occurred in the Fynbos Biome during the ten-year study period is shown in Figure 4-6. The indicated values are the cumulative number of fire detections that occurred within each 0.2°x0.2° cell. There are three factors that could potentially contribute to the cumulative count: 1) There may be more than one fire detection event for an individual fire that spreads over a large area or burns over multiple days, 2) There can be fire detections due to completely independent fires at different locations within each cell and 3) There can be fire detections that relate to repetitive fires that occurred over the same land area, but multiple years apart from one another. Given the multiple factors affecting the cumulative fire count, caution should be taken when interpreting the spatial variability of fires based on the MODIS active-fires detections.

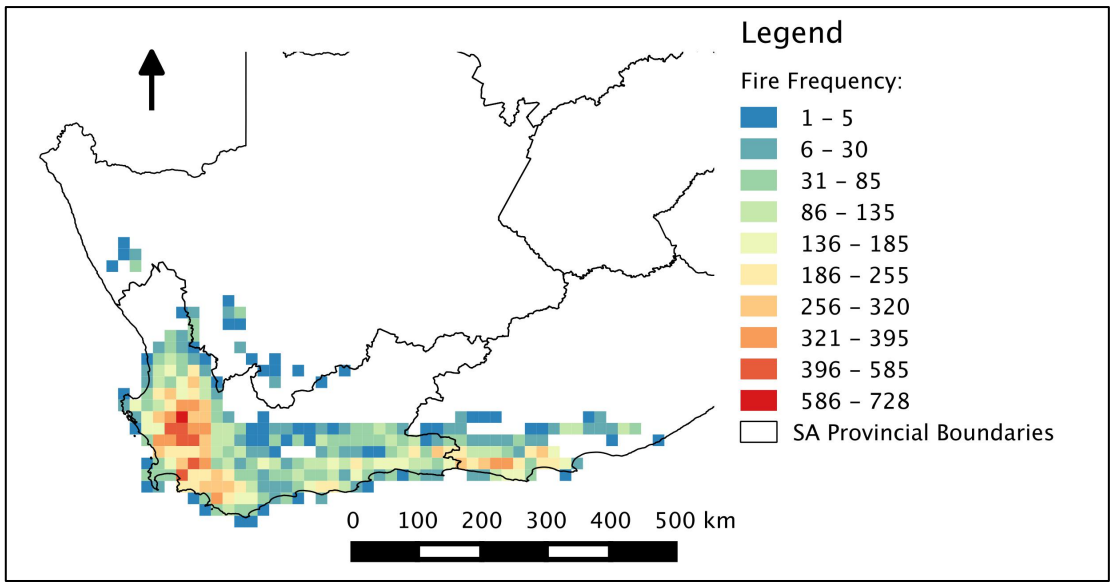

Figure 4-6: Count of fire detections in the Fynbos Biome during the study period showing spatial variability of fire occurrence.

In Figure 4-6 it can be observed that the fire detection hot spots tend to occur furthest away from the Fynbos Biome boundaries, in the centre of the domain. The coastal areas tend to have a lower cumulative fire count, which can probably be attributed to the lower fire danger created by the influence of the ocean. As observed in Figure 4-1 and Figure 4-7, the ocean reduces the fire danger along the coastal region of South Africa by limiting the minimum relative humidity and maximum temperature respectively. However, the FDI continues to increase beyond the domain of the Fynbos Biome, moving towards the South African interior (Figure 4-7). This suggests that along the non-coastal boundary of the Fynbos Biome, the fuel and ignition wildfire ingredients have stronger control over the occurrence of wildfires. This could be due to biome boundary vegetation gradients – mixtures and mosaics of fire-prone and fire-retardant vegetation types – as well as reduced population densities, leading to less anthropogenic ignitions.

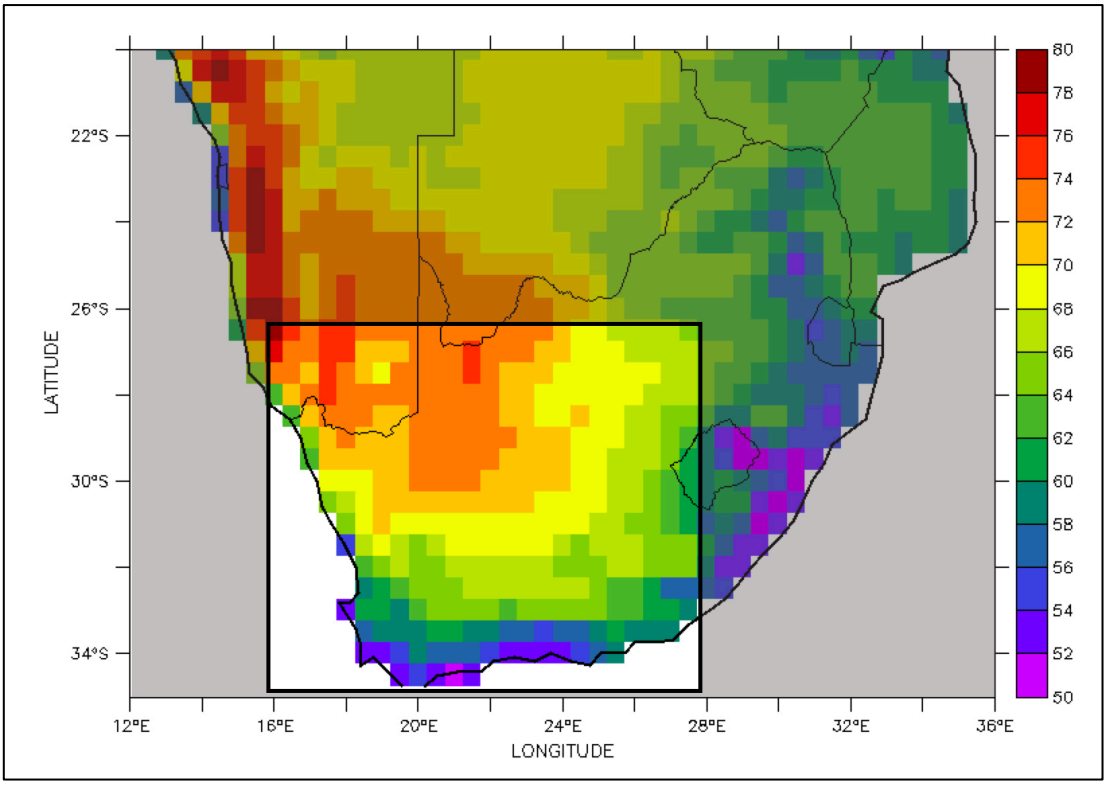

Figure 4-7: Mean Fire Danger Index over all days in the study period. The highlighted window matches the map area displayed in Figure 4-6.

While the Figure 4-6 would appear to show more fires in the western part of the region, when taking into account the width of the biome, there is no noteworthy difference in the cumulative fire counts. However, the seasonality of fires in the two regions may differ as shown by Southey (2009) and Van Wilgen *et al.* (2010).

4.2.3 Fire occurrence thresholds

The histograms in Figure 4-8 show the distributions of the FDI and its constituent variables for all fire detection events. The resulting distributions should be interpreted with caution because the categorical ranges of the FDI and its constituent variables in the respective histograms do not occur with equal frequencies in space and time. Therefore the shape of the distribution has little relevance. However, these distributions do suggest threshold values for fires to occur. For example, there were no fire events that occurred when the FDI was below 32 and less than 1.4% of the total number of fire events occurred when the FDI was below 50. The threshold FDI value of 32 or 50

respectively provides a theoretical limit for the possibility of fire occurrence, given a user-specified degree of error, but does not provide any measure of the probability of an actual fire event.

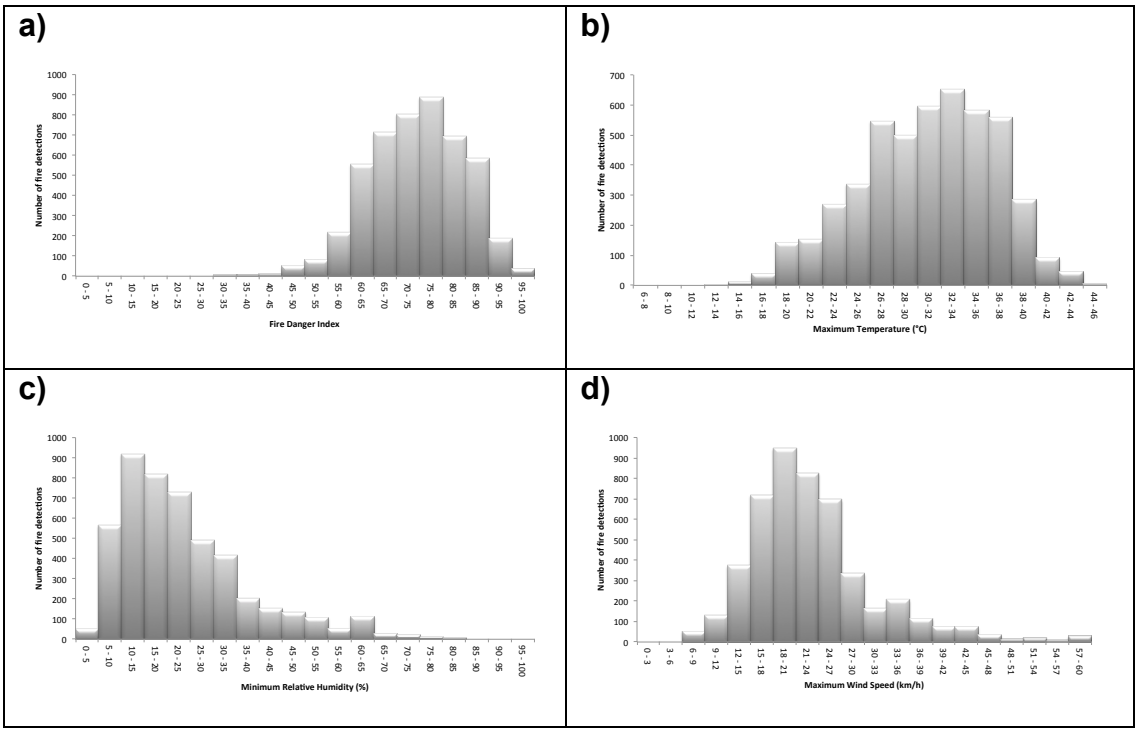

Figure 4-8: Histograms of the a) Fire Danger Index, b) Maximum surface temperature, c) Minimum surface relative humidity, and d) Maximum surface wind speed at the locations of fire detection events.

Using a user-specified error of 5%, the threshold values identified for fire occurrence are: a FDI value of 57, a maximum surface temperature of 21°C, a minimum relative humidity of 55%, and a maximum surface wind speed of 12.7km/h. Note that the usability of these threshold values in practice is somewhat restricted due to the relatively low temporal resolution of the atmospheric reanalysis data used in this study. Micro-scale conditions can deviate substantially from the 0.5°x0.5° mean.

4.2.4 Relationship between fire intensity and FDI

The scatterplot of fire intensity and Fire Danger Index, as well as the scatterplots of fire intensity and each its three constituent variables, are shown in Figure 4-9 for all the fire detections. There appears to be no

evidence of a relationship between the FDI and fire intensity, confirmed by a correlation factor of 0.0044 between the two variables. Similarly, there is no identifiable relationship between 1) fire intensity and maximum surface temperature, 2) between fire intensity and minimum surface relative humidity, and 3) between fire intensity and maximum surface wind speed. The corresponding correlations between fire intensity and each of the three FDI constituent variables are 1) -0.0204, 2) 0.0196 and 3) 0.0473 respectively.

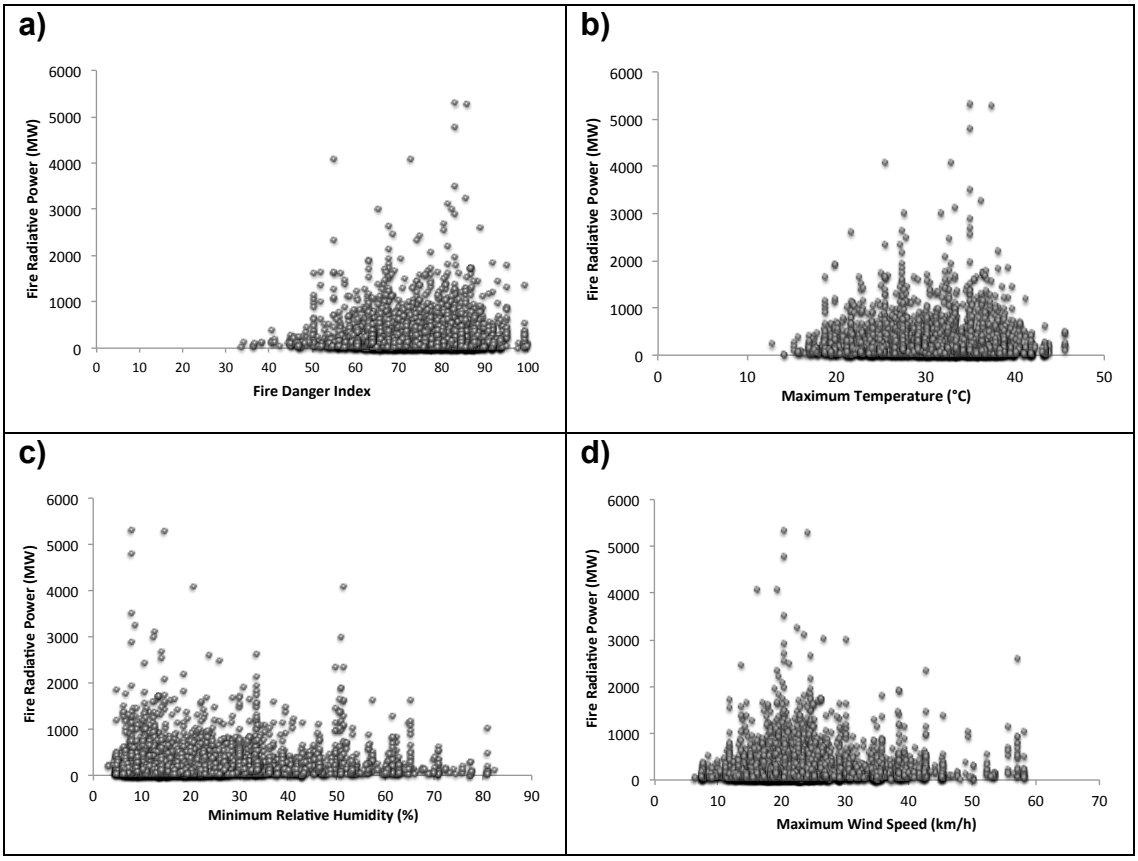

Figure 4-9: Scatterplots showing the relationship between Fire Intensity and the a) Fire Danger Index, b) Maximum surface temperature, c) Minimum surface relative humidity, and d) Maximum surface wind speed for all fire detection events.

These results contradict the current understanding of the relationship between the FDI and fire intensity found in the literature. It is widely accepted that a higher FDI, manifesting itself as higher temperatures, lower relative humidity and higher wind speeds, will increase the fire behaviour and fire intensity (Everson *et al.*, 1988; Rothermal, 1972; Willis *et al.,* 2001). This positive correlation between the FDI and fire intensity is also accepted in fire

management practice and is easily observed in the field during fire events. A possible reason for these contradictory results could be due to the relatively low spatial resolution of the atmospheric reanalysis data used in this study as well as the exclusion of rainfall in the calculation of the FDI. However, it is more likely that the conditions of the fuel (one of the ingredients for wildfire) have a disproportionately higher effect on fire intensity than the weather ingredient. Therefore, if the fuel conditions remained constant, changes in the weather variables/FDI would affect the fire intensity. Although not an ingredient of wildfire as described in the literature review of this study, topography is an additional factor that can affect fire intensity (Everson *et al.*, 1988; Rothermal, 1972; Teie, 2009). For example, an increase in terrain slope results in increased fire intensity due to pre-heating of vegetation upslope of the fire by the convective and radiant heat of the flames. The topography also affects micro-scale winds that in turn affect the amount of pre-heating of vegetation downwind of the fire (Teie, 2009).

4.3 The classification of the FDI pattern over South Africa

The classification of SOMs into 16 distinct nodes is shown in Figure 4-10. As a consequence of the SOMs technique, the four corner nodes [Node (1), Node (4), Node (13), and Node (16)] display the most extreme variations in the spatial patterns of the FDI anomaly. The remaining nodes show a relatively smooth transition between these four extreme states.

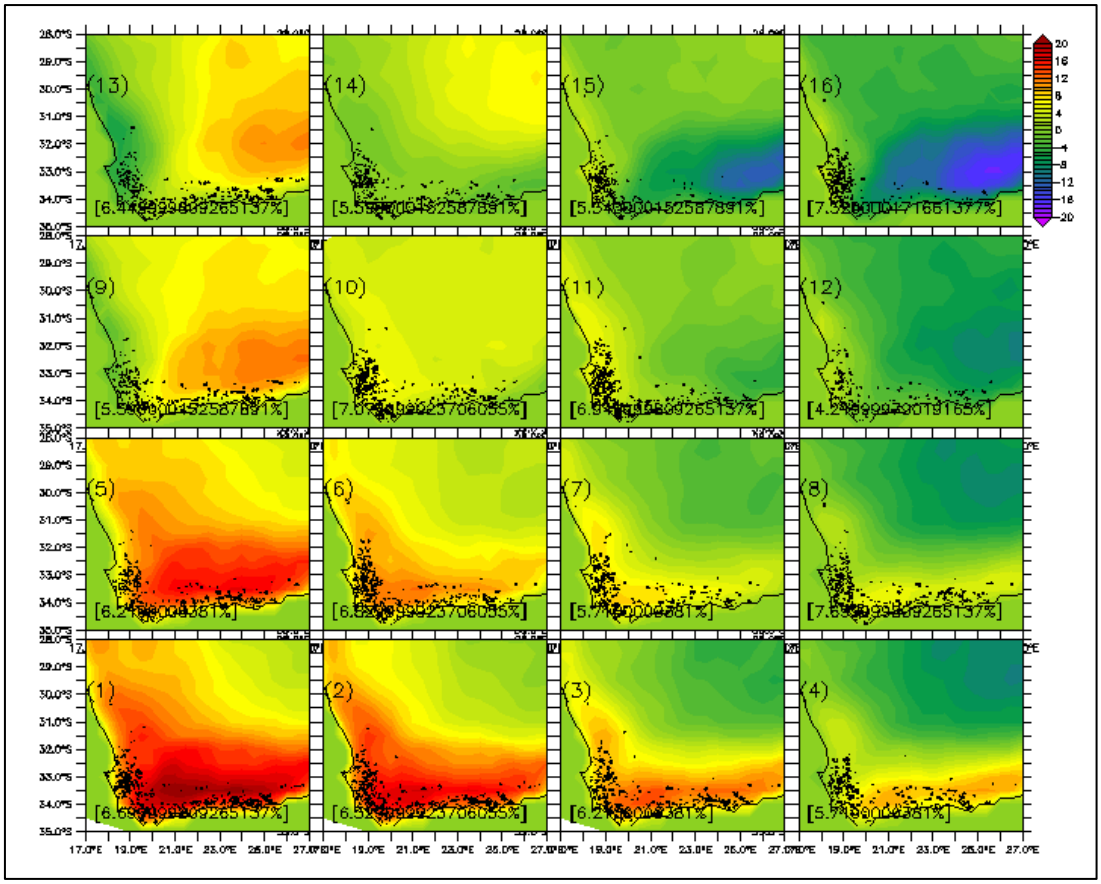

Figure 4-10: Resulting nodes of Self Organising Maps technique displaying spatial variation in FDI anomaly on days when fires occurred. The number in square brackets represents the relative node occurrence frequency, while the number in round brackets represents the node identification number. Black dots are indicative of fire locations that occurred within each node.

Node (1) depicts the extreme case where the FDI anomaly has the largest positive deviations over the entire extent of the Fynbos Biome. The majority of the Western Cape of South Africa has a 15 unit positive deviation in the FDI and this influence extends northwards into the Northern Cape and eastwards into the Eastern Cape. The highest FDI anomaly occurs in a band that extends parallel to the south coast, north of the Cape Fold Mountains. The north-eastern interior of South Africa has a smaller FDI anomaly, but it is still positive.

In Node (4) the area of the highest positive FDI is closely confined to the south coast of the country. Even within this band the highest positive FDI anomaly of 10 units is only half that of Node (1). There is also a very weak

positive anomaly that extends northwards from the Western Cape. From these positive FDI anomaly regions, there is a relatively smooth transition to a moderate negative FDI anomaly in the north-eastern interior.

Unlike Node (1) and Node (4), that show a southwest to northeast negative gradient in the spatial pattern of the FDI anomaly, Node (13) shows a strong west to east positive gradient. This is the only node that has a moderate negative FDI anomaly along the west coast of the country that extends up into the Northern Cape and is also one of only three nodes that show a smaller positive anomaly in the west of the domain, compared to the east of the domain.

Node (16) depicts the final extreme case with a weak positive FDI anomaly, tied closely to the west coast, with a strong negative FDI anomaly extending eastward along the south coast. The FDI in the rest of the country's interior appears to be fairly close to the mean FDI.

The spatial locations of the actual fire events that occurred within each node are relatively uniform across all nodes. This deviates from the expectation that more fires would occur where the positive FDI anomalies are greatest. There are a number of plausible explanations for this unexpected result. It is possible that while weather is important for producing an environment conducive to burning, one of the other ingredients of wildfire may be a stronger regulator for the actual timing and location of fires within the Fynbos Biome. Furthermore, fires that occurred within areas of negative FDI anomalies could also be due to prescribed burn fire detections that could not be excluded from the fire dataset. Planned prescribed burning operations usually take place on days where there is reduced fire risk. Finally, the methods in this study fail to account for the influence of weather on days preceding the actual fire day. Weather on preceding days will have a particularly strong influence on the vegetation fuel state, as hotter and drier days will reduce the fuel moisture and therefore increase the vegetation's propensity to burn.

In Figure 4-10, it can be observed that all nodes occur with a similar relative frequency during the ten-year study period. However, as shown in Figure 4-11, there is a difference in the seasonal frequency of the nodes.

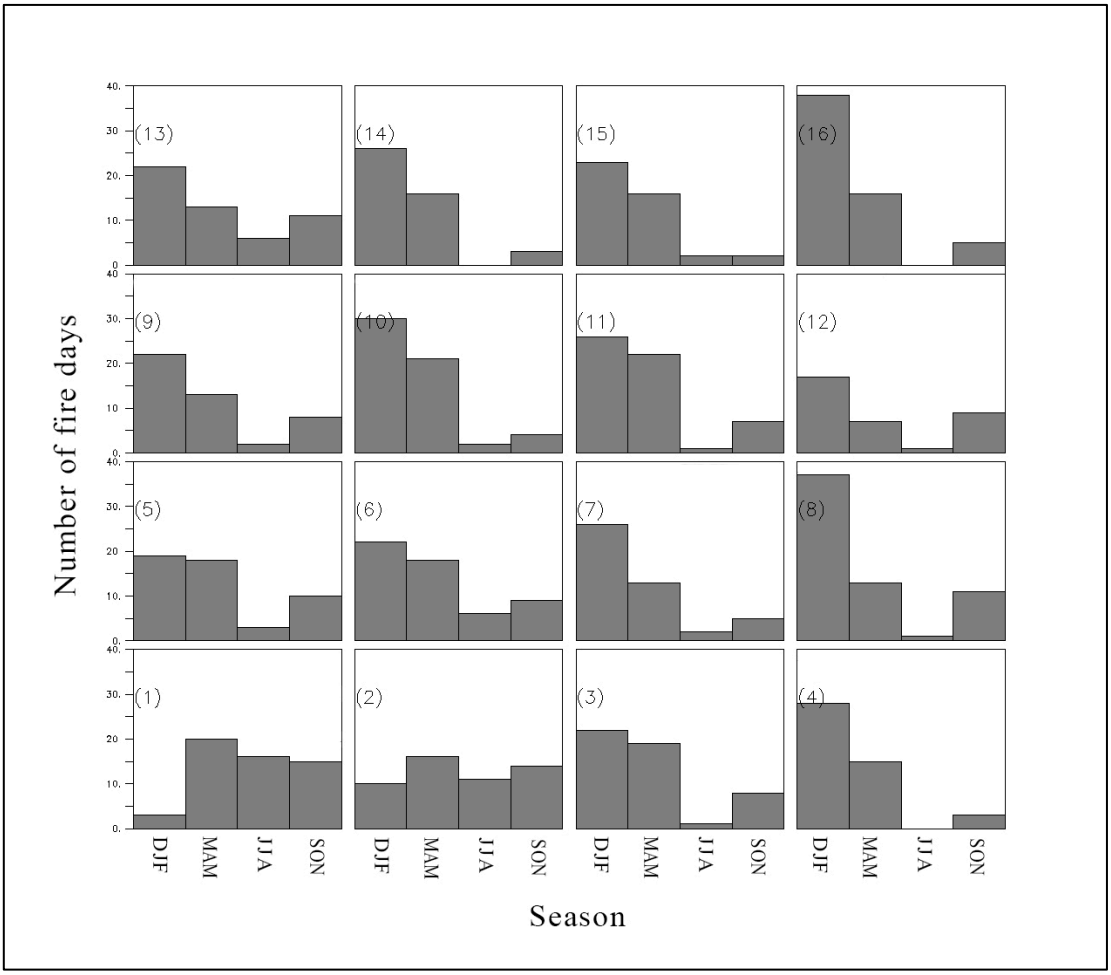

Figure 4-11: Seasonality of the resulting SOMs nodes. The number in round brackets represents the node identification number.

Earlier analysis of the fire data used in this study was typical of a summer fire regime with the majority of fire days occurring in the DJF season. As expected, most nodes occur with the highest frequency in the DJF season. However, not only do Node (1) and Node (2) not have their highest frequency in the DJF season, but the DJF season is also when these two nodes occur least frequently. Similarly, all nodes occur with the least frequency in the JJA season, with the exception of Node (1) and Node (2). Other observations of interest include: Node (4), Node (14) and Node (16) do not occur even once

during the JJA season throughout the study period. Furthermore, Node (2) appears to occur with a consistent frequency throughout the year.

In addition to the seasonality of the different nodes, there is also weak evidence of longer-term trends in the occurrence of each of the nodes as shown in Figure 4-12.

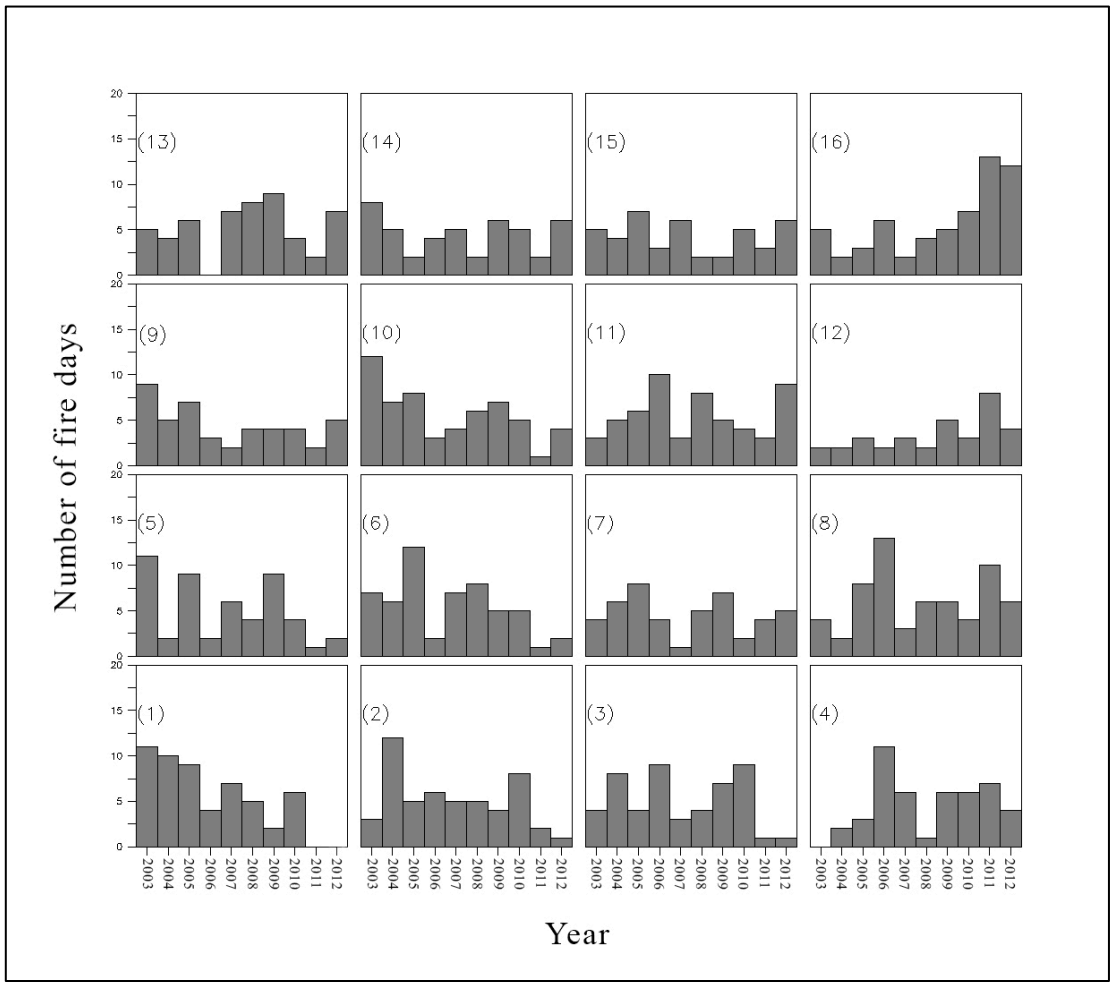

Figure 4-12: Interannual variability in the occurrence of the resulting SOMs nodes. The number in round brackets represents the node identification number.

This trend analysis is limited due to the short length of the study period. Earlier analysis also revealed a negative trend in the annual number of fire days during the study period. This negative trend seems most apparent in Node (1), Node (2) and Node (3) with very few fire days occurring in the last two years of the study period. Node (1) seems to be completely absent from

the final two years of the study period. In most other nodes a visually identifiable trend is either absent or very weak. However, in contrast to the overall negative trend in the number of fire days over the study period, Node (16) appears to have a strong positive trend, while Node (8) and Node (12) seem to have a weaker positive trend.

4.4 Atmospheric features that produce fire-conducive conditions

The majority of the resulting nodes from the SOMs analysis occur with greatest frequency in the DJF season, corresponding with the summer fire regime in the Fynbos Biome. This section looks exclusively at the DJF season, but the results for the MAM, JJA and SON (shown in the appendices section) can be interpreted in the same manner. The atmospheric conditions and processes that increase the propensity for wildfires in the DJF season can be identified by exploring the spatial variation in the FDI constituent variables, as well as the geopotential height and wind vectors at the 850mb and 500mb levels respectively. The focus of this discussion is on the extreme state corner nodes [Node (4), Node (13) and Node (16)]. Node (1) will be discussed as a special case because it occurs very infrequently during the dominant DJF season.

Figure 4-13 is the DJF seasonal component of the SOMs results in Figure 4-10. The pattern of the spatial variation in the maximum surface temperature anomalies on fire day events (Figure 4-14) very closely corresponds to the spatial pattern in the FDI anomalies, evidenced by a mean correlation of 0.9348 ± 0.0503 (Table 4-1). This highlights the relative importance of maximum surface temperature in the calculation of the FDI, in addition to the role it plays in producing a fire-conducive environment.

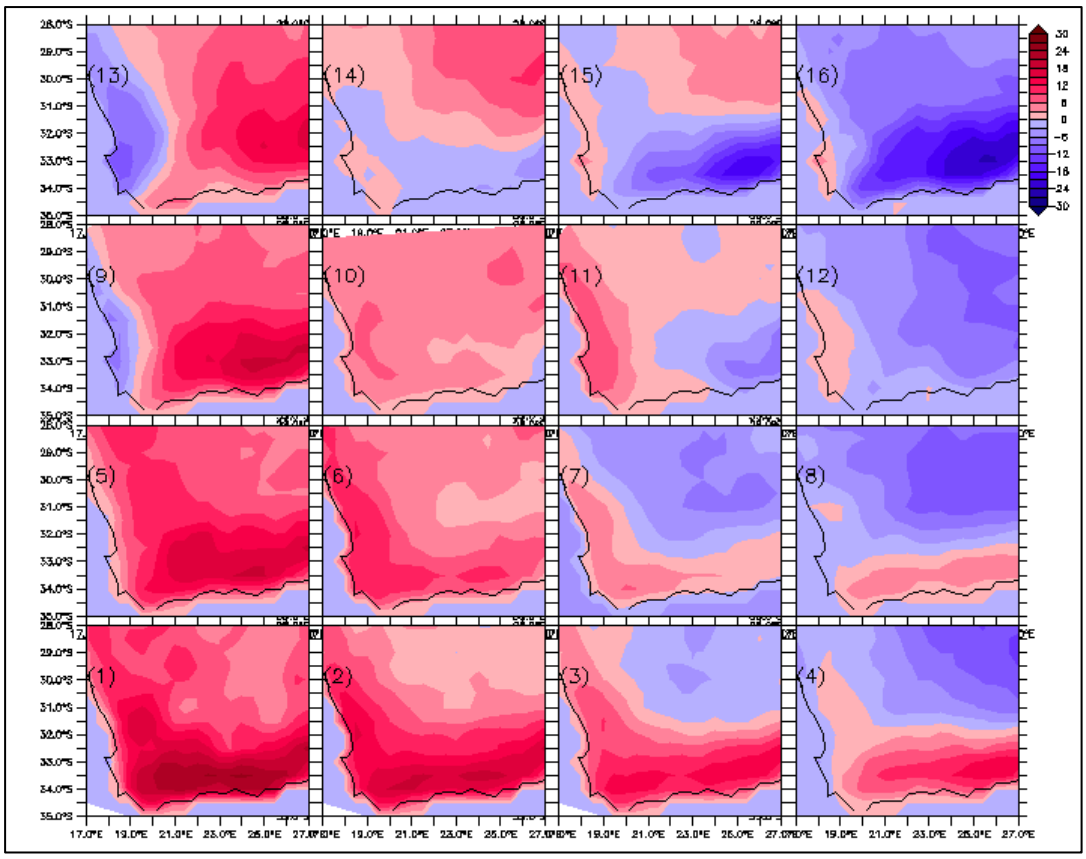

Figure 4-13: DJF season anomalies of the Fire Danger Index on the day of fire for each node. The number in round brackets represents the node identification number.

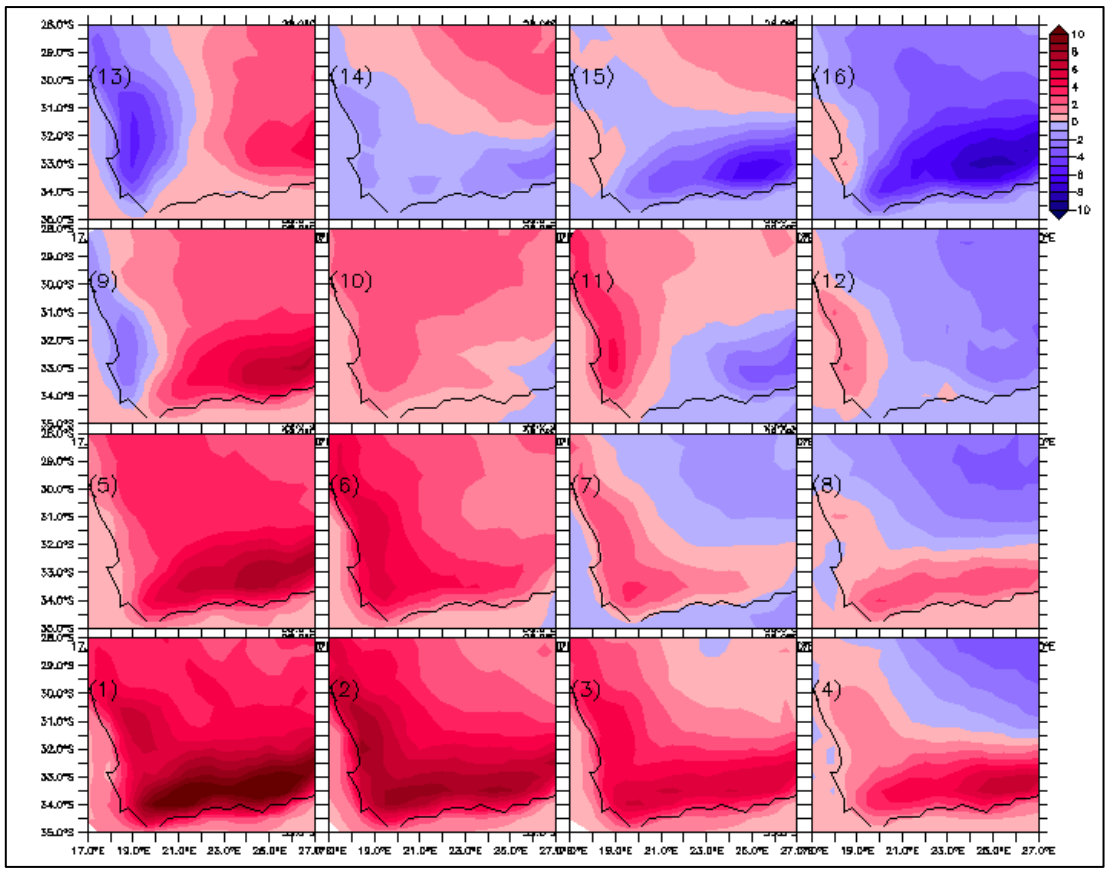

Figure 4-14: DJF season anomalies of maximum surface temperature (°C) on the day of fire for each node. The number in round brackets represents the node identification number.

Table 4-1: Correlations between the DJF FDI anomaly nodes and the respective DJF nodes of each of the FDI constituent variables.

Node Number	Maximum Temperature	Minimum Relative Humidity	Maximum Wind Speed
Node 1	0.9178	-0.7742	0.3628
Node 2	0.9085	-0.9530	0.7249
Node 3	0.9535	-0.9380	0.8531
Node 4	0.9919	-0.9823	0.7421
Node 5	0.9298	-0.8004	0.4539
Node 6	0.8151	-0.7197	0.6200
Node 7	0.9032	-0.9093	0.7335
Node 8	0.9840	-0.9835	0.6894
Node 9	0.9523	-0.9535	0.6393
Node 10	0.8415	-0.7681	0.3895
Node 11	0.9145	-0.9059	0.4536
Node 12	0.9613	-0.9517	0.7679
Node 13	0.9648	-0.9710	0.8862
Node 14	0.9616	-0.9334	0.7985
Node 15	0.9793	-0.9796	0.6897
Node 16	0.9773	-0.9793	0.6830
Average	0.9348 ± 0.0503	-0.9064 ± 0.0885	0.6555 ± 0.1605

Similarly, the pattern of the spatial variation in the minimum surface relative humidity anomalies on fire day events (Figure 4-15) very closely corresponds to both the spatial pattern in the FDI anomalies and maximum surface temperature anomalies, but has deviations in the opposite directions. The mean correlation between the FDI composites and minimum relative humidity composites is -0.9064 ± 0.0885 (Table 4-1). The inverse relationship between surface temperature and relative humidity is a fundamental property of the atmosphere. An increase in temperature of a given air mass – without affecting its water vapour content – will increase the saturation vapour

pressure of that air mass, leading to a reduction in the relative humidity of the air mass (Lawrence, 2005). Therefore it is maximum surface temperature and minimum surface relative humidity that are used to calculate the Burning Index component in the FDI calculation and together have the strongest influence in producing wildfire-conducive conditions.

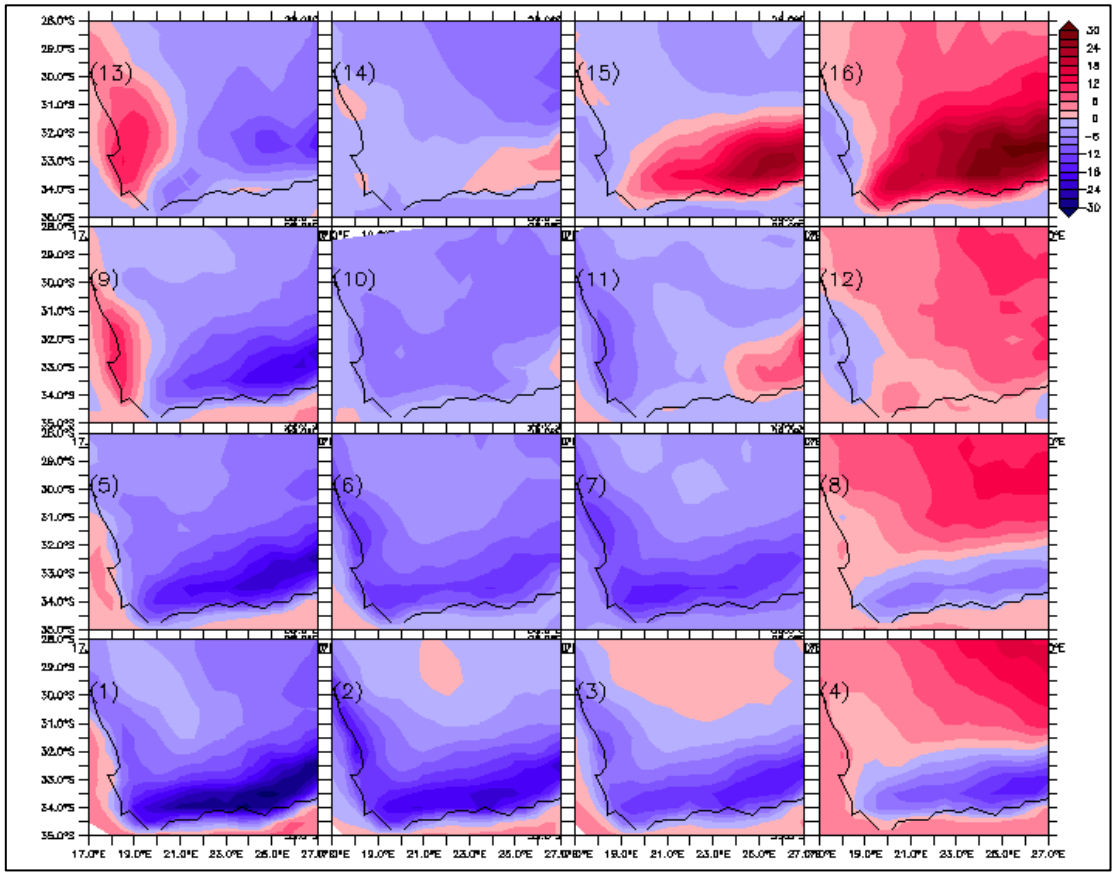

Figure 4-15: DJF season anomalies of minimum surface relative humidity (%) on the day of fire for each node. The number in round brackets represents the node identification number.

The pattern of spatial variation in surface wind speed anomalies on fire day events (Figure 4-16) does show some resemblance to the variation in the FDI anomalies, but this relationship appears much weaker than with maximum temperature and minimum relative humidity. This weaker relationship – mean correlation of 0.6555 ± 0.1605 (Table 4-1) – suggests that wind speed may have a limited role in producing a fire-conducive environment even though it is known to play an important role in fire behaviour (Rothermal, 1972; Teie, 2009). A possible explanation for the weak relationship between the FDI

anomalies and wind speed anomalies in these results is the insufficient spatial resolution of the wind speed data. Micro-scale wind conditions, especially due to localised topography, can deviate substantially in both magnitude and direction from the synoptic scale average. Therefore, in order to capture the real influence of wind speed on the FDI, higher resolution wind data would be required. The insufficient resolution of the wind speed data could also help explain why wildfires are occurring in areas with negative FDI anomalies in these results.

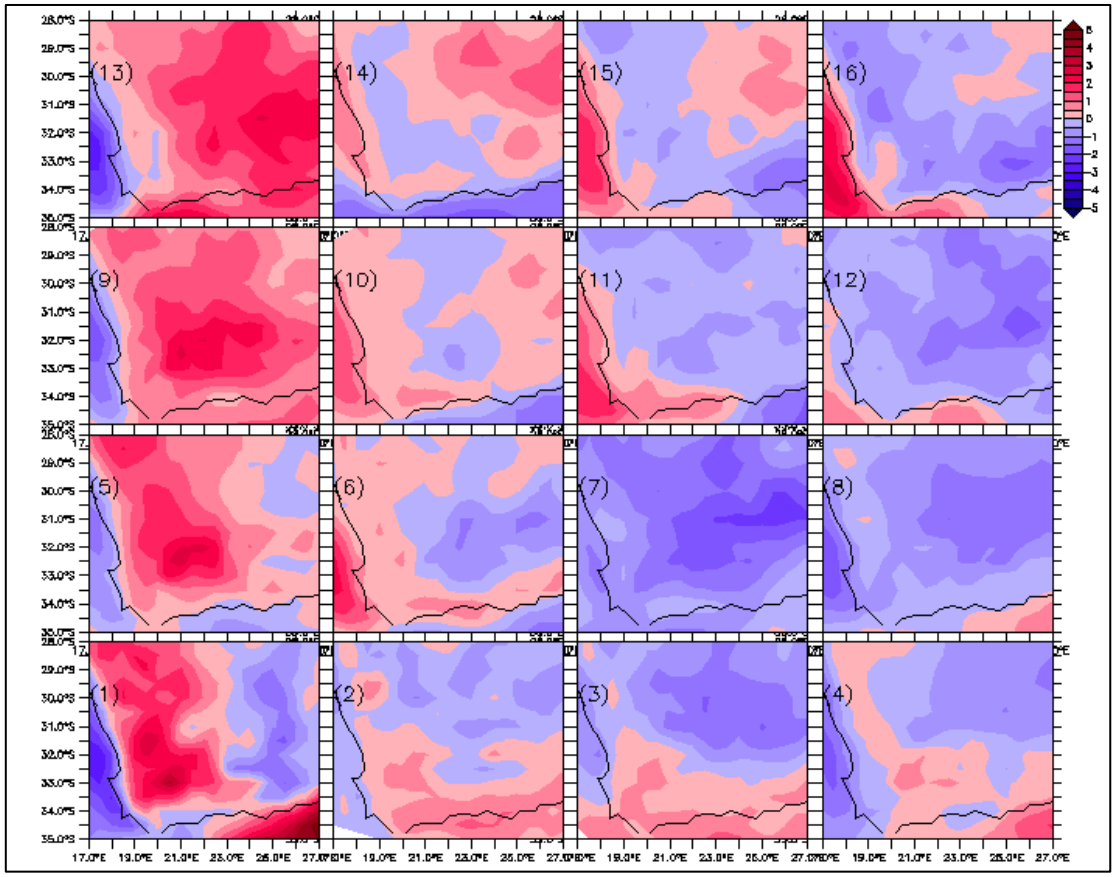

Figure 4-16: DJF season anomalies of maximum surface wind speed ($m.s^{-1}$) on the day of fire for each node. The number in round brackets represents the node identification number.

At the spatial resolution of the atmospheric data used in this study, maximum surface temperature and minimum surface relative humidity (which are used together to calculate the Burning Index in the FDI) have the largest influence in defining the spatial variation in the FDI anomaly on fire days. The atmospheric processes that produce the spatial variation in the FDI

constituent variables can be identified by examining the geopotential height anomalies and actual geopotential heights at both the 850mb and 500mb levels as shown in Figure 4-17, Figure 4-18, Figure 4-19 and Figure 4-20.

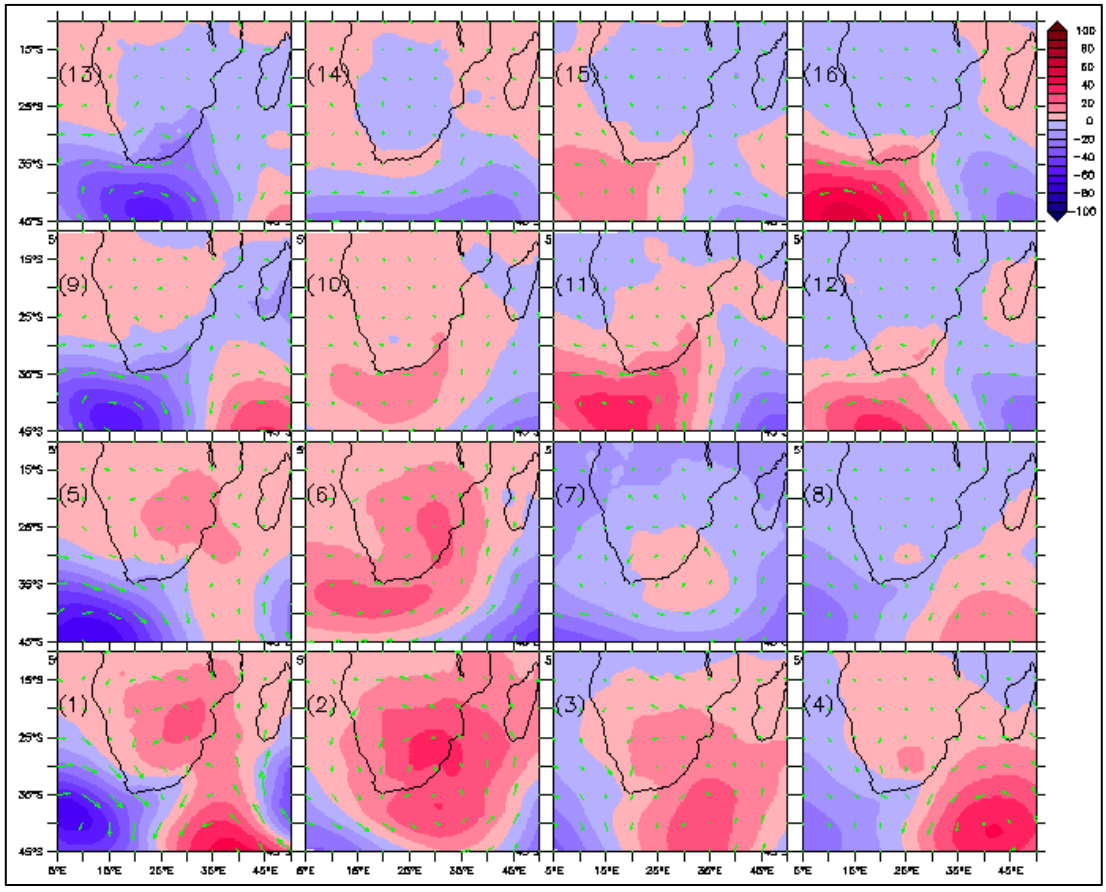

Figure 4-17: DJF season Anomalies of Geopotential Height (m) and Wind Vectors at 850mb level, on the day of fire for each node. The number in round brackets represents the node identification number.

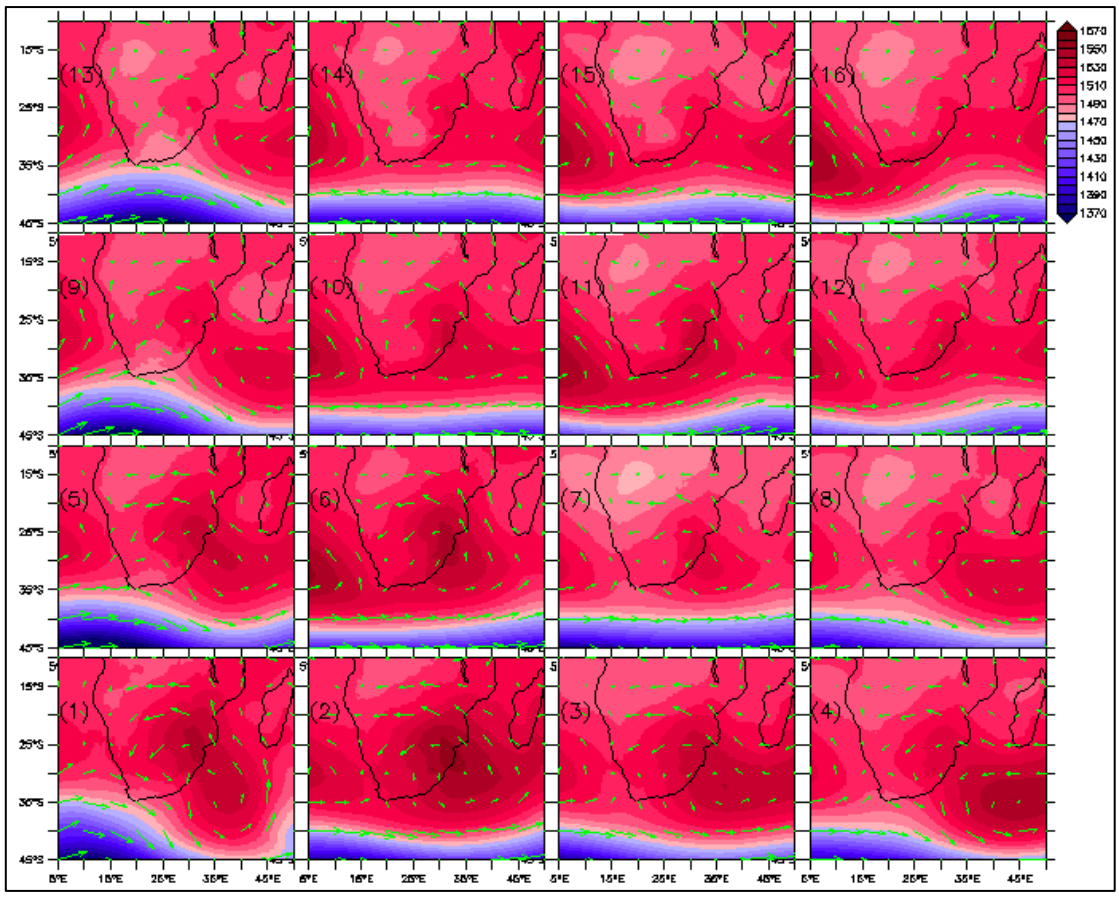

Figure 4-18: DJF season Actual Geopotential Height (m) and Wind Vectors at 850mb level, on the day of fire for each node. The number in round brackets represents the node identification number.

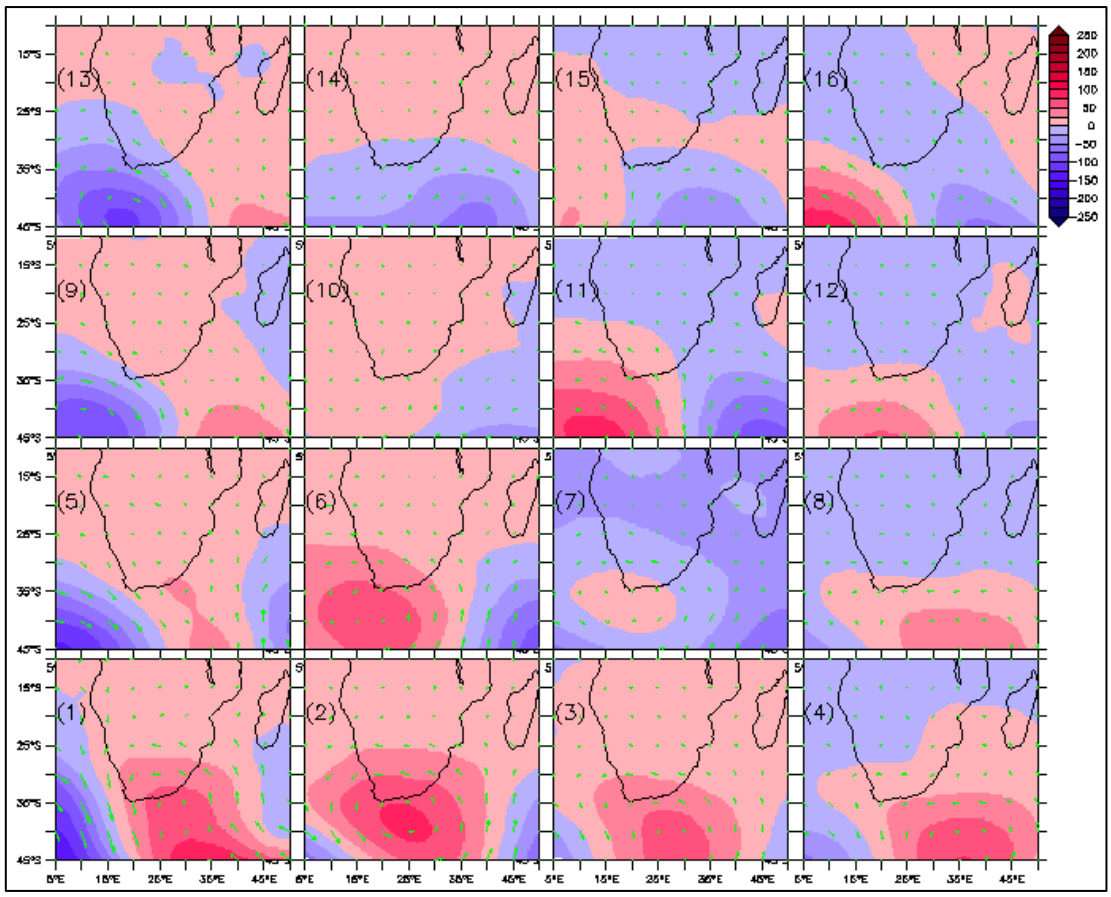

Figure 4-19: DJF season Anomalies of Geopotential Height (m) and Wind Vectors at 500mb level, on the day of fire for each node. The number in round brackets represents the node identification number.

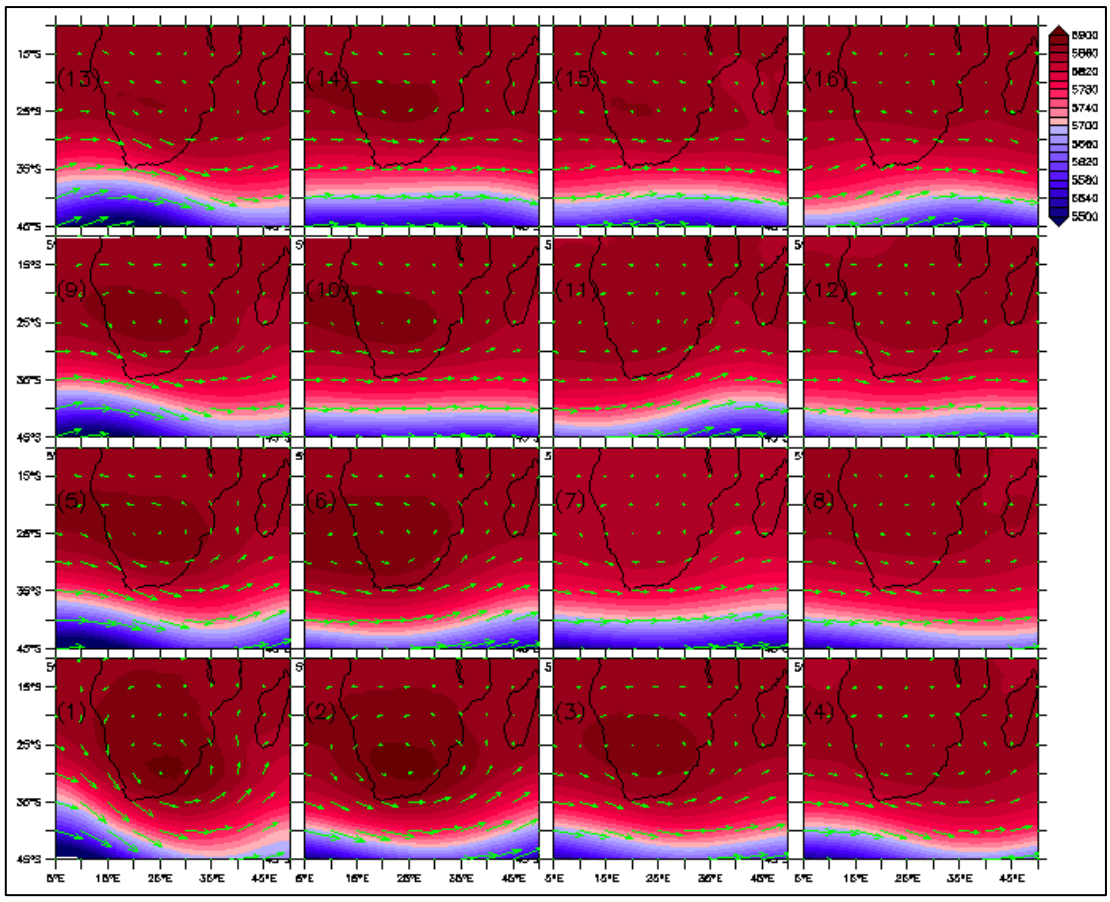

Figure 4-20: DJF season Actual Geopotential Height (m) and Wind Vectors at 500mb level, on the day of fire for each node. The number in round brackets represents the node identification number.

4.4.1 Node (4)

In the case of Node (4) there is a positive geopotential height anomaly of the Southern Indian Anticyclone and a negative geopotential height anomaly of the Southern Atlantic Anticyclone evident at both the 850mb and 500mb levels. The cumulative strengthening of the Southern Indian Anticyclone and weakening of the Southern Atlantic Anticyclone leads to an increased flow of air from the Indian Ocean into the Southern African interior. This moist and relatively cooler air mass will displace the existing air mass in the Southern African interior, resulting in a higher minimum relative humidity and lower maximum temperature. The drier and warmer air mass that was displaced from the interior moves southwards towards the domain of the Fynbos Biome, leading to a decrease in the minimum relative humidity and in increase in the maximum temperature along the south coast of South Africa. In a narrow

band along the southwest coast of South Africa, it appears that the potential increase in the FDI anomaly, associated with the displacement of the continental air mass described above, is offset by a reduction in the wind speed along the west coast as a result of the weakening of the Southern Atlantic Anticyclone. In addition to the effects of the horizontal air mass movements there is also some evidence of a weak positive geopotential height anomaly cell over the Eastern Cape at the 850mb level. This suggests that there may be a faint, localised increase in the downward vertical movement of dry air from the upper atmosphere, which would further reduce the minimum relative humidity along the southeast coast of South Africa.

Therefore, there is strong evidence that the simultaneous strengthening of the Southern Indian Anticyclone and weakening of Southern Atlantic Anticyclone will lead to an increase in the FDI over the Fynbos Biome and the rest of the south coast, but will lead to a decrease in the FDI over the Southern African interior.

4.4.2 Node (16)

Node (16) manifests itself almost as the opposite case to Node (4). There is a strong positive geopotential height anomaly and ridging of the Southern Atlantic Anticyclone and a moderate negative geopotential height anomaly of the Southern Indian Anticyclone evident at both the 850mb and 500mb levels. Due to the strengthening and ridging of the Southern Atlantic Anticyclone, combined with the weakening of the Southern Indian Anticyclone, the dominant air mass movement established is a northward movement of cold and moist polar maritime air from the Southern Ocean up over the southern coast of South Africa. This large-scale air mass movement has the effect of reducing the maximum temperature and increasing the minimum relative humidity over most of South Africa, with the strongest influence occurring within the Fynbos Biome. The strong negative FDI anomaly created by the large-scale air mass movement is offset in a narrow band along the west coast due to the development of a very strong, localised south-easterly wind. The micro-scale influence of this prevailing south-easterly wind would greatly

enhance the FDI at a micro-scale, but this is not captured in the results of this study. As seen from the SOMs results in Figure 4-10, Node (16) was the second most frequent case leading to wildfire events. The localities of the fire events in Node (16) are focused along the west coast of South Africa, which is most likely due to the influence of the strong south-easterly wind in the region. However, there are a surprisingly large number of fire events that occur in the eastern half of the Fynbos Biome. This could be ascribed to lightning strikes, which are one of the major sources of ignition of wildfires in the eastern half of the Fynbos Biome (Cowling *et al.*, 2004; Southey, 2009; Tadross *et al.,* 2005). When the Great Escarpment and the Cape Fold Mountains orographically lift the polar maritime air – which has high convective available potential energy – thunderstorms will develop, leading to potential lightning strikes and high, localised wind speeds. Because the FDI calculation does not take lightning activity into account, the FDI is underestimated in regions where high fire potential exists. There may be a need for a modification factor to be included in the Lowveld FDI, which would be used exclusively in the eastern portion of the Fynbos Biome. Wind direction would be the determinant variable in this factor. It is the southerly winds that lead to potential thunderstorm development and should increase the value of the FDI when observed.

In summary, a strengthening and ridging of the Southern Atlantic Anticyclone, combined with a weakening of the Southern Indian Anticyclone, will lead to a strong negative FDI anomaly over most of the Fynbos Biome, extending up in to South Africa's interior. Only a narrow band of the west coast shows a small positive FDI anomaly. Furthermore, as observed in Figure 4-12, there is some evidence of an increasing annual trend in the atmospheric processes identified in Node (16) and therefore it is recommended that these specific conditions be studied further.

4.4.3 Node (13)

In the case of Node (13) there is very little change to the Southern Indian Anticyclone and Southern Atlantic Anticyclone. However, there is a strong

negative geopotential height anomaly between the two anticyclones, located directly south of the African continent. This is evident at both the 850mb and 500mb levels. The negative geopotential height anomaly is a result of a northward shift of the mid-latitude cyclone/front. Cold and moist polar maritime air from the Southern Ocean is drawn along the west coast of South Africa by a south-westerly wind, reducing the maximum temperature and increasing the minimum relative humidity. Along the east coast and in the interior of South Africa, there is an increase in maximum temperature and a reduction in relative humidity as warm and dry tropical continental air is transferred southward from Central Africa. Therefore, a northward shift in the mid-latitude cyclone produces a negative FDI anomaly along the west coast of South Africa and the Fynbos Biome, but a positive FDI anomaly along the south coast, east coast and interior of South Africa. Similarly to Node (16), there are many fire events in Node (13) that are located where there is a negative FDI anomaly (along the west coast in this case). These fire events can probably be attributed to ignition sources (lightning strikes as well as intentional and unintentional anthropogenic ignitions) playing a more prominent role than wildfire-conducive weather.

4.4.4 Special Case - Node (1)

Node (1) presents a very interesting case as it leads to an equivalent number of fire events to the other nodes, but only 3 of the fire events in Node (1) occur in the DJF fire season as observed in Figure 4-11. First the DJF atmospheric conditions of Node (1) will be discussed, for comparison with [Node (4), Node (13) and Node (16)] in the DJF season already analysed. Secondly, the atmospheric conditions of Node (1) in the other seasons will be compared to those in the DJF season.

In the DJF season for Node (1), there is a strong negative geopotential height anomaly to the southwest of South Africa with a strong positive geopotential height anomaly to the southeast of South Africa, extending up into the eastern interior of the country. These anomalies are the result of a northward shift in the mid-latitude cyclone (southwest of South Africa) and Southern

Atlantic Anticyclone, combined with the strengthening and westward shift of the Southern Indian Anticyclone. Comparing the actual geopotential height composite of Node (1) in Figure 4-18 with the mean geopotential heights per season in Figure 4-2, it appears that the actual geopotential height composite of Node (1) more closely resembles the mean geopotential height composite of the MAM and JJA seasons. Nevertheless, these unseasonal atmospheric conditions lead to a positive FDI anomaly over South Africa, with the anomaly being highest over the Fynbos Biome. Node (1) differs from Node (4), Node (13) and Node (16) in that the relative positions and strengths of the mid-latitude cyclone, Southern Atlantic Anticyclone and Southern Indian Anticyclone respectively are such that no polar maritime air is conveyed to South Africa's land. The majority of the land surface of South Africa is exposed to tropical continental air that is transferred southward, increasing maximum temperature and reducing minimum relative humidity. The FDI anomaly is probably higher over the Fynbos Biome due to the northerly katabatic wind transferring the continental air down the Great Escarpment, which will result in a further increase in maximum temperature over the Fynbos Biome. As the atmospheric conditions in Node (1) produce the highest overall positive FDI over Southern Africa and the Fynbos Biome, it can be expected that when these conditions do occur, they are more likely to lead to wildfires than atmospheric conditions in other nodes. It can therefore be assumed that the low frequency of fire events is due to the infrequent occurrence of the atmospheric conditions in Node (1) during the DJF season, as opposed to the infrequent occurrence of wildfires when the atmospheric conditions of Node (1) occur.

Comparing the geopotential height anomaly composites of Node (1) across all four seasons in Figure 4-21, it can be observed that the deviations from the seasonal mean geopotential heights are very similar. Looking at the resultant actual geopotential heights for Node (1), the key synoptic atmospheric features are all located in the same positions despite the season. Only the strength of the resulting synoptic features differs amongst the seasons, with the JJA season having the strongest and the DJF season having the weakest features at the 850mb level. Therefore, if the atmospheric

features identified in Node (1) occur at any time in the year, highly conducive wildfire conditions are produced. This is confirmed in Figure 4-22, showing the overall positive FDI anomalies in all four seasons with the highest anomalies occurring in the JJA season.

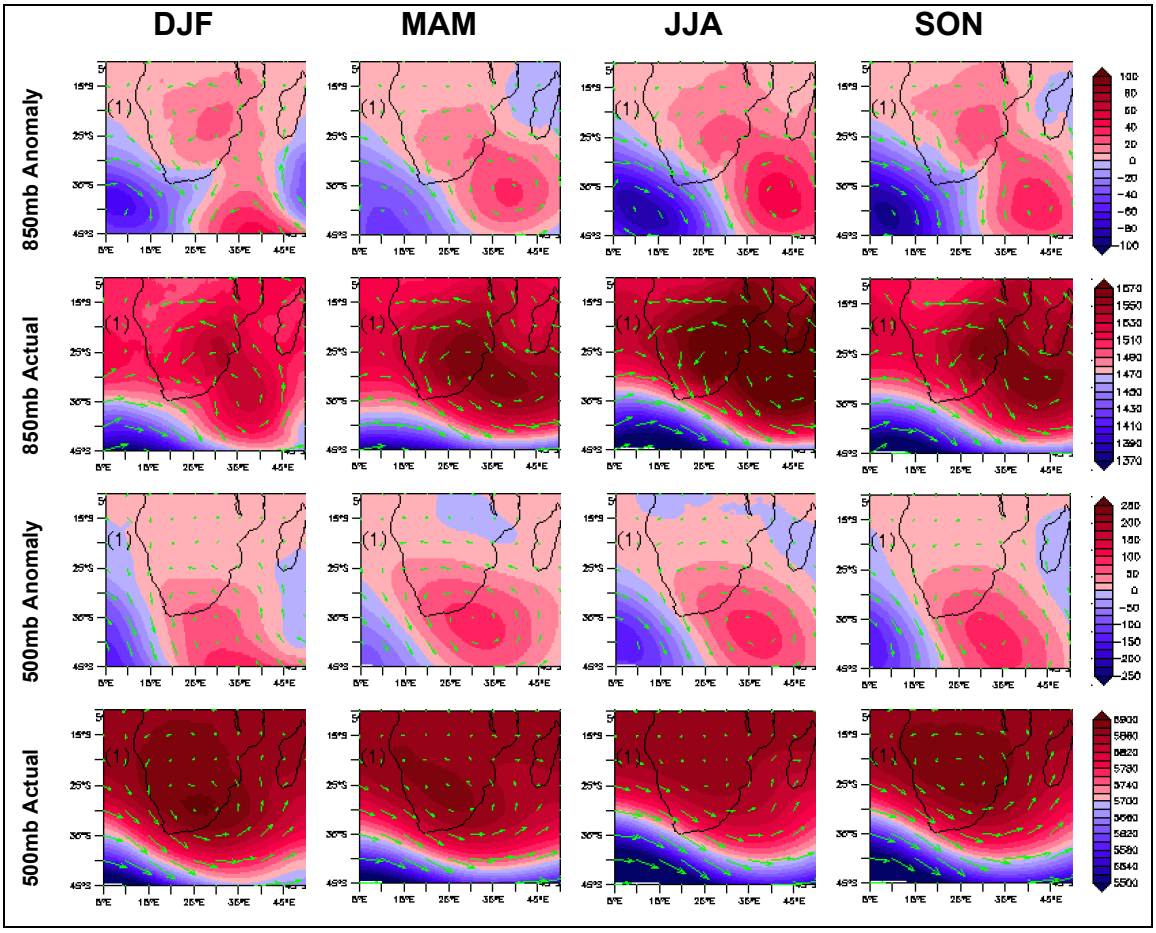

Figure 4-21: The Anomalies and Actual values of Geopotential Height (m) and Wind Vectors for Node (1) for the DJF, MAM, JJA and SON seasons at both the 850mb and 500mb levels.

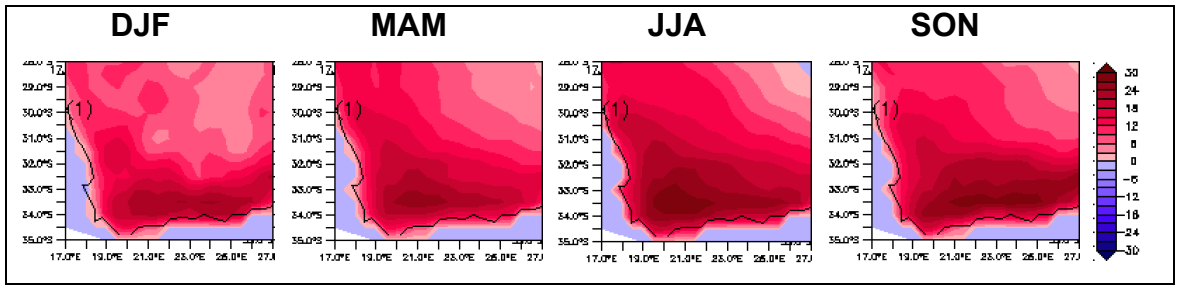

Figure 4-22: The FDI anomalies on the days of fire events for Node (1) for the DJF, MAM, JJA and SON seasons.

As discussed earlier, there is a decreasing annual trend in Node (1), with no fire events occurring in the last two years of the study period as observed in Figure 4-12. Therefore, the relative importance of the node in producing atmospheric conditions that lead to fire events may be becoming increasingly redundant. However, the atmospheric conditions of Node (1) should still be considered for further study, as it may occur due to a temporal atmospheric cycle with a period greater than that of the study.

4.5 Ability of atmospheric circulation features to be used as a fire forecasting tool

A composite for the 1) Fire Danger Index, 2) geopotential height anomaly at the 850mb level and 3) geopotential height anomaly at the 500mb level was determined for all 16 of the resulting SOMs nodes and for each of the four seasons. By comparing the number of days that these composites occurred with the number of actual fire days, the potential for using the node-specific atmospheric circulation features to improve the predictability of wildfire events is determined. This analysis focuses on the comparison between the three composites of the DJF season, as shown in Figure 4-23, using Node (13) as the reference node for the interpretation.

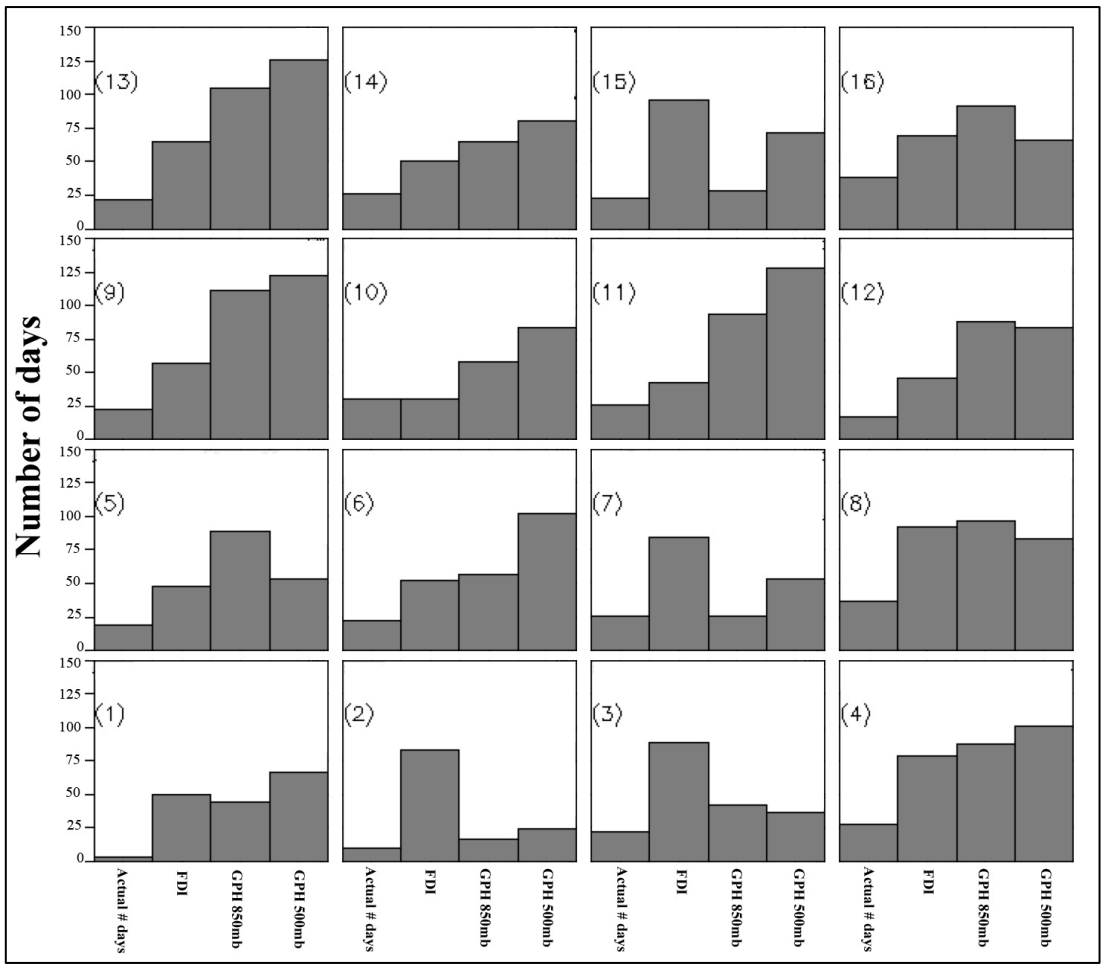

Figure 4-23: Comparison between: The actual number of fire days that occurred in the DJF season [Column 1] and the number of days the DJF FDI composite [Column 2], the DJF geopotential height anomaly at the 850mb level composite [Column 3] and the DJF geopotential height anomaly at the 500mb level composite [Column 4] occurred during the entire study period, for each of the resulting SOMs nodes. The number in round brackets represents the node identification number.

In the case of Node (13), the previously identified FDI composite for the DJF season occurred on 65 out of the total number of 3652 days during the study period, but fires only occurred on 22 of these days. This suggests that on 34% of the days when the DJF FDI composite of Node (13) was experienced, all three of the wildfire ingredients were present for a fire to occur. However, on the remaining 66% of the days when the DJF FDI composite of Node (13) was experienced, either the fuel or ignition or both wildfire ingredient conditions were not met and this consequently limited the occurrence of a wildfire. While this result provides no information on whether the weather ingredient of wildfire can be the limiting factor of wildfire occurrence, it does

show that the fuel or ignition or both the fuel and ignition ingredients can act as the limit of wildfire occurrence. Similarly, the percentages of days that fires actually occurred, relative to the number of days when the DJF FDI composite for each of the respective nodes occurred, are listed in Table 4-2 and there are some substantial differences amongst the different nodes. Fires occurred on 100% of the days that the DJF FDI composite of Node (10) occurred, indicating that all three wildfire ingredients were present on each day. At the opposite extreme, Node (1) has a 6% fire occurrence, which suggests that the fuel or ignition or both the fuel and ignition wildfire ingredients are almost always absent. The corollary to this statement is that weather is almost never a limiting ingredient under these conditions. However, caution should be taken when interpreting the result of Node (1) because, as discussed earlier, Node (1) only led to three fires days during the DJF season. Therefore the DJF FDI composite for Node (1) may not be representative.

Table 4-2: The percentage of days that fires occurred relative to the number of days the DJF FDI composite occurred during the study period, for each of the resulting SOMs nodes.

Node #	Percentage fire occurrence
Node 1	6%
Node 2	12%
Node 3	25%
Node 4	35%
Node 5	40%
Node 6	42%
Node 7	31%
Node 8	40%
Node 9	39%
Node 10	100%
Node 11	60%
Node 12	37%
Node 13	**34%**
Node 14	52%
Node 15	24%
Node 16	55%

Returning to the case of Node (13), it is observed in Figure 4-23 that the DJF geopotential height (850mb) anomaly composite occurred on 105 days, but it only resulted in conditions matching the DJF FDI composite on 65 days. There are a number of possible explanations why the atmospheric circulation features identified in the DJF geopotential height (850mb level) anomaly composite might not always lead to the corresponding FDI pattern observed in the DJF FDI composite:

- The identified atmospheric circulation features represent a dynamic state of the atmosphere that results in the horizontal and vertical movement of air masses. It is the movement of these air masses over the Fynbos Biome that has a controlling influence on the FDI. Even if the atmospheric circulation features on different days are identical and lead to the same air mass trajectories, the inherent properties or state of the air masses themselves may be different. Therefore, the FDI on a given day is dependent on the state of the atmosphere leading up to that given day. This provides further justification for the need to research the atmospheric conditions and features on the days prior to fire days.
- The spatial resolution of the reanalysis data may be inadequate to resolve small-scale atmospheric circulation features that might have a dominant effect on the FDI in localised regions.
- Low-level atmospheric wind jets may have no signature in the geopotential height at the 850mb level, but could still influence the FDI at the surface.
- The potential effects of the atmospheric boundary layer are not considered in this study.

Although the true sources of error are net yet discovered, the actual percentage of the DJF FDI composite occurrence, listed for all nodes in Table 4-3, provides some indication about whether the respective atmospheric circulation features can be used as a tool for predicting wildfire potential. When the percentage is very low, as in the case of 46% for Node (11), the associated atmospheric circulation features do not lead to a consistent pattern in the FDI over the Fynbos Biome. Therefore, the DJF geopotential height (850mb level) anomaly composite for this node cannot be used as a reliable predictive tool. However, where the percentage is close to 100% – as

in the case of Node (4), Node (6) and Node (8) – the associated atmospheric circulation features result in consistent patterns in the FDI respectively and can therefore be reliably used as a tool for predicting wildfire potential. Finally, there are also cases where the percentage DJF FDI composite occurrence is much greater than 100%. This could be due to one or more of the potential sources of error listed above, but can also be caused by numerous unidentified and different atmospheric circulation features, which may all produce the same pattern in the FDI. In these cases the actual number of fire days were very close to the number of days the geopotential height (850mb level) anomaly occurred, which could suggest that the respective atmospheric circulation features may be a better predictive tool for forecasting fire potential than the FDI itself. Further research is required to support this claim.

Table 4-3: The percentage of days that the DJF FDI composite occurred, relative to the number of days the DJF geopotential height (850mb level) anomaly composite occurred, for each of the resulting SOMs nodes.

Node #	Percentage DJF FDI composite occurrence
Node 1	114%
Node 2	488%
Node 3	212%
Node 4	91%
Node 5	54%
Node 6	91%
Node 7	323%
Node 8	95%
Node 9	51%
Node 10	52%
Node 11	46%
Node 12	52%
Node 13	**62%**
Node 14	77%
Node 15	343%
Node 16	76%

Returning to the case of Node (13) for a final comparison, it is observed in Figure 4-23 that the DJF geopotential height (500mb level) anomaly composite occurs on 126 days, but the DJF geopotential height (850mb level)

anomaly composite occurs on only 105 days. Just as the identified atmospheric circulation features at the 850mb level are the forcing behind the surface air mass movements that largely determine the spatial pattern in the FDI at the surface, so is the dynamic state of the upper atmosphere (500mb level) responsible for forcing the lower-level atmospheric circulation features (850mb level). This forcing between the upper and lower levels of the atmosphere is complex and non-linear. Therefore, particular atmospheric circulation features at the 500mb level may not always result in the same atmospheric circulation features at the 850mb level. Similar potential sources of error may occur in the geopotential height (500mb level) anomaly composite where the spatial resolution of the reanalysis data is inadequate to resolve important smaller-scale circulation features. This could also result in the geopotential height anomaly composite at the 850mb level occurring on more days than at the 500mb level – as in the case of Node (16) for example. Atmospheric circulation features that are evident at both the 850mb level and the 500mb level, like the strong negative geopotential height anomaly for Node (13) discussed in the previous section, are generally stronger atmospheric systems that occur with longer durations. Therefore, in cases where an atmospheric circulation feature is evident at both levels of the atmosphere and the respective geopotential height composites occur with relatively equal frequency, there is stronger evidence for supporting the use of that particular atmospheric circulation feature as a tool for forecasting wildfire potential. Consequently the predictive power of a particular atmospheric circulation feature in creating wildfire-conducive conditions is strongest for nodes where there is a relatively equal occurrence of the FDI composite and the geopotential height anomaly composites at both the 850 and 500mb levels. Therefore, the atmospheric circulation feature in Node (4) is probably more useful in forecasting fire potential than Node (13).

The relationship between the actual number of fires that occurred in the MAM season and the three MAM composites, as shown in Figure 4-24, can be interpreted in the same manner as in Figure 4-23 for the DJF season. An interesting difference between the DJF season and the MAM season is that although the MAM season only had 69% of the fire days that the DJF season

had, all three of the MAM seasonal composites occurred on more days during the study period than the respective DJF composites. This result suggests that even though the MAM season has more fire-conducive days than the DJF season, either the fuel or ignition or both the fuel and ignition wildfire ingredient conditions were not met more often, resulting in fewer fires. Furthermore, it is expected that these fire-conducive weather conditions are closer to the threshold values for fire occurrence. This would imply that even though weather is not the limiting wildfire ingredient on these days, it would reduce the potential for fire and the risk of fire spread. Furthermore, Node (2), Node (4) and Node (6) in Figure 4-24 display the case where all three MAM composites occurred on a similar number of days. This advocates that the atmospheric features identified for these nodes could be reliably used as an alternative or supplementary tool for predicting fire occurrence in the future. Caution should however be taken when using these results, as ecological prescribed burns are usually performed during the MAM season on days specifically chosen for the weather conditions, amongst other factors (Van Wilgen *et al*., 1992). Because the MODIS active-fires data used in this study cannot distinguish between wildfires and ecological prescribed burns, the MAM composites on which this comparison is based may contain a bias.

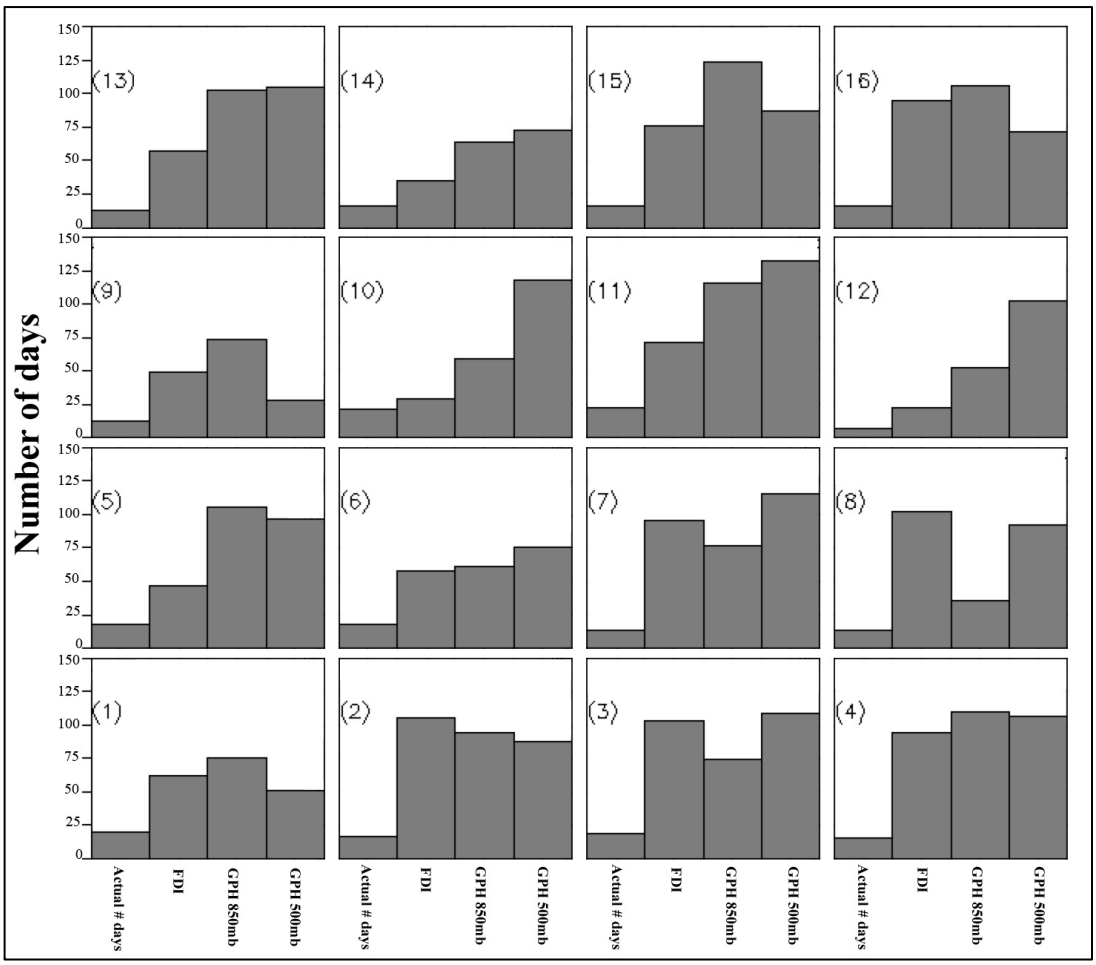

Figure 4-24: Comparison between: The actual number of fire days that occurred in the MAM season [Column 1] and the number of days the MAM FDI composite [Column 2], the MAM geopotential height anomaly at the 850mb level composite [Column 3], and the MAM geopotential height anomaly at the 500mb level composite [Column 4] occurred during the entire study period, for each of the resulting SOMs nodes. The number in round brackets represents the node identification number.

The relationship between the actual number of fires that occurred in the SON season and the three SON composites, as shown in Figure 4-25, shows a very similar result to the respective comparison for the MAM season. While only 48% of fire days occurred during the SON season relative to the MAM season, the percentage of the number of fire days and the number of days the FDI composite occurred for both the MAM and SON seasons is very similar at 28% and 25% respectively. This suggests that the fuel or ignition or fuel and ignition wildfire ingredient conditions have similar importance in both seasons. However, there appears to be a much bigger disparity between the occurrence of each SOMs composite per node, when compared to the results

for the DJF and MAM seasons. Therefore the atmospheric features identified for the SON season would not be able to sufficiently aid in the prediction of wildfires. Just like the unavoidable inclusion of ecological prescribed burns in the MAM season could potentially create a bias in the MAM composites, prescribed stack burning operations could create a bias in the SON composites. This is because stack burns are performed on weather specific days in the SON season to clear alien vegetation and vegetation from cleared firebreaks.

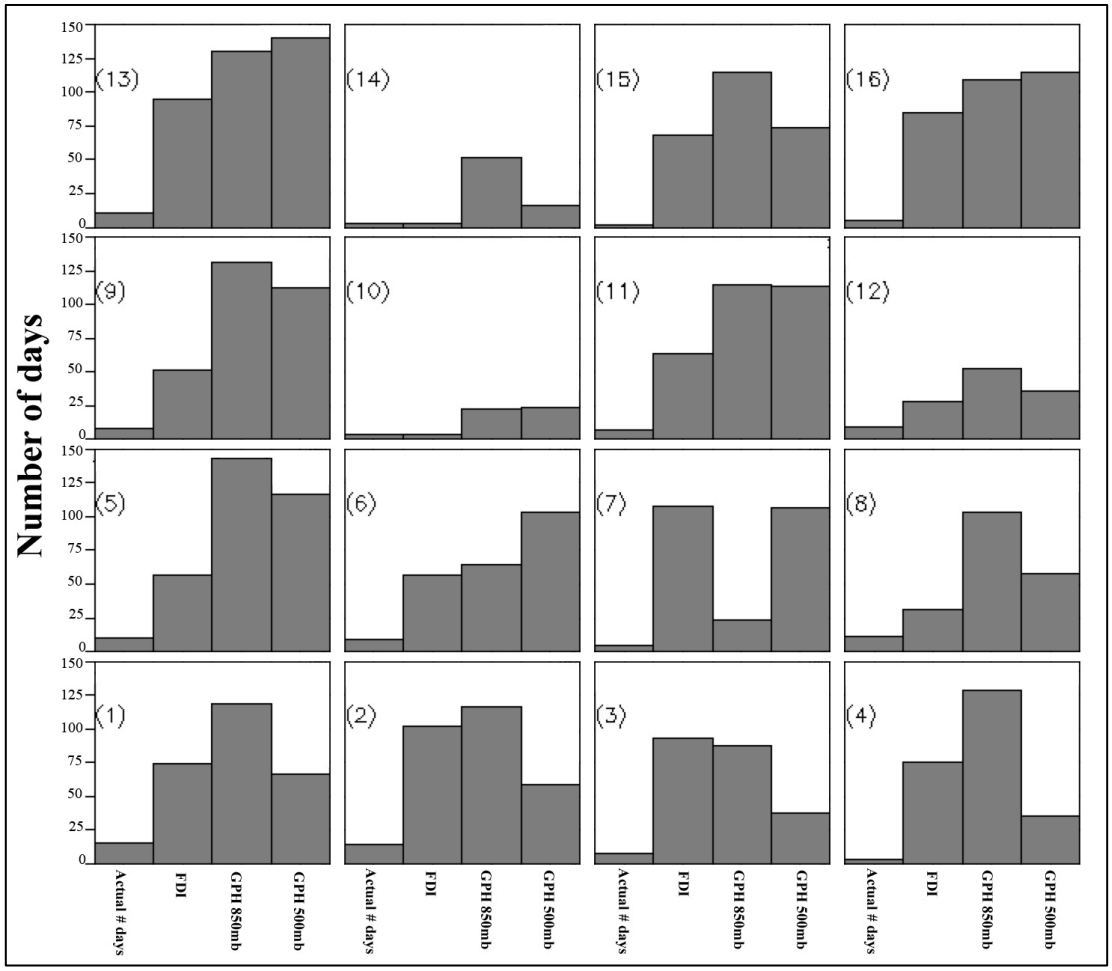

Figure 4-25: Comparison between: The actual number of fire days that occurred in the SON season [Column 1] and the number of days the SON FDI composite [Column 2], the SON geopotential height anomaly at the 850mb level composite [Column 3], and the SON geopotential height anomaly at the 500mb level composite [Column 4] occurred during the entire study period, for each of the resulting SOMs nodes. The number in round brackets represents the node identification number.

Finally, the number of days that the three JJA composites occurred, relative to the number of actual fire days in the JJA season and each other, are shown in Figure 4-26. When analysing the seasonality of the nodes classified by the SOMs technique (Figure 4-11) it was shown that Node (4), Node (14) and Node (16) did not occur during the JJA season and therefore there are no results for these nodes in the JJA season. There were a total of 54 fire days that occurred during the study period in the JJA season, which is 14.6% of the number of fire days that occurred in the DJF season. Therefore the respective JJA composites for each node are established on an average of 3.38 fire days. Extreme caution should therefore be taken when using the JJA composites, as they may not be representative of the true dynamics for each node. As more data becomes available with time, more data relating to fires that occur during the JJA season will be presented, which will improve these findings. Despite the very small sample size of fires in the JJA season, there does seem to be relatively good congruence amongst the number of days that each of the three JJA composites occurred, particularly in Node (9), Node (11), Node (13) and Node (15). Therefore it is possible that the atmospheric circulation features identified in these nodes may still improve the predictability of wildfires within the JJA season. However, fires only occur on an average of 5% of the number of days that the JJA composites occur suggesting that a combination of the fuel and ignition wildfire ingredients play an even more important role in the JJA season relative to the other seasons. Nevertheless, this result is more likely a manifestation of a sampling bias.

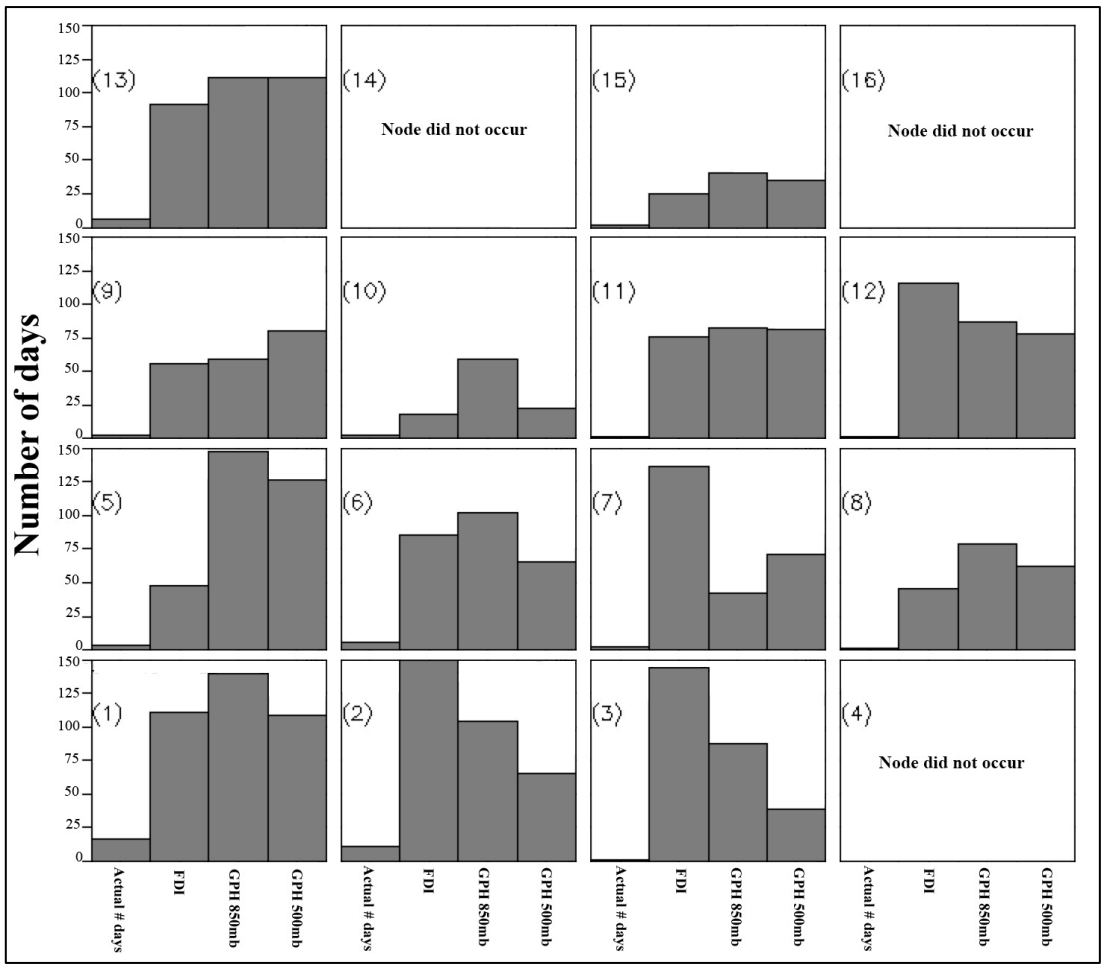

Figure 4-26: Comparison between: The actual number of fire days that occurred in the JJA season [Column 1] and the number of days the JJA FDI composite [Column 2], the JJA geopotential height anomaly at the 850mb level composite [Column 3], and the JJA geopotential height anomaly at the 500mb level composite [Column 4] occurred during the entire study period, for each of the resulting SOMs nodes. The number in round brackets represents the node identification number.

Chapter 5. Conclusions and Recommendations

5.1 Conclusions

Although fires are an ecological imperative in the Fynbos Biome, they generally have severe negative impacts on humans. Changes to the natural fire regime of the Fynbos Biome, both by natural and anthropogenic mechanisms, impact natural ecological functioning with negative conservation consequences. It can also exacerbate the harmful effects on people. With the adoption of the proactive integrated management approach, efforts are being made to maintain the natural fire regime and mitigate the detrimental ecological and social effects of wildfires.

This minor-dissertation has investigated the relationship between MODIS active-fires data and the accompanying synoptic-scale atmospheric conditions obtained from the Climate Forecasting System Reanalysis datasets. The aim of this investigation was to improve our understanding of the synoptic-scale atmospheric circulation features that induce favourable conditions for wildfire in the Fynbos Biome, with the view to better-informed fire management. This study set out to achieve this aim by first investigating the characteristics of fire occurrence in the Fynbos Biome over a ten-year study period (2003-2012). This was followed by the classification and identification of the dominant synoptic-scale atmospheric circulation features that are linked to wildfire in the region. Finally, the associations between fire days, the pattern of widespread fire danger and the linked atmospheric features were assessed.

The investigation of the fire occurrence characteristics revealed that:

- The MODIS active-fires data reproduces the known seasonality of wildfires in the Fynbos Biome, showing a dominant summer fire regime, but also the occurrence of a few winter fires. However, the highest correlation between the FDI over the Western Cape and number of fire days per month ($r = 0.7331$) occurred with a one-month lag in the number of fire days per month.
- There was an average of 80.4 ± 11.5 fire days per year, with a decreasing trend evident in the number of fire days per year. This negative trend was believed to only represent a short negative random walk in an overall positive trend in the number of fire days per year, which could not be identified due the short study period. This negative trend loosely matches the negative trend in the annual FDI over the Western Cape.
- Some evidence was established that the state of the El Niño Southern Oscillation might impact the number of fire days per year in the Fynbos Biome (El Niño events appear to result in an increased number of fire days per year).
- The fire count density was found to be highest in the central areas of the Fynbos Biome – away from the South African coastline and the biome boundary respectively.
- The threshold values required for fire occurrence in the Fynbos Biome (5% error) were identified as a FDI value of 57, a maximum surface temperature of 21°C, a minimum surface relative humidity of 55% and a maximum surface wind speed of 12.7km/h.
- Despite the known relationship between weather and fire behaviour, no evidence of a relationship between the FDI and fire intensity was found in this study. This was attributed to the relatively greater importance of fuel and topography in determining fire intensity, neither of which were controlled for in this analysis.

In order to identify the dominant synoptic-scale atmospheric circulation features that are associated with wildfire, the Self Organising Maps (SOMs) technique was used to classify the FDI anomaly over the Fynbos Biome on the days that fires occurred. Most of the nodes occurred with highest

frequency in the DJF season, but two of them occurred with their lowest frequency in the same season. This suggested that the resulting SOMs nodes should be distinguished by their seasonal components. This study classified 16 atmospheric features associated with wildfires for each of the four seasons. However, only the four major synoptic-scale atmospheric circulations – most distinct from one another – that usually induce wildfire in the Fynbos Biome during the DJF season, were identified and described as:

- The cumulative strengthening of the Southern Indian Anticyclone and weakening of the Southern Atlantic Anticyclone, at both the 850mb and 500mb levels respectively, that produces a positive FDI anomaly limited to the Fynbos Biome.
- The cumulative weakening of the Southern Indian Anticyclone and the strengthening and ridging of the Southern Atlantic Anticyclone, at both the 850mb and 500mb levels respectively, that produces a negative FDI anomaly extending beyond the bounds of the Fynbos Biome. It was suggested that fires occurring in the areas with negative FDI anomalies were a probable result of lightning strikes, which are not taken into account in the calculation of the FDI.
- The development of a strong negative geopotential height anomaly between the Southern Indian Anticyclone and Southern Atlantic Anticyclone (south of the African continent), that produces a positive FDI anomaly limited to the western region of the Fynbos Biome, but which also produces a negative FDI anomaly over the rest of the Fynbos Biome extending into the South African interior.
- An approaching mid-latitude frontal system that manifests as the cumulative strengthening of the Southern Atlantic Anticyclone with the development of a positive geopotential height anomaly located to the southeast of South Africa, extending up into the country's interior. This atmospheric feature produces a positive FDI anomaly extending beyond the bounds of the Fynbos Biome, regardless of the season it occurs in. However, only three fires occurred under this atmospheric feature in the DJF season, which can be attributed to the low occurrence of the feature itself in this season.

The associations between fire days, the pattern of widespread fire danger and the linked synoptic-scale atmospheric features were assessed in order to determine whether the identified atmospheric features in this study could be used as a tool to help predict the potential for wildfires to occur. The results of the analysis in this study showed that:

- Wildfires do not always occur on days when the weather provides fire-conducive conditions. Therefore, the fuel, ignition or both of these wildfire ingredients must act as the limit for the occurrence of wildfires on these days.
- Some of the atmospheric features identified, which were strong enough to be constantly defined at both the 850mb and 500mb levels, consistently produce the same patterns of the FDI over the Fynbos Biome. Therefore these atmospheric features could be used as a supplement – or even as an alternative – to the FDI for identifying fire-conducive days.
- There were other weaker atmospheric features (not consistently defined at both the 850mb and 500mb levels) that showed minimal congruence to the associated pattern of the FDI in the Fynbos Biome. Therefore, these atmospheric features cannot be used to reliably identify fire-conducive days.
- It is possible that a few of the identified atmospheric features may be even better at identifying fire-conducive days than the FDI. However, given the limitations of the analysis, further research is required to validate this finding.

The main limitations of this study were the constrained study period of only 10 years, the inability to remove prescribed burns from the MODIS active-fires data and the relatively low resolution of the atmospheric reanalysis data. Given these limitations, case studies are needed to establish these findings.

This minor-dissertation advances our scientific understanding of the synoptic-scale atmospheric features that are associated with wildfire in the Fynbos

Biome of South Africa, despite its limitations. Furthermore, this study not only provides evidence that the gained knowledge can supplement the Fire Danger Index's ability to predict wildfire, but it may even lead to an improvement on it. Therefore, this study provides a proof of principal that by incorporating knowledge of prevailing synoptic-scale atmospheric features into fire monitoring, fire management can be improved in any fire-prone eco-region worldwide, aiding the globally informed biodiversity conservation agenda.

5.2 Recommendations for further research

The limitations identified in this minor-dissertation can be resolved in future research. The satellite remote-sensing products and atmospheric circulation models are continually advancing with time and researchers may be able to access the prescribed burn fire records for the region. Resolving these limitations will certainly produce more robust results. Notwithstanding, the results of this minor-dissertation need to be validated to establish the findings. Therefore it is suggested that the following steps be taken in order to further this work:

1) Exclude prescribed burn fire detections from among the active-fires dataset.
2) Extend the study period as more data become available.
3) Use higher resolution gridded atmospheric data when it becomes available.
4) Identify the synoptic features on each of the days prior to fire events in addition to identifying the synoptic features on the days of fire events.
5) Use the new official formula for calculating the Lowveld Fire Danger Index.
6) Validate the findings of this study by replicating it for other regions where synoptic atmospheric features have been linked to wildfires, in order to compare the findings.
7) Validate how well the identified atmospheric features perform as a fire forecasting tool over a different period of fire occurrence (e.g. 2013 to present).

Acknowledgements

The author would like to acknowledge the following people:

- My parents for the opportunities and privileges they have provided me with through the years.
- My wife Aletta Harrison for the love, care and patience.
- Dr Babatunde Abiodun for being a mentor, colleague and a friend – whose guidance, encouragement and enthusiasm was unwavering.
- Dr Pippin Anderson for helping me to finish this minor-dissertation and for providing emotional support during the process.
- My parents-in-law for their daily thoughts and prayers.
- The Climate Systems Analysis Group for their financial support.
- The Volunteer Wildfire Services for advancing my knowledge, skills and passion for wildfire management.

References

Abiodun, B.J., Abba Omar, S., Lennard, C. & Jack, C. 2015. Using regional climate models to simulate extreme rainfall events in the Western Cape, South Africa. *International Journal of Climatology*. Doi: 10.1002/joc.4376.

Allan, R.J. 2000. 'ENSO and climatic variability in the last 150 years', *in El Niño and the Southern Oscillation: Multiscale variability, Global and Regional Impacts*. eds H.F. Diaz & V. Markgraf. Cambridge University Press: Cambridge. pp: 3-56 .

AndyNixPix, 2015. *Figure 1-6 [Left] Properties under threat on the wildland-urban interface of Table Mountain National Park and the suburb of Lakeside*. [Photograph]. Available (Online): http://www.climbing.co.za/2015/03/still-burning/ [Accessed 2015, 9th July].

Archibald, S., Nickless, A., Govender, N. Scholes, R.J. & Lehsten, V. 2010. Climate and the inter-annual variability of fire in southern Africa: a meta-analysis using long-term field data and satellite-derived burnt area data. *Global Ecology and Biogeography*. **19**: 794-809.

Banitz, E. Evaluation of short-term weather forecasts in South Africa. *Water SA*. **27**(4): 489-498.

Bett, A.K., Zhao, M., Dirmeyer, P.A. & Beljaars, A.C.M. 2006. Comparison of ERA-40 and NCEP/DOE near-surface data sets with other ISLSCP-II data sets. *Journal of Geophysical Research*. **111**: D22S04. DOI: 10.1029/2006JD007174.

Bond, W.J., Midgley, G.F., & Woodward, F.I. 2003. What controls South African vegetation – climate or fire?. *South African Journal of Botany*, **69**: 79 – 91.

Bosilovich, M., Chen, J., Robertson, F.R. & Adler, R.F. 2008. Evaluation of global precipitation in reanalyses. *Journal of Applied Meteorology and Climatology*. **47**: 2279–2299.

Bromwich, D.H., Nicolas, J.P. & Monaghan, A.J. 2011. An Assessment of precipitation changes over Antarctica and the Southern Ocean since 1989 in contemporary global reanalyses. *Journal of Climate*. **24**: 4189–4209.

CapeNature, 2015. *Table Mountain Ghost Frog*. Available (Online): http://www.capenature.co.za/fauna-and-flora/table-mountain-ghost-frog/ [Accessed 2015, 9th July].

CISL Research Data Archive. 2013. *Climate Forecast System Reanalysis*. [Data]. Available (Online): http://rda.ucar.edu/#!lfd?nb=y&b=proj&v=NCEP%20Climate%20Forecast%20System%20Reanalysis [Accessed 2013, February - June].

City of Cape Town. n.d. *Figure 1-7: [Right] Fire education programme*. [Photograph]. Available (Online): http://www.capetown.gov.za/EN/FIREANDRESCUE/Pages/Publiceducation.aspx [Accessed 2015, 9th July].

Cody, M.L. 1986. 'Diversity, rarity, and conservation in Mediterranean-climate regions', in *Conservation biology: the science of scarcity and diversity*. ed M.E. Soulé. Sinauer: Sunderland, Massachusetts. pp: 122-152.

Cowling, R.M., MacDonald, I.A.W. & Simmons, M.T. 1996. The Cape Peninsula, South Africa: Physiographical, biological and historical background to an extraordinary hot-spot of biodiversity. *Biodiversity and Conservation*. **5**: 527–550.

Cowling, R.M., Richardson, D.M. & Pierce, S.M. 2004. *Vegetation of South Africa*. Cambridge University Press: Cambridge.

Csiszar, I., Abuelgasim, A., Li, Z., Jin, J., Fraser, R. & Hao, W. 2003. Interannual changes of active fire detectability in North America from long-term records of the advanced very high resolution radiometer. *Journal of Geophysical Research*. **108**(D2). DOI: 10.1029/2001JD001373

DailyMail, 2015. *Figure 1-6 [Right] Geofrey Collings' home in Tokai was one of 13 houses that were either entirely or partly destroyed*. [Photograph]. Available (Online): http://www.dailymail.co.uk/news/article-2978982/Wildfires-rage-South-African-tourist-haven.html [Accessed 2015, 12th March].

de Klerk, H. 2008. A pragmatic assessment of the usefulness of the MODIS (Terra and Aqua) 1-km active fire (MOD14A2 and MYD14A2) products for mapping fires in the fynbos biome. *International Journal of Wildland Fire*. **17**: 166-178.

de Ronde, C. 2002. 'Wildland fire-related fatalities in South Africa – A 1994 Case study and looking back at the year 2001', in *Forest Fire Research & Wildland Fire Safety*. ed. D.X. Viegas. Millpress: Rotterdam. pp: 1-7.

Erasmus, R. 2013. *How Wildfires Start*. Available (Online): http://envirowildfire.co.za/how-wildfires-start/ [Accessed 2015, 22nd May].

Everitt, B.S., Landau, S., Leese, M. and Stahl, D. 2011. *Cluster Analysis*. 5th edition. John Wiley & Sons: New York.

Everson, T.M., Van Wilgen, B.W. & Everson, C.S. 1988. Adaptation of a model for fire danger rating in the Natal Drakensberg. *South African Journal of Science*. **84**: 44-49.

Gardner, A.E. 2015a. *Figure 1-3 [Left] The Fynbos endemic Orange-breasted sunbird (Anthobaphes violacea) sitting on a burnt protea bush*. [Photograph]. Supplied personally on 13th July 2015.

Gardner, A.E. 2015b. *Figure 1-5 [Centre*] *Seeding as a post-fire reproductive strategy*. [Photograph]. Supplied personally on 13th July 2015.

Geldenhuys, C.J. 1994. Bergwind Fires and the Location Pattern of Forest Patches in the Southern Cape Landscape, South Africa. *Journal of Biogeography*. **21**(1): 49-62.

Giglio, L., Descloitres, J., Justice, C.O. & Kaufman, Y.J. 2003. An enhanced contextual fire detection algorithm for MODIS. *Remote Sensing of Environment*. **87**: 273–282.

Gill, A.M. & Stephens, S.L. 2009. Scientific and social challenges for the management of fire-prone wildland–urban interfaces. *Environmental Research Letters*. **4**. DOI: 10.1088/1748-9326/4/3/034014.

Goldammer, J.G. & Crutzen, P.J. 1993. *Fire in the environment: Scientific rationale and summary of results of the Dahlem Workshop*. John Wiley & Sons: Chechester.

Goldblatt, P. & Manning, J.C. 2002. Plant diversity of the Cape Region of southern Africa. *Annals of the Missouri Botanical Garden*. **89**: 281–302.

Gower, J.C. 1967. A Comparison of Some Methods of Cluster Analysis. *Biometrics*. **23**(4): 623-637.

Hann, W.J. & Bunnell, D.L. 2001. Fire and land management planning and implementation across multiple scales. *International Journal of Wildland Fire*. **10**: 389-403.

Harris, S. 2006. *Figure 1-2: King Protea (Protea cynaroides) – The national flower of South Africa*. [Photograph]. Available (Online): https://www.flickr.com/photos/7693168@N05/536902500 [Accessed 2015, 9th July].

Hewitson, B.C. 2013. EGS4038F Seminar – 18 April 2013. University of Cape Town. South Africa.

Hewitson, B.C. & Crane, R.G. 2002. Self-organizing maps: applications to synoptic climatology. *Climate Research*. **22**: 13-26.

Jolliffe, I.T. 2002. *Principal Component Analysis*. 2nd edition. New York: Springer.

Kalabokidis, K., Palaiologou, P., Gerasopoulos, E., Giannakopoulos, C., Kostopoulou, E. & Zerefos, C. 2015. Effect of Climate Change Projections on Forest Fire Behavior and Values-at-Risk in Southwestern Greece. *Forests*. **6**(6): 2214-2240.

Keetch, J.J. & Byram, G.M. 1968. *A Drought Index for Forest Fire Control*. United States Department of Agricultural Forest Service Research Paper SE-38.

Kipfmueller, K.F. & Swetnam, T.W. 2000. 'Fire-climate interactions in the Selway-Bitterrot Wilderness Area. Proceedings of Wilderness Science in a Time of Change: A Conference', in *RMRS-P-15-VOL-5*. eds D.N. Cole, S.F. McCool, D.J. Parsons & P.J. Brown. USDA Forest Service. pp: 270-275.

Kohonen T., Hynninen J., Kangas J. and Laaksonen J. 1995. *SOM_PAK: the self-organizing map program package*. Helsinki University of Technology, Laborotory of Computer and Information Science, Espoo, Finland.

Kohonen, T. 1997. *Self-organising maps*. Springer: Berlin.

Köppen, W.P. 1931. *Grundriss der Klimakunde*. W. de Gruyter: Berlin.

Kraaij, T., Cowling, R.M., Van Wilgen, B.W. & Schutte-Vlok, A. 2013. Proteaceae juvenile periods and post-fire recruitment as indicators of minimum fire return interval in eastern coastal Fynbos. *Applied Vegetation Science*. **16**: 84-94.

Kramer, J. 2006. *Figure 1-7 [Centre] The "look what you have done" fire prevention campaign*. [Photograph]. Available (Online): https://www.flickr.com/photos/capelight/102291721 [Accessed 2015, 9th July].

Kruger, F.J., Forsyth, G.G., Kruger, L.M., Slater, K., Le Maitre, D.C. Matshate, J. 2006. 'Classification of Veldfire Risk in South Africa for the Administration of the Legislation regarding Fire Management', in *Proceedings of 5th International Conference on Forest Fire Research*. ed D.X. Viegas. Elsevier: Amsterdam. pp: 27-30.

Lawrence, M.G. 2005. The relationship between relative humidity and the dewpoint temperature in moist air: A simple conversion and applications. *Bulletin of the American Meteorological Society*, **86**(2): 225-233.

Li, Z., Fraser, R., Jin, J., Abuelgasim, A.A., Csiszar, I., Gong, P., Pu, R. & Hao, W. 2003. Evaluation of algorithms for fire detection and mapping across North America from satellite. *Journal of Geophysical Research*. **108**: 1–12.

Linn, R., Winterkamp, J., Edminster, C., Colman, J.J. & Smith, W.S. 2007. Coupled influences of topography and wind on wildland fire behaviour. *International Journal of Wildland Fire*. **16**(2): 183–195.

Liu, Y., Weisberg, R.H. & Mooers, C.N.K. 2006. Performance evaluation of the self-organising map for feature extraction. *Journal of Geophysical Research*. **111**(C5): 1978-2012.

McArthur, A.G. 1958. 'The preparation and use of fire danger tables', in *Proceedings Fire Weather Conference*, ed L.J. Dwayer, Bureau of Meteorology: Melbourne.

Millán, M.M., Estrela, M.J. & Badenas, C. 1998. 'Synoptic analysis of meteorological processes relevant to forest fire dynamics on the spanish mediterranean coast', in *Large Forest Fires.* ed J.M. Moreno. Backhuys Publishers: Leiden. pp. 1-30.

Mucina, L. & Rutherford, M.C. (eds.). 2006. 'The Vegetation of South Africa, Lesotho and Swaziland', in *Strelitzia 19*. South African National Biodiversity Institute: Pretoria.

NASA-FIRMS, 2011. *MODIS Hotspot / Active Fire Detections*. [Data]. Available (Online): http://earthdata.nasa.gov/data/nrt-data/firms [Accessed 2013, 16th February].

NOAA. 2015. *Historical El Nino/ La Nina episodes (1950-present)*. [Data]. Available (Online): http://www.cpc.noaa.gov/products/analysis_monitoring/ensostuff/ensoyears.shtml [Accessed 2015, 24th June].

O'Hara, S.A. *Figure 1-1 The Five Mediterranean eco-regions (shaded dark green) that are located within the mid-latitudes. The Fynbos Biome is located predominantly in the Western Cape of South Africa*. [Figure]. Available (Online): http://gimcw.org/climate/map-world.cfm [Accessed 2015, 16th July].

Olivier, T. n.d. *Figure 1-5 [Left] Fire burning in Fynbos*. [Photograph]. Available (Online): http://overbergfpa.co.za/news/all/fynbos-fire-management-goes-high-tech/ [Accessed 2015, 13th July].

Papadopoulos, A., Paschalidou, A.K., Kassomenos, P.A. & McGregor, G. 2013. On the association between synoptic circulation and wildfires in the Eastern Mediterranean. *Theoretical and Applied Climatology*. DOI: 10.1007/s00704-013-0885-1.

Parr, C.L. & Chown, S.L. 2003. Burning issues for conservation: A critique of faunal fire research in Southern Africa. *Austral Ecology*. **28**: 384-395.

Pausas J.G. & Ribeiro, E. 2013. The global fire-productivity relationship. *Global Ecology and Biogeography*. **22**: 728-736.

Punj, G. and Stewart, D.W. 1983. Cluster Analysis in Marketing Research: Review and Suggestions for Application. *Journal of Marketing Research*. **20**(2): 134-148.

Rabie, M. 2015. *Figure 1-5 [Right] Resprouting as a post-fire reproductive strategy*. [Photograph]. Available (Online): http://mariorabiephotography.blogspot.com/2015/03/out-of-ashes-comes-new-life.html [Accessed 2015, 13th July].

Rao, C.R. 1964. The use and interpretation of principal component analysis in applied research. *Sankhya*. **26**: 329-358.

Reason, C.J.C. & Rouault, M. 2002. ENSO-like decadel variability and South African rainfall. *Geophysical Research Letters*. **29**(13). DOI: 10.1029/2002GL014663.

Reggie. 2010. *Figure 1-7 [Left] Today's fire danger rating signboard outside the entrance to the Table Mountain National Park*. [Photograph]. Available (Online): https://namibsands.files.wordpress.com/2010/02/02-fire-warning.jpg [Accessed 2015, 9th July].

Reush, D.B., Alley, R.B. & Hewitson, B.C. 2005. Relative Performance of Self-Organizing Maps and Principal Component Analysis in Pattern Extraction from Synthetic Climatological Data. *Polar Geography*. **29**(3): 188-212.

Rothermal, R.C. 1972. *A mathematical model for predicting fire spread in wildland fuels*. Research Paper INT-RP-115. Ogden, UT: USDA Forest Service, Intermountain Forest and Range Experiment Station.

Roy, D.P., Lewis, P.E. & Justice, C.O. 2002. Burned area mapping using multitemporal moderate spatial resolution data – a bi-directional reflectance model-based expectation approach. *Remote Sensing of Environment*. **83**: 263–286.

Roy, D.P., Frost, P., Justice, C.O., Landmann, T., Le Roux, J., Gumbo, K., Makungwa, S., Dunham, K. et al. 2005a. The Southern Africa Fire Network (SAFNet) regional burned area product validation protocol. International *Journal of Remote Sensing*. **26**: 4265–4292.

Roy, D.P., Jin, Y., Lewis, P.E. & Justice, C.O. 2005b. Prototyping a global algorithm for the systematic fire-affected area mapping using MODIS time series data. *Remote Sensing of Environment*. **97**: 137–162.

Saha, S., Moorthi, S., Pan, H.L., Wu, X., Wang, J., Nadiga, S., Tripp, P., Kistler, R. et al. 2010. The NCEP climate forecast system reanalysis. *Bulletins of the American Meteorological Society*. **91**: 1015–1057.

SANBI. n.d. *Figure 1-3 [Right] The critically endangered and endemic Table Mountain Ghost Frog (Heleophryne rosei)*. [Photograph]. Available (Online): http://www.sanbi.org/creature/table-mountain-ghost-frog [Accessed 2015, 13th July].

SANBI. 2006. *Vegetation Map of South Africa, Lesotho and Swaziland (2006)*. [Shapefile]. Available (Online): http://bgis.sanbi.org/vegmap/map.asp [Accessed 2013, 12th February].

San José, R., Luis Pérez, J., González, R.M., Pecci, J. & Palacios, M. 2014. Analysis of fire behaviour simulations over Spain with WRF-FIRE. *International Journal of Environment and Pollution*. **55**(1-4): DOI: 10.1504/IJEP.2014.065919.

SAWS. 2015. *Lowveld Fire Danger Index Map – Friday 12 June 2015*. Available (Online): http://www.weathersa.co.za/home/fire-index [Accessed 2015, 12th June].

Shlisky, A., 2007. 'Fire, ecosystems and people: threats and strategies for global biodiversity conservation', in *4th International Wildland Fire Conference*, Seville, Spain, p. 17.

Silva, J.S., Rego, F., Fernandes, P. & Rigolot, E. 2010. *Towards Integrated Fire Management – Outcomes of the European Project Fire Paradox*. European Forest Institute.

Southey, D. 2009. *Wildfires in the Cape Floristic Region: Exploring vegetation and weather as drivers of frequency*. Thesis presented for the Degree of Master of Science, Department of Botany, University of Cape Town, South Africa.

Staatskoerant. 2013. *Publication of the Fire Danger Rating System for General Information in terms of Section 9(1) on the National Veld and Forest Fire Act, 1998 *ACT NO. 101 of 1998)*. Notice 1099 of 2013. 15 November 2013.

Tadross, M., Jack, C. & Hewitson, B. 2005. On RCM-based projections of change in southern African summer climate. *Geophysical Research Letters*. **32**. DOI: 10.1029/2005GL024460.

Teie, W.C. 2009. *Fire Manager's Handbook on Veld and Forest fires: Strategy, Tactics and Safety*, ed C.F. Pool. 2nd edition. South African Institute of Forestry: Pretoria.

Teie, W.C., Weatherford, B.F. & Murphy, T.M. 2010. *Leadership for the Wildland Fire Officer: Leading in a Dangerous Profession*. Deer Valley Press: California.

Trigg, S. & Flasse, S. 2001. An evaluation of different bispectral spaces for discriminating burned shrub-savannah. *International Journal of Remote Sensing*. **22**: 2641–2647.

Turpie, J.K., Heydenrych, B.J. & Lamberth, S.J. 2003. Economic value of terrestrial and marine biodiversity in the Cape Floristic Region: Implications for defining effective and socially optimal conservation strategies. *Biological Conservation*. **112**: 233-251.

Tyson, P.D. 2000. The weather and climate of South Africa. Oxford University Press: Oxford.

Van Wilgen, B.W. 1984. Fire climates in the southern and western Cape province and their potential use in fire control and management. *South African Journal of Science*. **80**: 358-362.

Van Wilgen, B.W., Bond, W.J. & Richardson, D.M. 1992. Ecosystem Management. *The Ecology of Fynbos: Nutrients, Fire and Diversity* (ed Cowling, R.M.). 345-371. Oxford University Press: Cape Town.

Van Wilgen, B.W., Forsyth, G.G., de Klerk, H., Das, S., Khuluse, S. & Schmitz, P. 2010. Fire managementin Mediterranean-climate shrublands: a case study from the Cape Fynbos, South Africa. *Journal of Applied Ecology*. **47**: 631-638.

Wessa P. 2012. *Cross Correlation Function (v1.0.8) in Free Statistics Software (v1.1.23-r7)*. Office for Research Development and Education. [Software]. Available (Online): http://www.wessa.net/rwasp_cross.wasp/ [Accessed 2015, 12th June].

Willis, C., Van Wilgen, B.W., Tolhurst, K., Everson, C., D'abreton, P. Pero, L. & Flemming, G. 2001. *The development of a national fire danger rating system for South Africa*. Report No. ENV-P5C 2000-073, Division of Water, Environment of Forestry Technology, CSIR, Pretoria.

Wilson, A.M., Latimer, A.M., Silander Jr, J.A., Gelfand, A.E. & de Klerk, H. 2010. A Hierarchical Bayesian model of wildfire in a Mediterranean biodiversity hotspot: Implications of weather variability and global circulation. *Ecological Modelling*. **221**: 106-112.

Working on Fire. n.d. *FDI Alignment Chart*. [Pocket Card]. Kishugu – formerly FFA Group of Companies. South Africa.

Zhang, Q., Körnich H. & Holmgren. 2012. How well do reanalyses represent the southern African precipitation?. *Climate Dynamics*. **40**(3-4): 951-962.

Zhou, K., Liu, N. & Yuan, X. 2015. Effect of Wind on Fire Whirl Over a Line Fire. *Fire Technology*. DOI: 10.1007/s10694-015-0507-9.

Appendices

The attached appendices are the composites described in section 3.2.3 for the MAM, JJA and SON seasons. Using these composites, the dominant atmospheric features that produce fire-conducive conditions over the Fynbos Biome can be identified. The included appendices for the MAM, JJA and SON seasons respectively, grouped by the composite variable, are:

Appendices 1 to 3: Fire Danger Index anomalies ..... **99 - 101**

Appendices 4 to 6: Maximum surface temperature anomalies ..... **102 - 104**

Appendices 7 to 9: Minimum surface relative humidity anomalies .... **105 - 107**

Appendices 10 to 12: Maximum surface wind speed anomalies ..... **108 - 110**

Appendices 13 to 15: Anomalies of geopotential height and associated wind vectors at the 850mb level ..... **111 - 113**

Appendices 16 to 18: Actual geopotential height and associated wind vectors at the 850mb level ..... **114 - 116**

Appendices 19 to 21: Anomalies of geopotential height and associated wind vectors at the 500mb level ..... **117 - 119**

Appendices 22 to 24: Actual geopotential height and associated wind vectors at the 500mb level ..... **120 - 122**

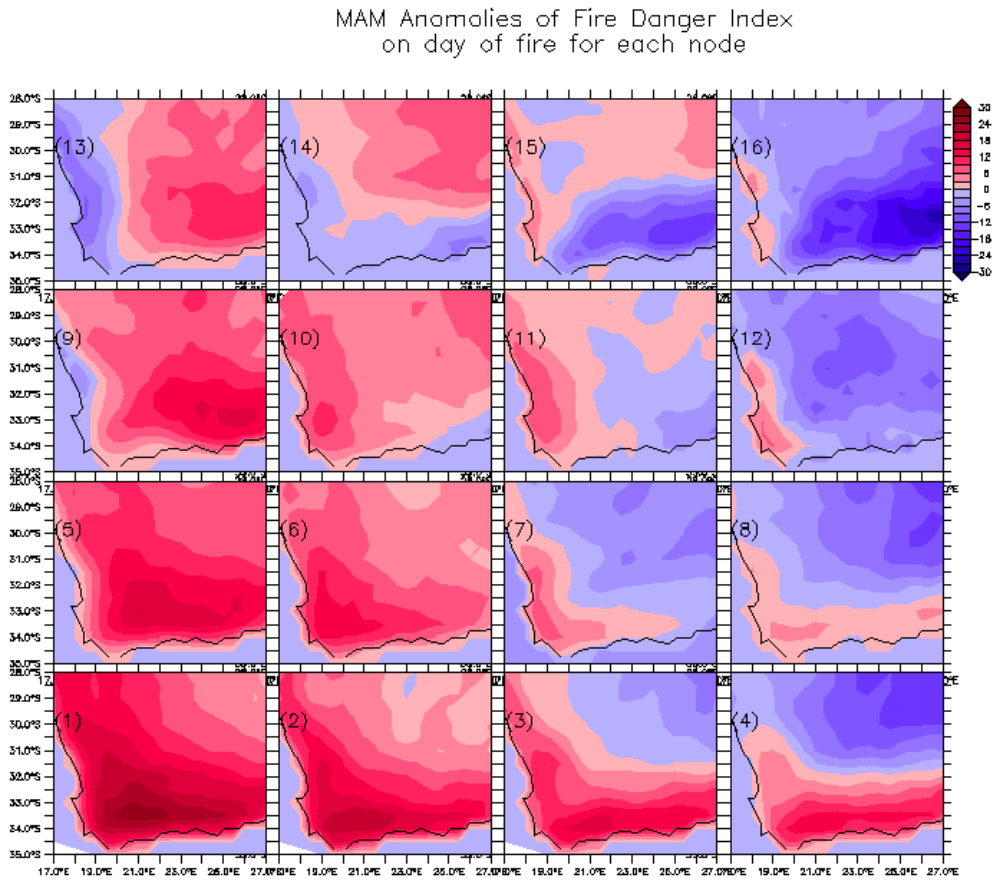

Appendix 1: MAM season anomalies of the Fire Danger Index on the day of fire for each node. The number in round brackets represents the node identification number.

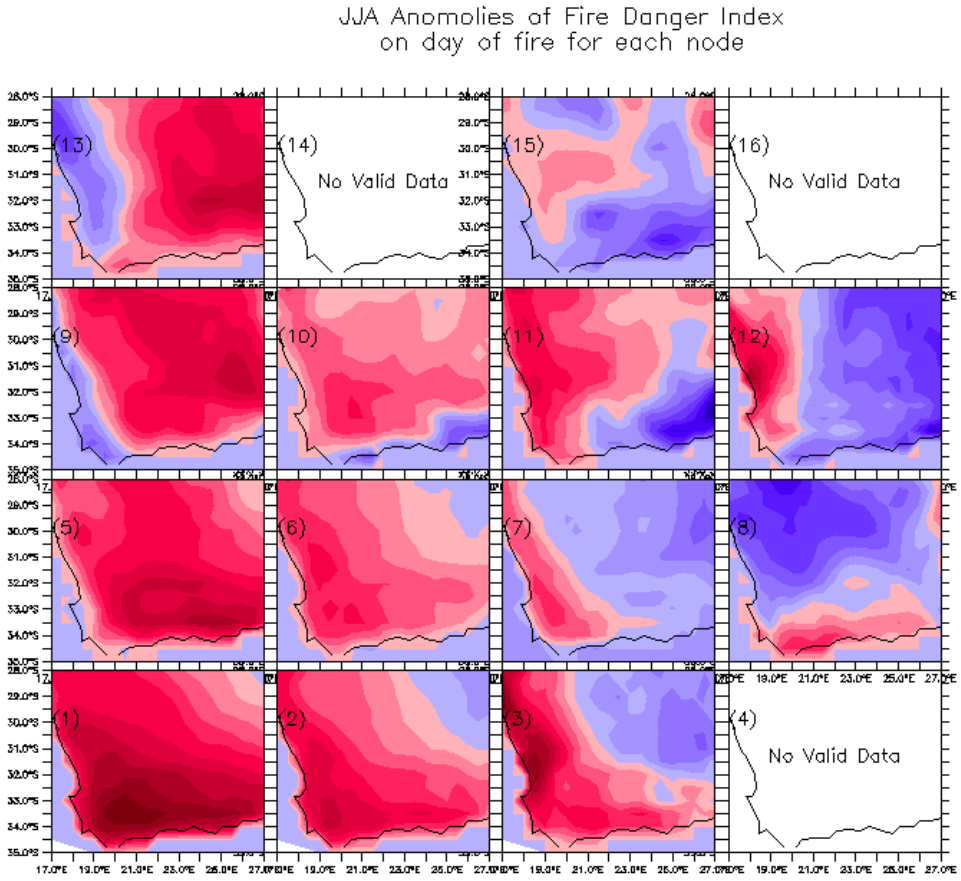

Appendix 2: JJA season anomalies of the Fire Danger Index on the day of fire for each node. The number in round brackets represents the node identification number.

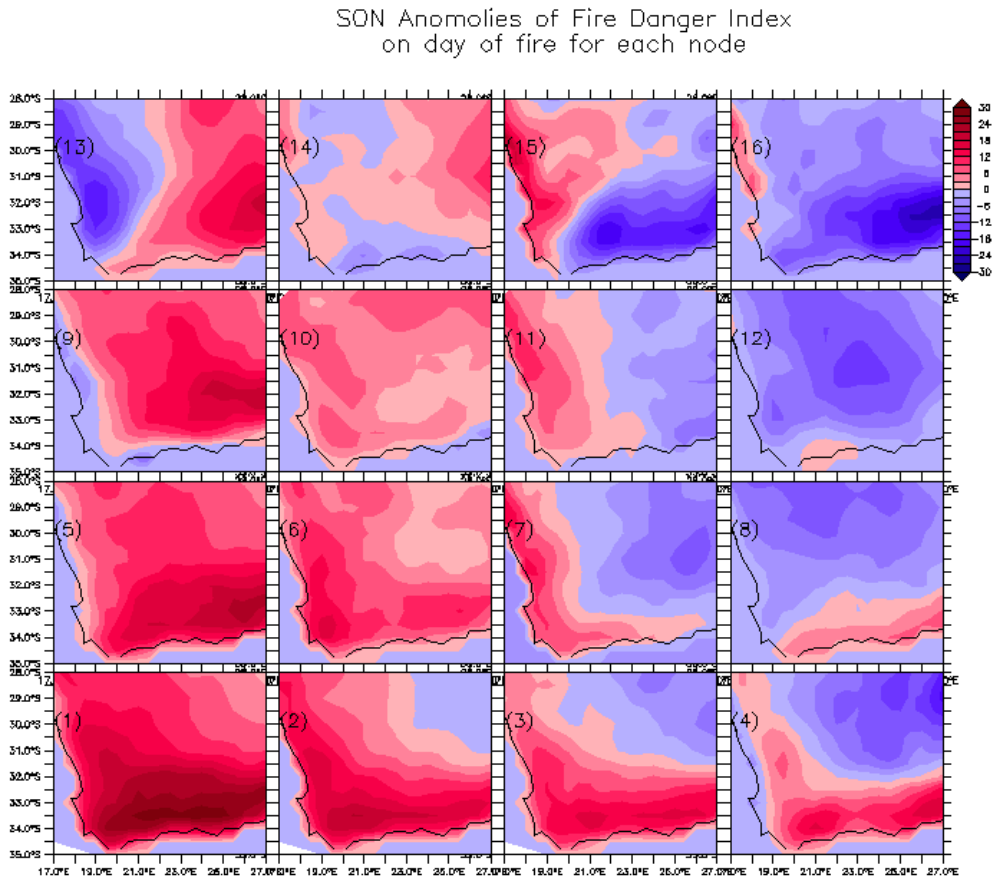

Appendix 3: SON season anomalies of the Fire Danger Index on the day of fire for each node. The number in round brackets represents the node identification number.

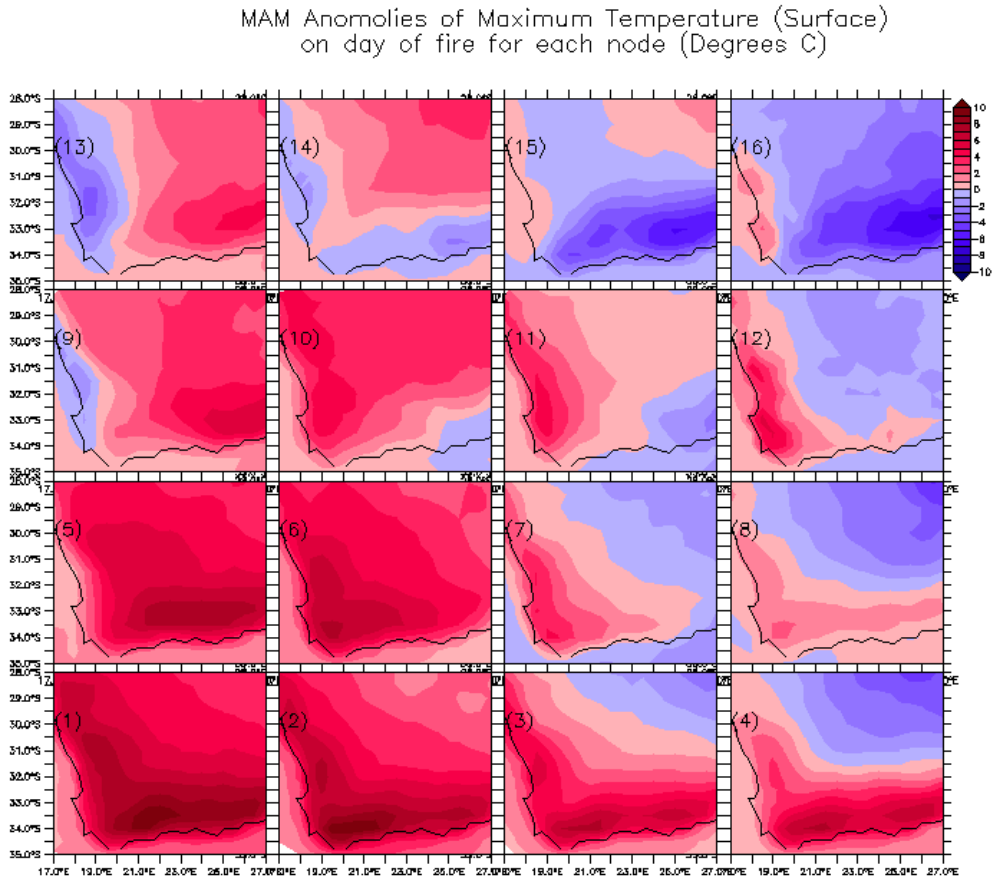

Appendix 4: MAM season anomalies of maximum surface temperature (°C) on the day of fire for each node. The number in round brackets represents the node identification number.

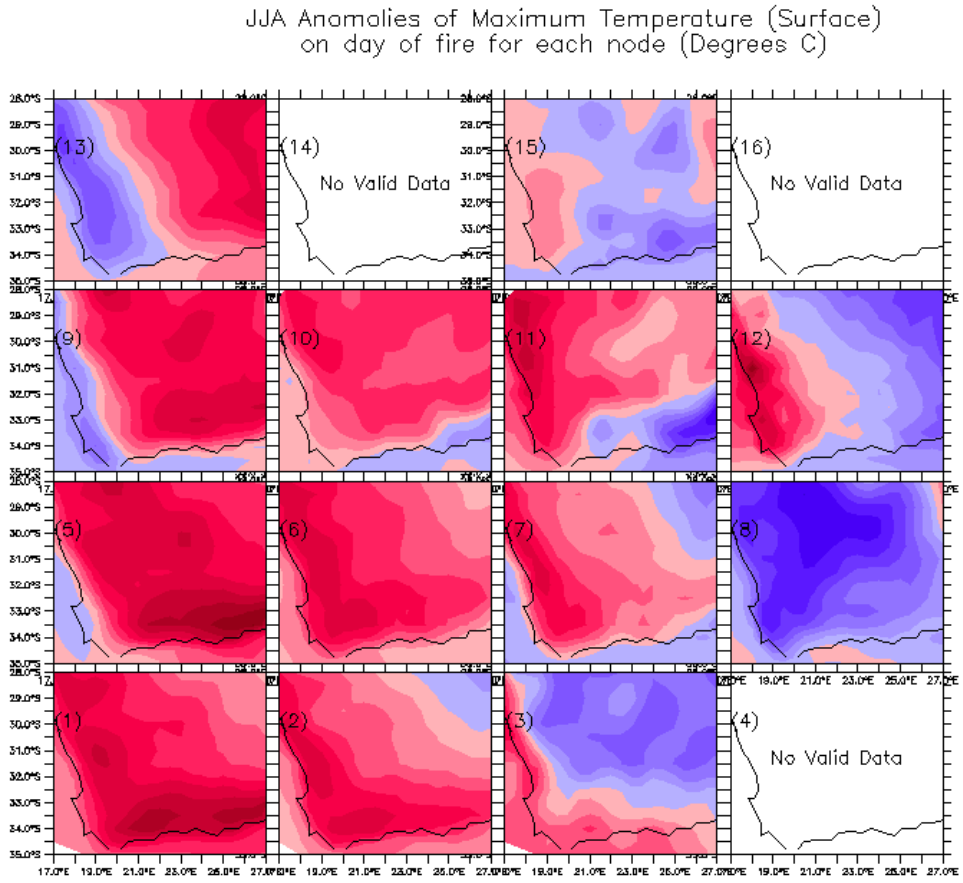

Appendix 5: JJA season anomalies of maximum surface temperature (°C) on the day of fire for each node. The number in round brackets represents the node identification number.

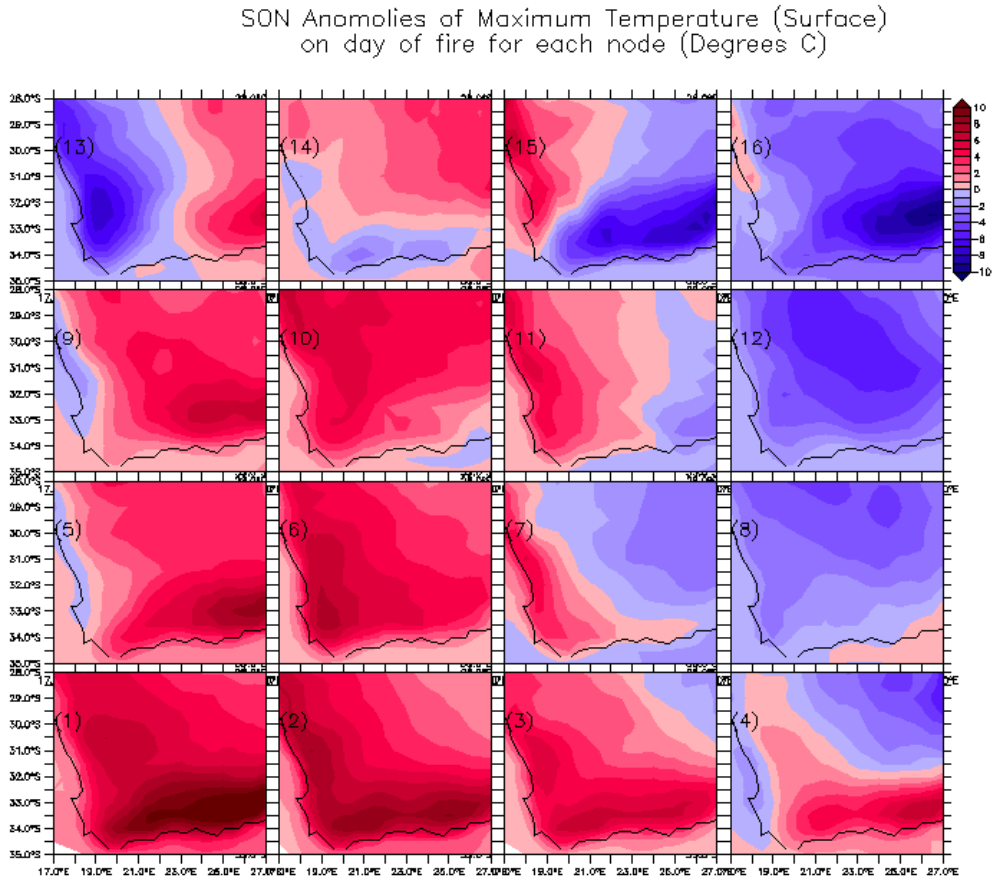

Appendix 6: SON season anomalies of maximum surface temperature (°C) on the day of fire for each node. The number in round brackets represents the node identification number.

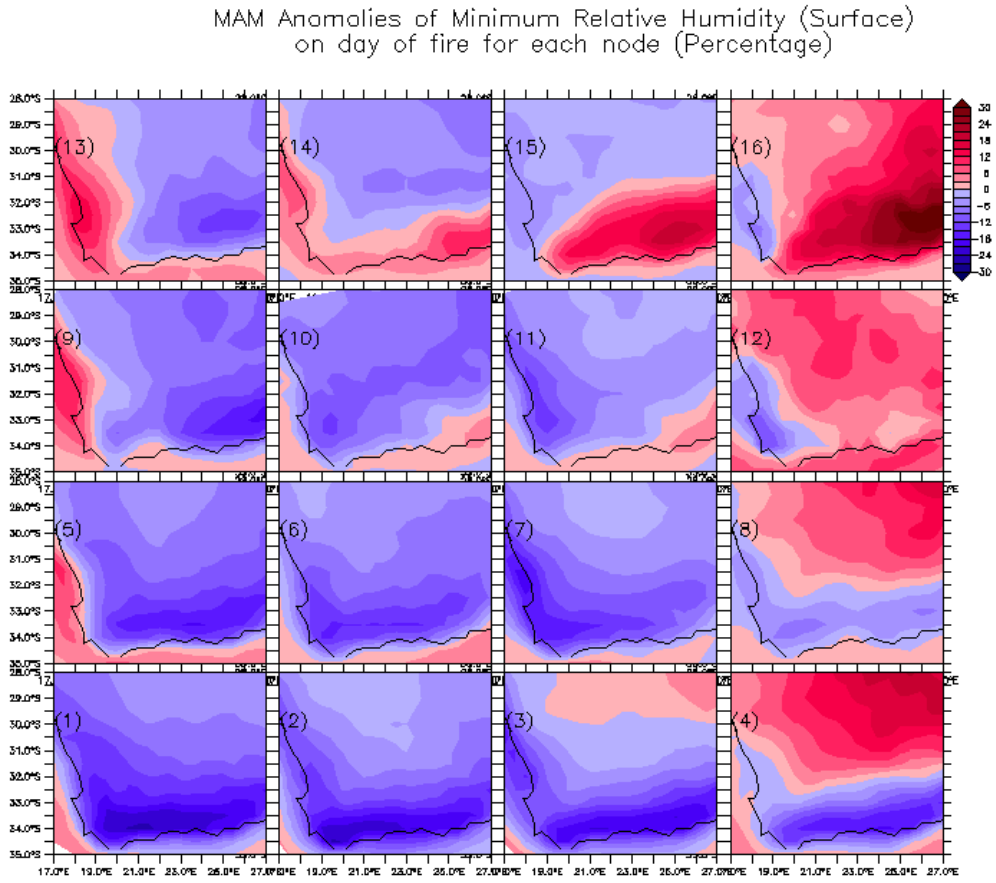

Appendix 7: MAM season anomalies of minimum surface relative humidity (%) on the day of fire for each node. The number in round brackets represents the node identification number.

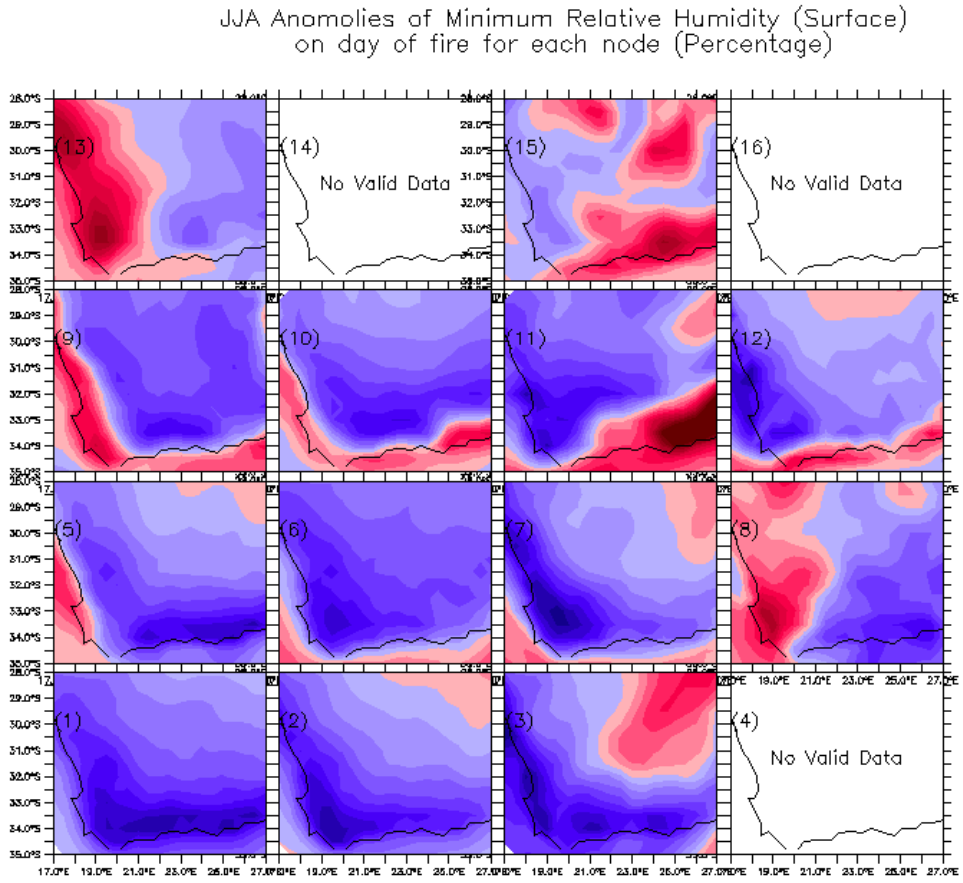

Appendix 8: JJA season anomalies of minimum surface relative humidity (%) on the day of fire for each node. The number in round brackets represents the node identification number.

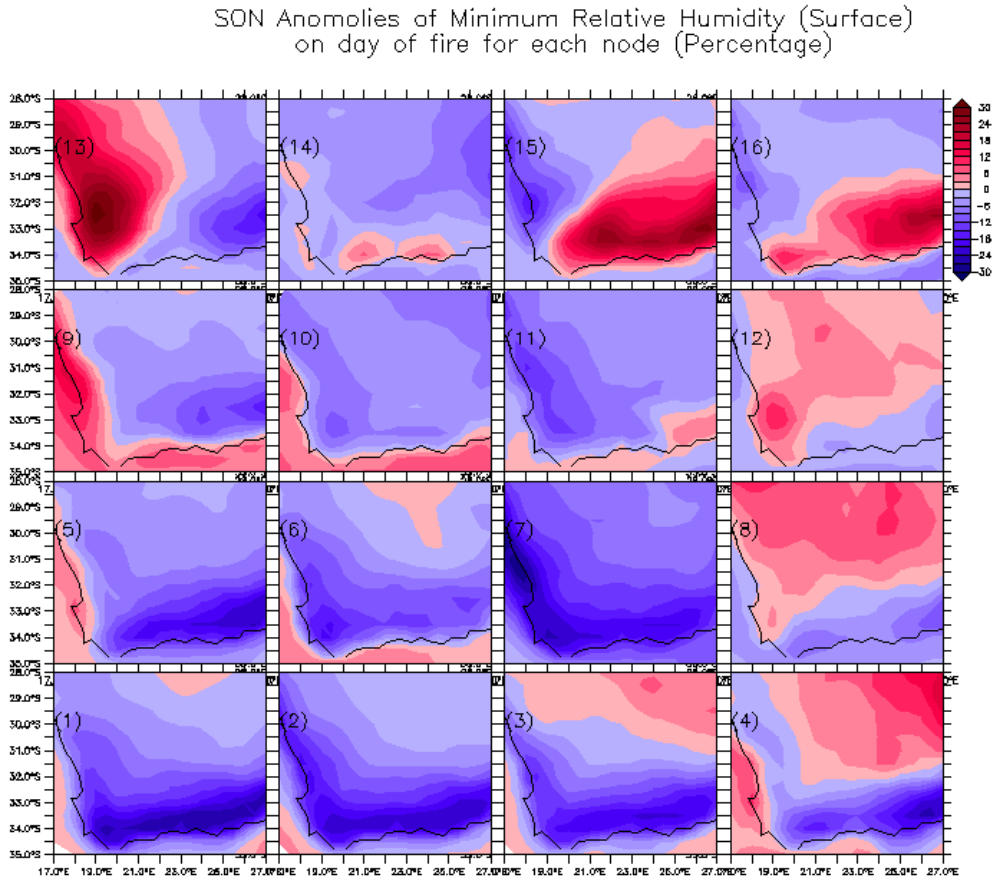

Appendix 9: SON season anomalies of minimum surface relative humidity (%) on the day of fire for each node. The number in round brackets represents the node identification number.

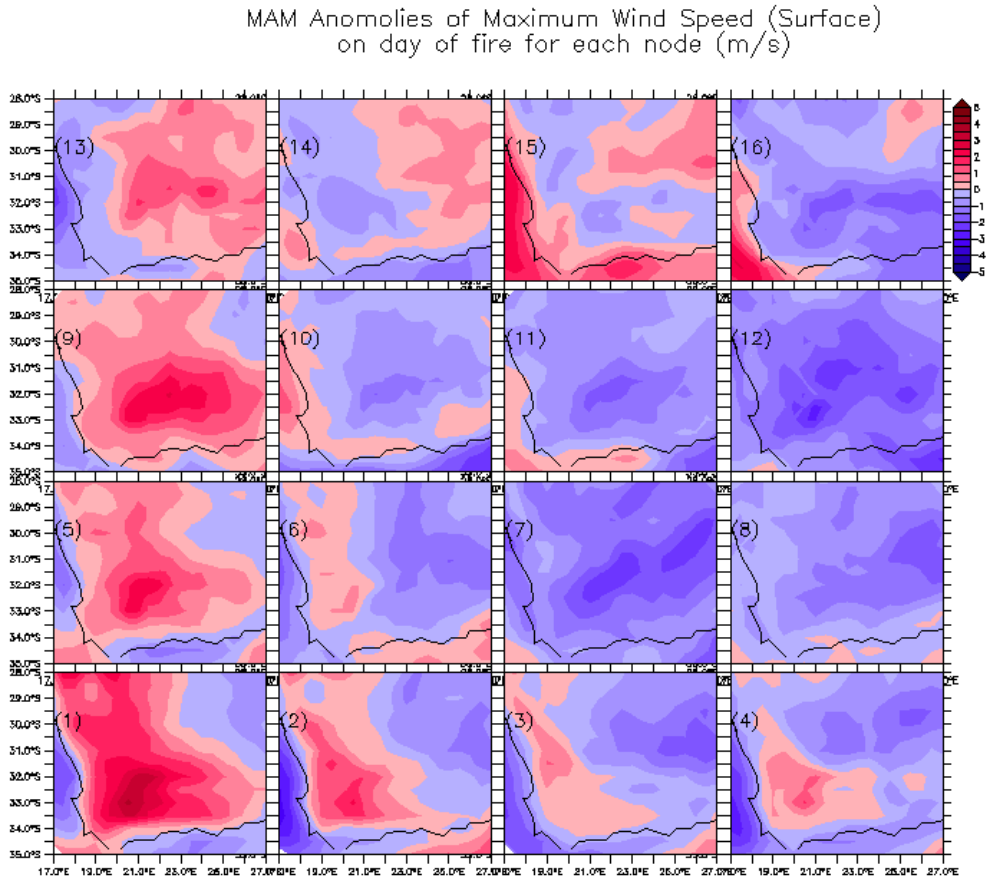

Appendix 10: MAM season anomalies of maximum surface wind speed ($m.s^{-1}$) on the day of fire for each node. The number in round brackets represents the node identification number.

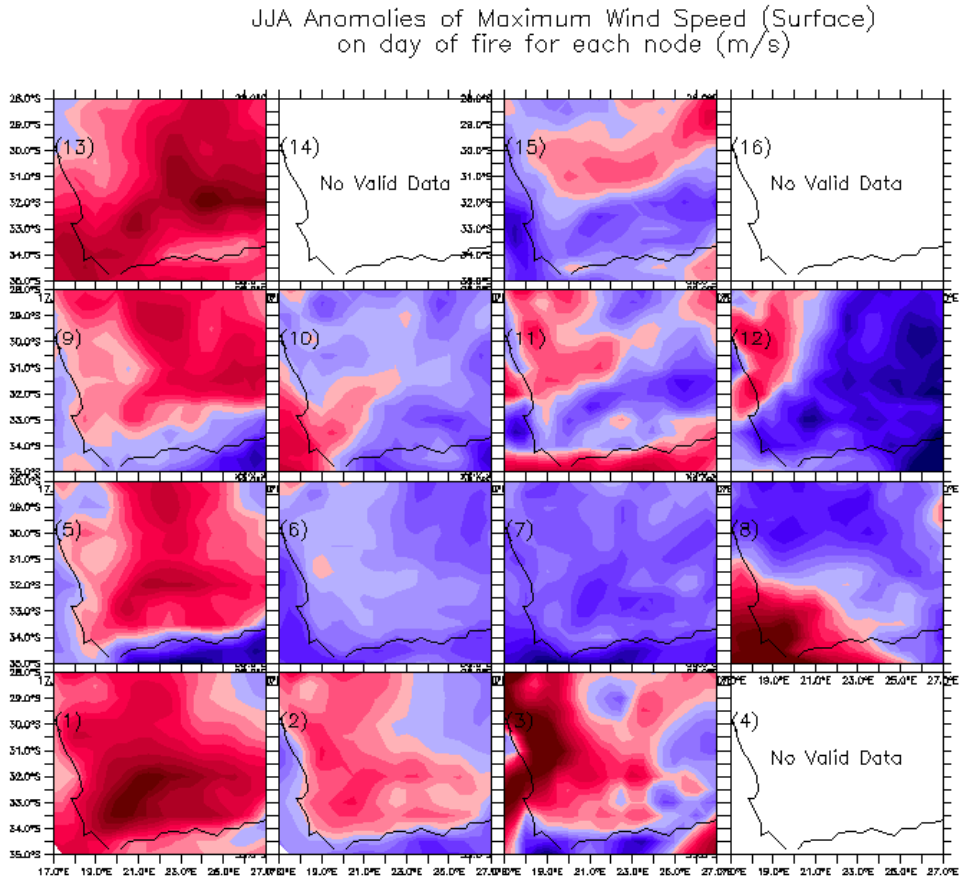

Appendix 11: JJA season anomalies of maximum surface wind speed ($m.s^{-1}$) on the day of fire for each node. The number in round brackets represents the node identification number.

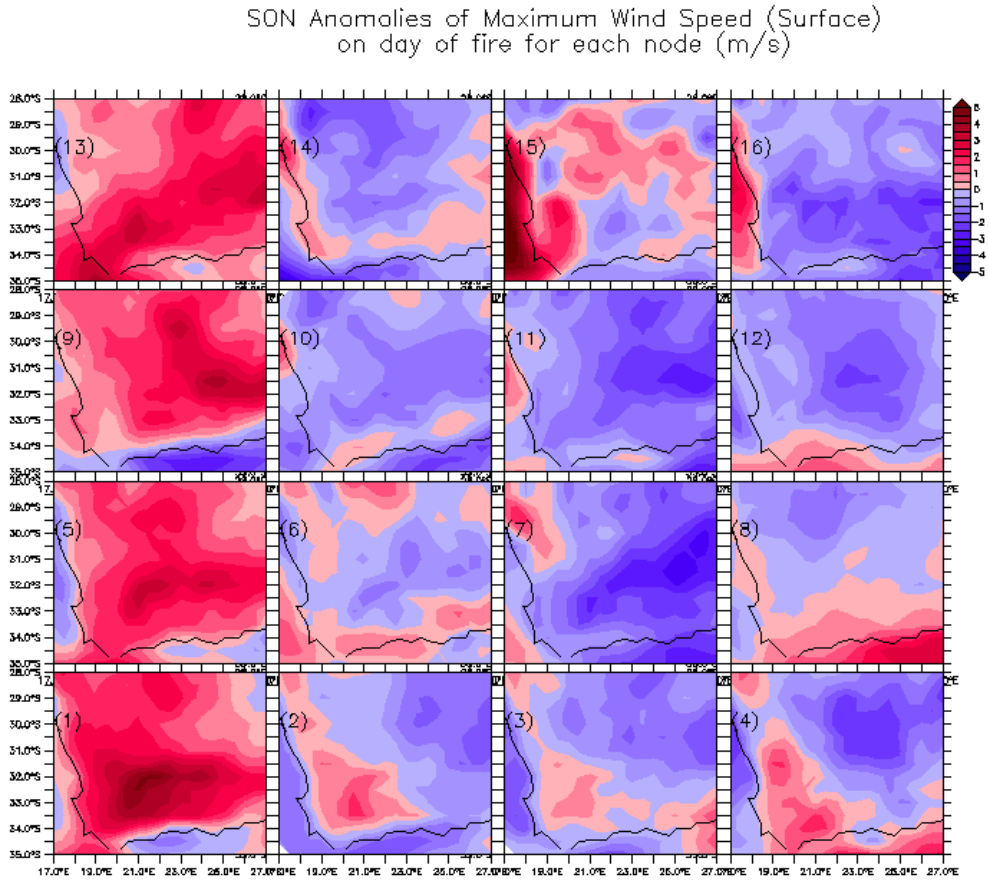

Appendix 12: SON season anomalies of maximum surface wind speed ($m.s^{-1}$) on the day of fire for each node. The number in round brackets represents the node identification number.

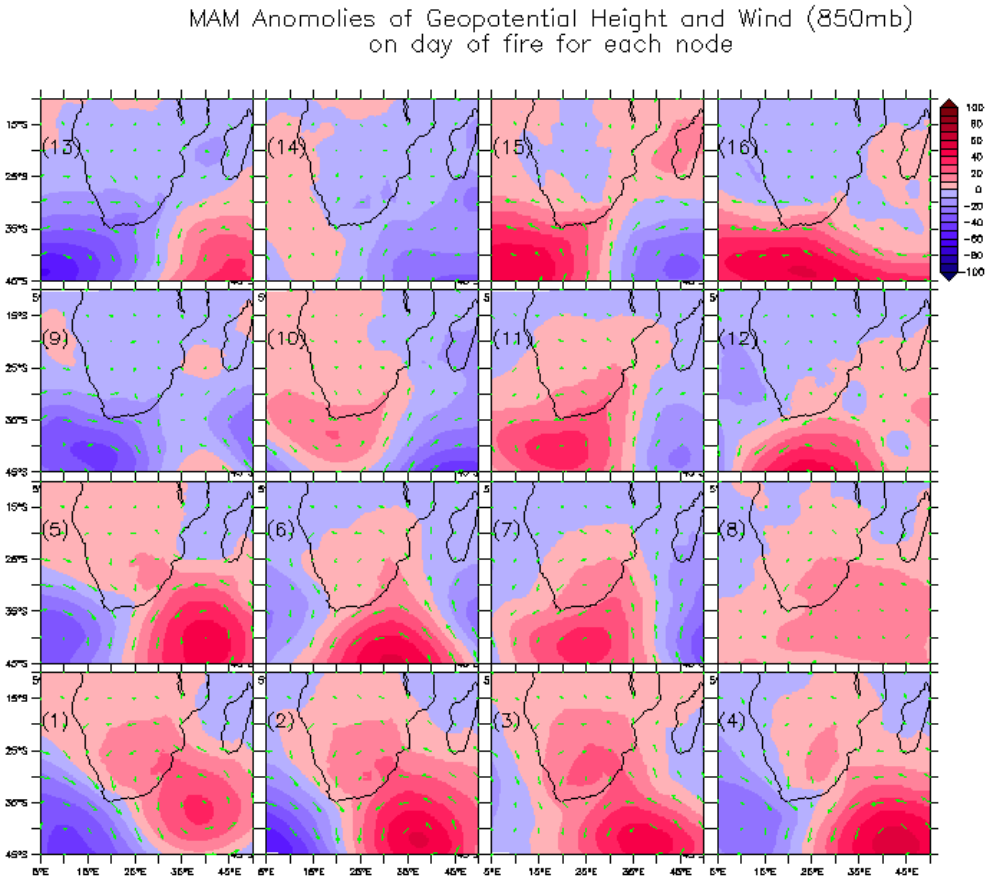

Appendix 13: MAM season Anomalies of Geopotential Height (m) and Wind Vectors at 850mb level, on the day of fire for each node. The number in round brackets represents the node identification number.

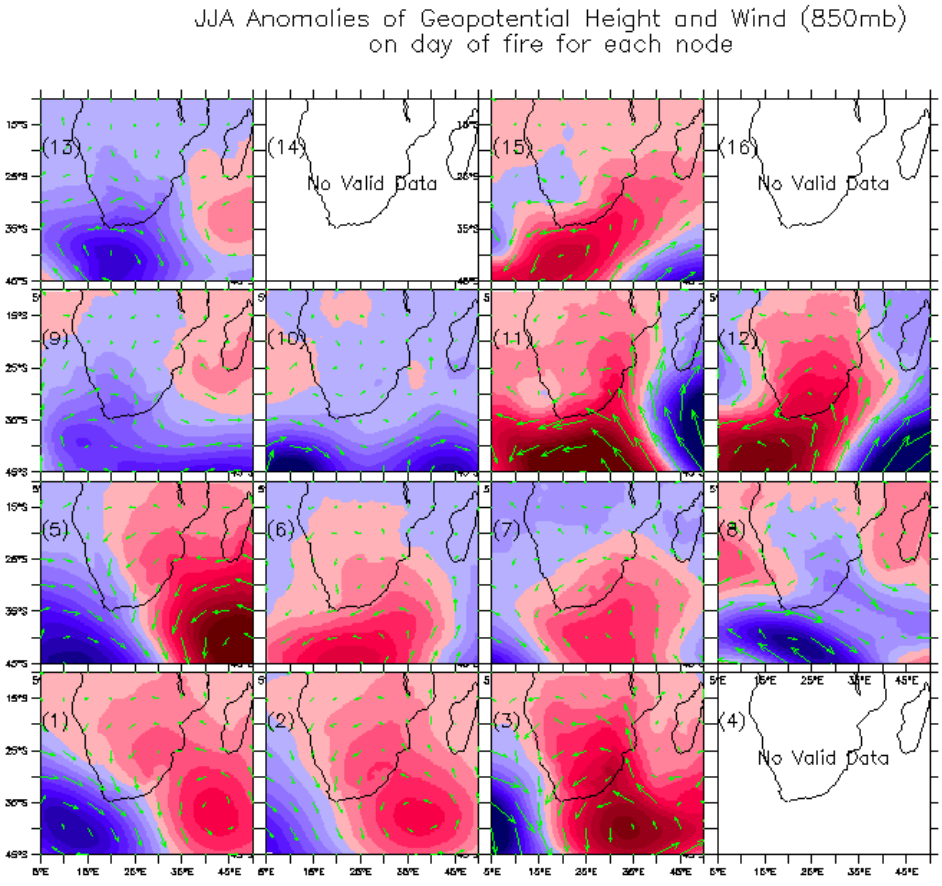

Appendix 14: JJA season Anomalies of Geopotential Height (m) and Wind Vectors at 850mb level, on the day of fire for each node. The number in round brackets represents the node identification number.

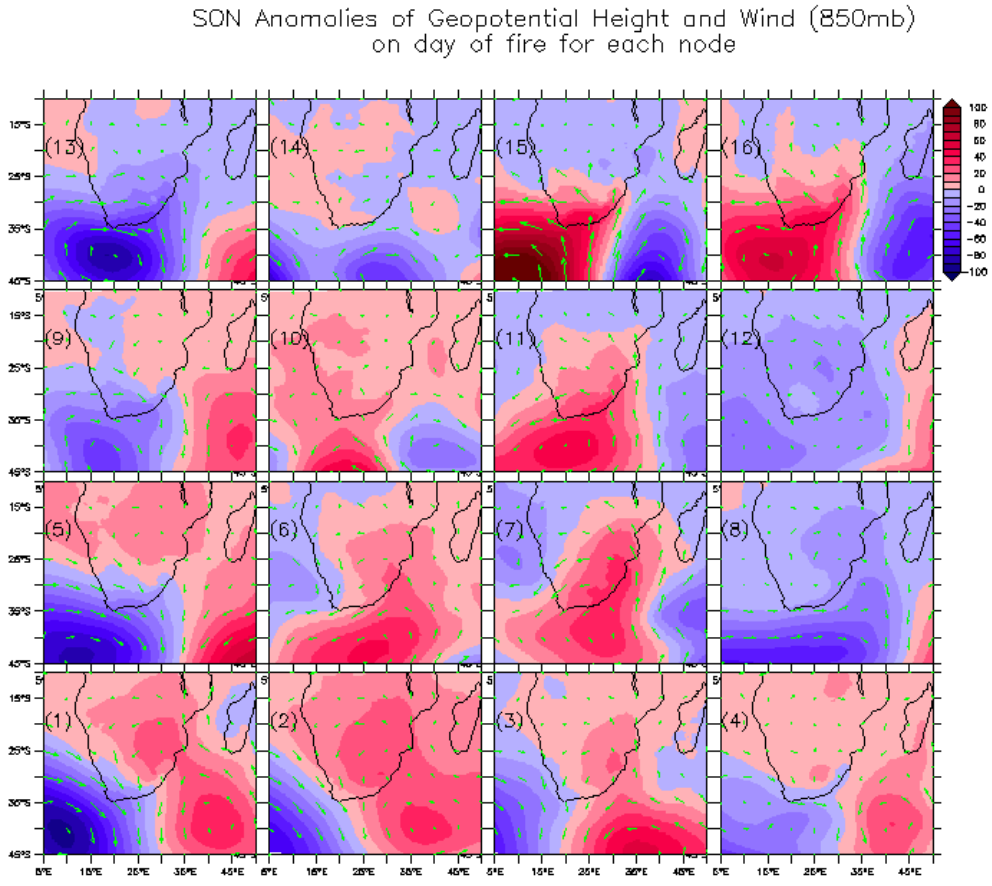

Appendix 15: SON season Anomalies of Geopotential Height (m) and Wind Vectors at 850mb level, on the day of fire for each node. The number in round brackets represents the node identification number.

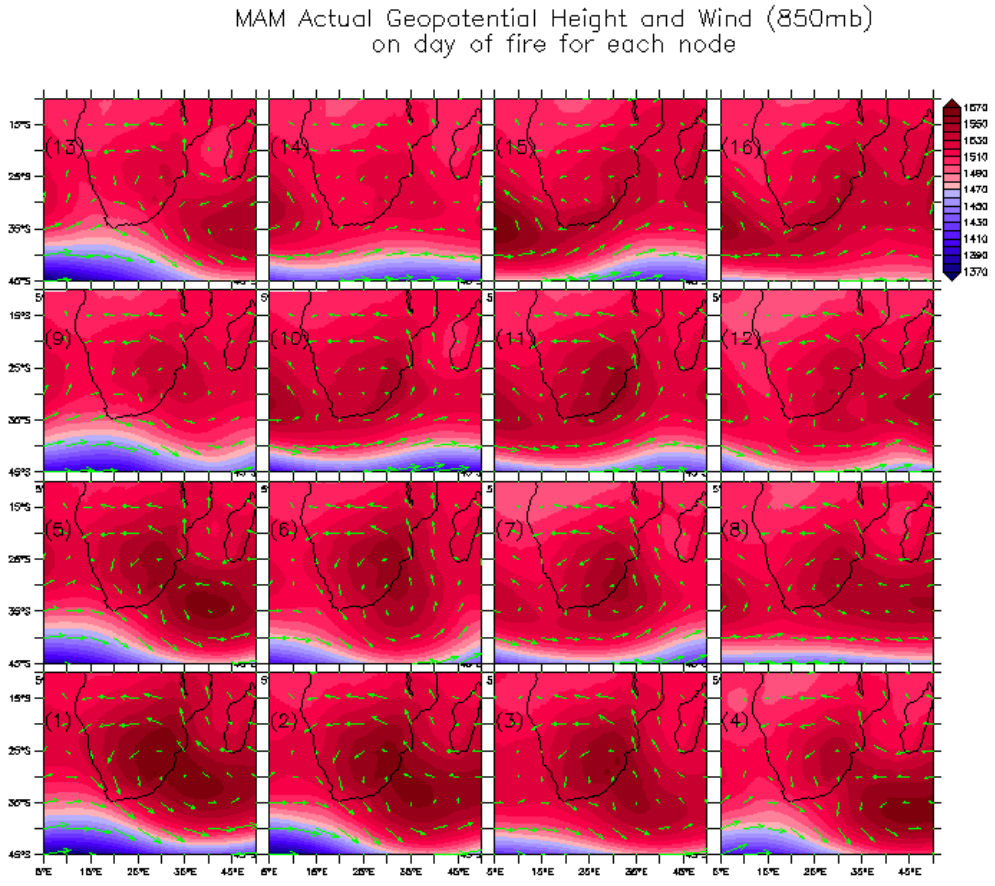

Appendix 16: MAM season Actual Geopotential Height (m) and Wind Vectors at 850mb level, on the day of fire for each node. The number in round brackets represents the node identification number.

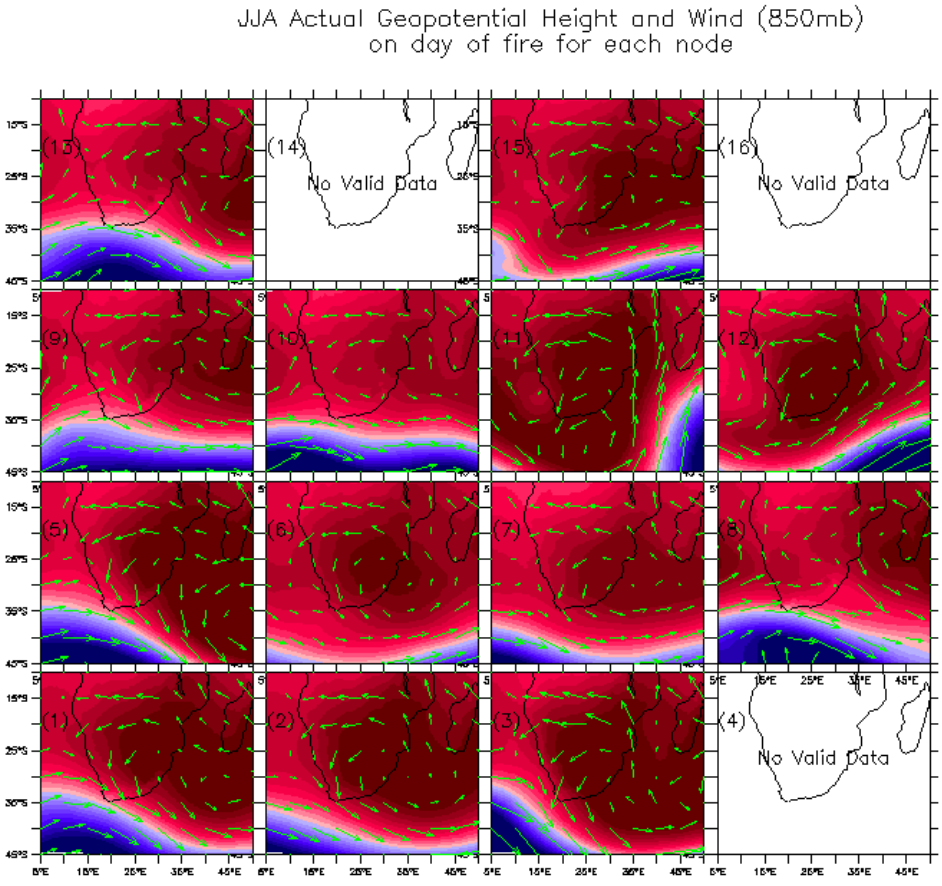

Appendix 17: JJA season Actual Geopotential Height (m) and Wind Vectors at 850mb level, on the day of fire for each node. The number in round brackets represents the node identification number.

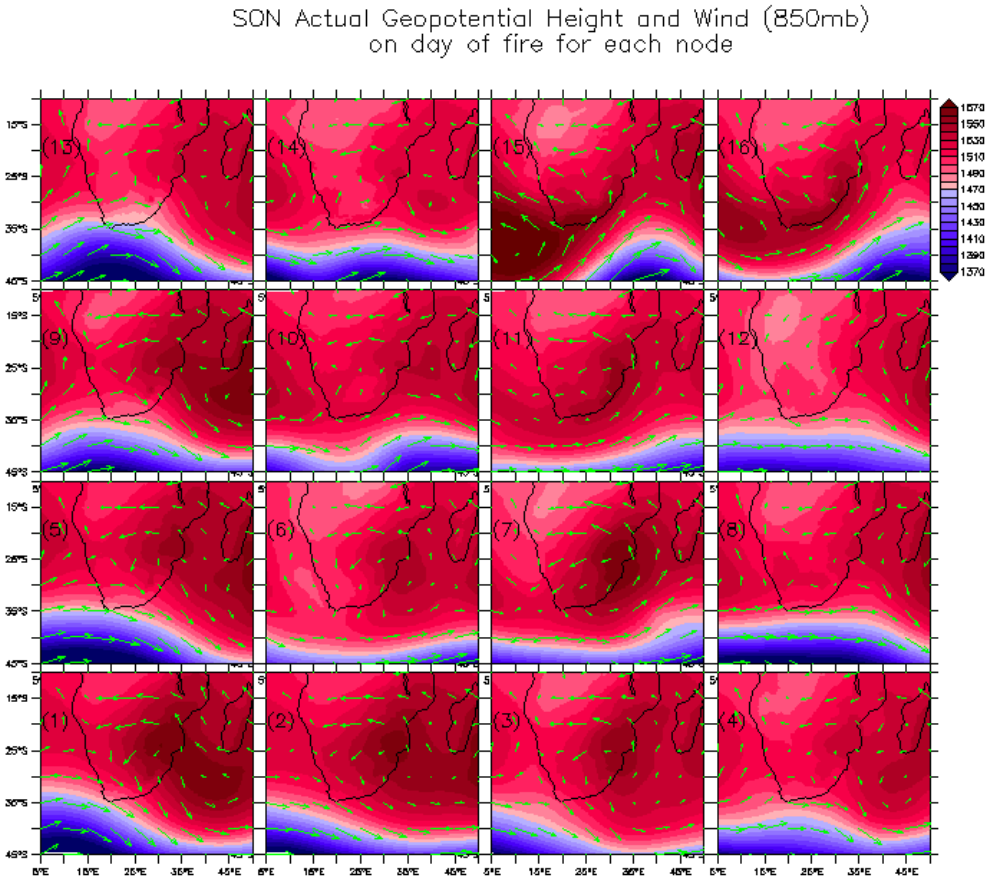

Appendix 18: SON season Actual Geopotential Height (m) and Wind Vectors at 850mb level, on the day of fire for each node. The number in round brackets represents the node identification number.

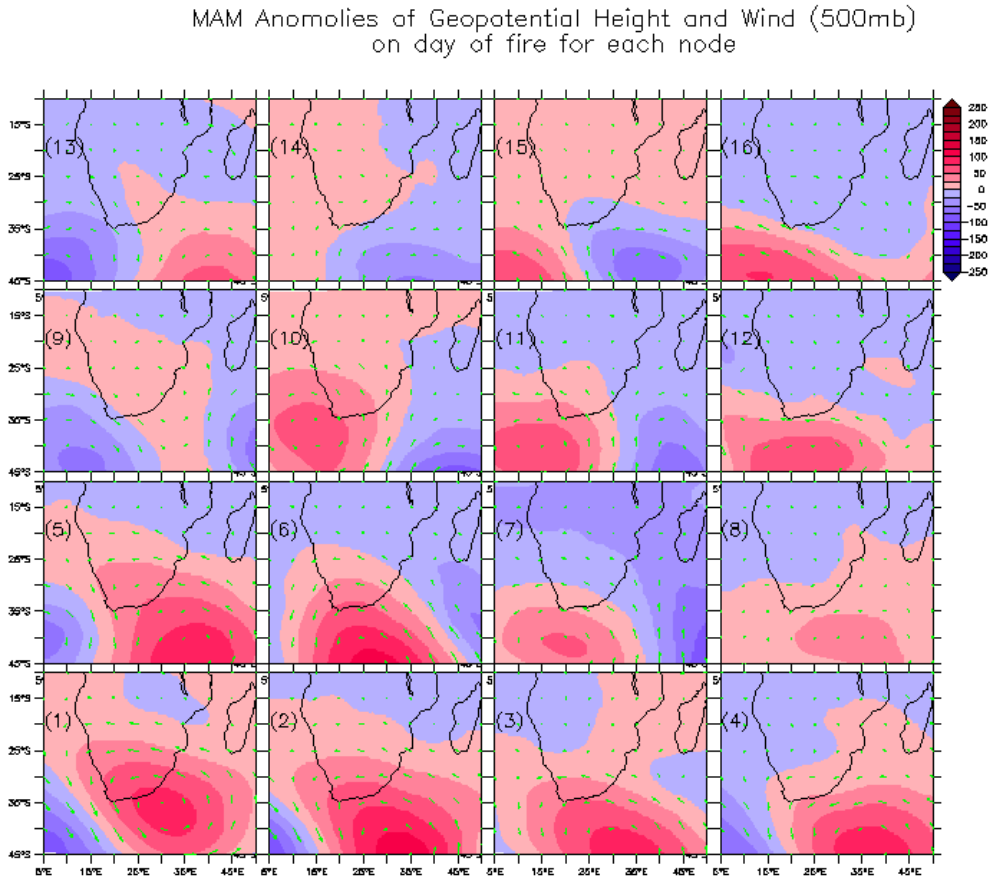

Appendix 19: MAM season Anomalies of Geopotential Height (m) and Wind Vectors at 500mb level, on the day of fire for each node. The number in round brackets represents the node identification number.

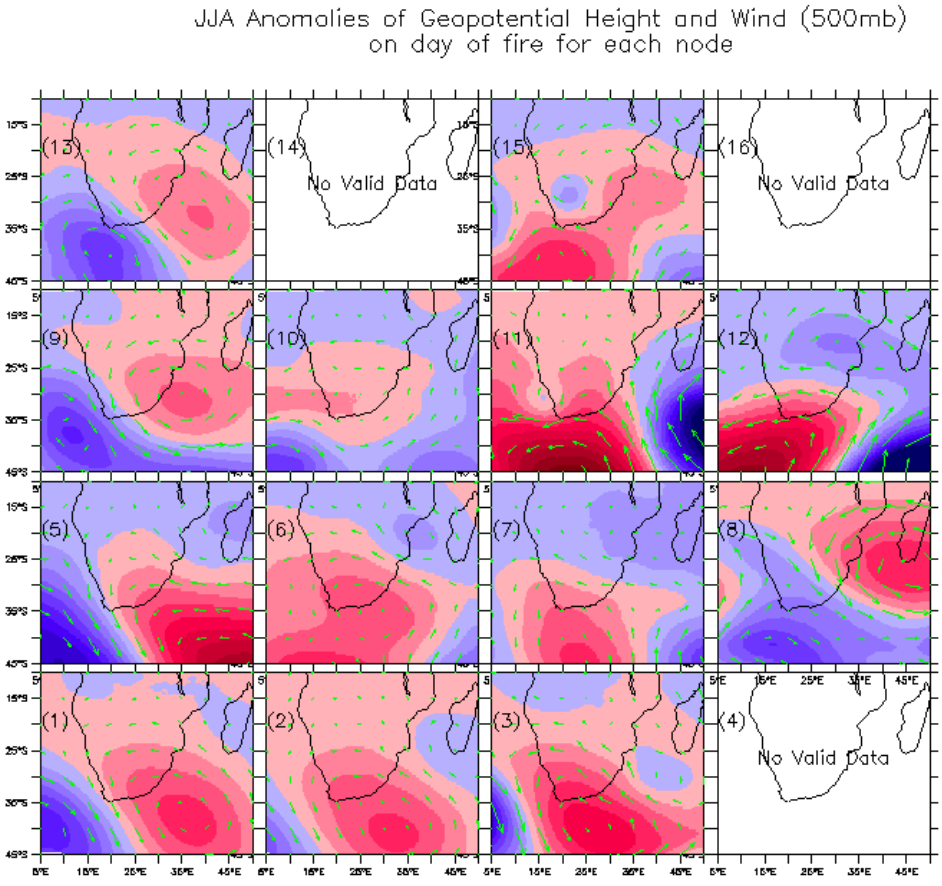

Appendix 20: JJA season Anomalies of Geopotential Height (m) and Wind Vectors at 500mb level, on the day of fire for each node. The number in round brackets represents the node identification number.

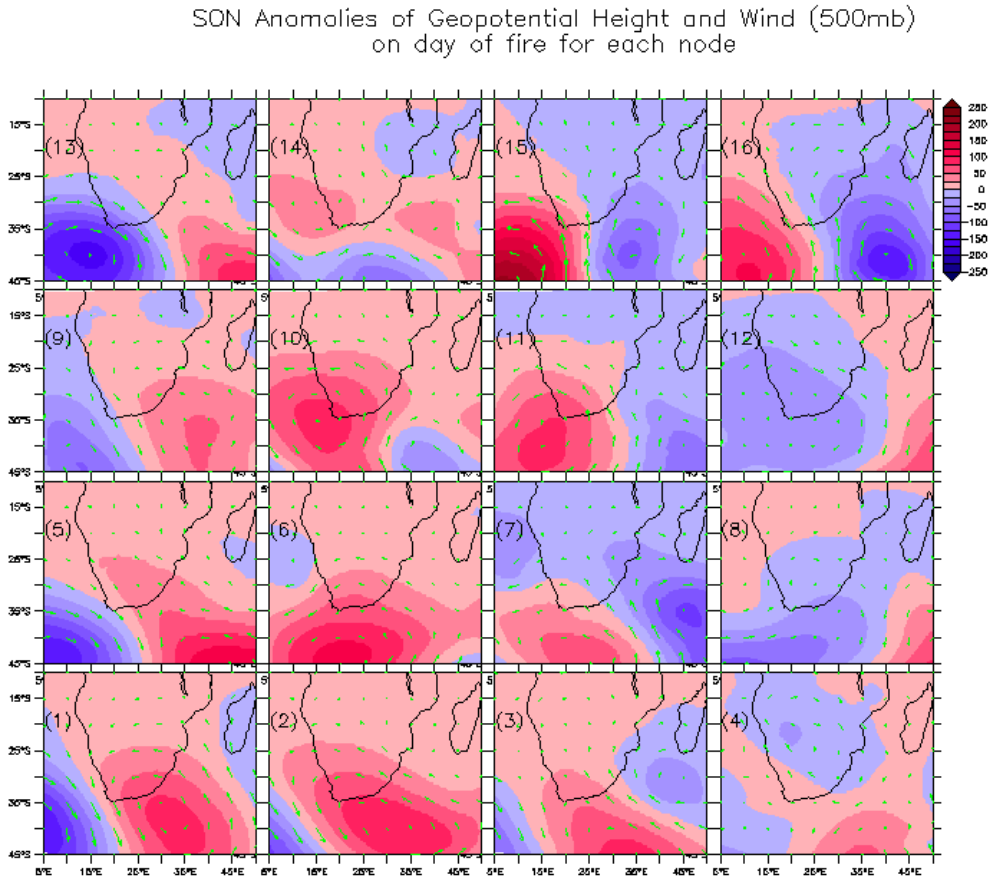

Appendix 21: SON season Anomalies of Geopotential Height (m) and Wind Vectors at 500mb level, on the day of fire for each node. The number in round brackets represents the node identification number.

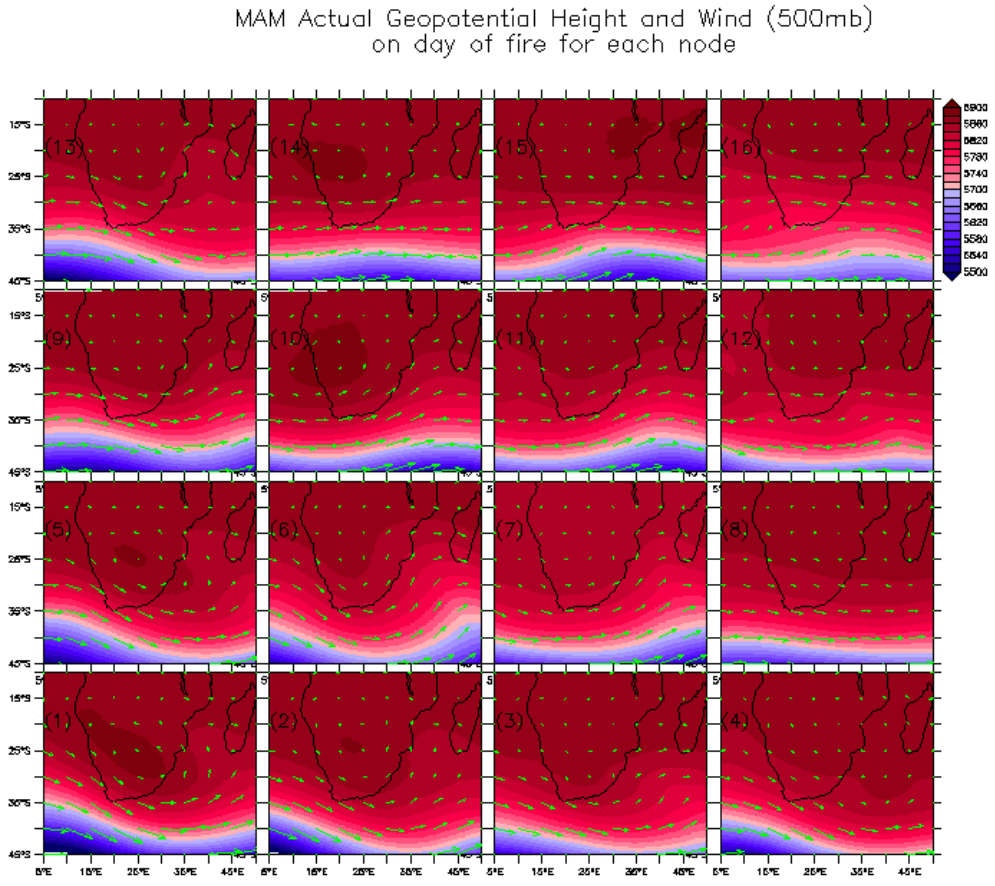

Appendix 22: MAM season Actual Geopotential Height (m) and Wind Vectors at 500mb level, on the day of fire for each node. The number in round brackets represents the node identification number.

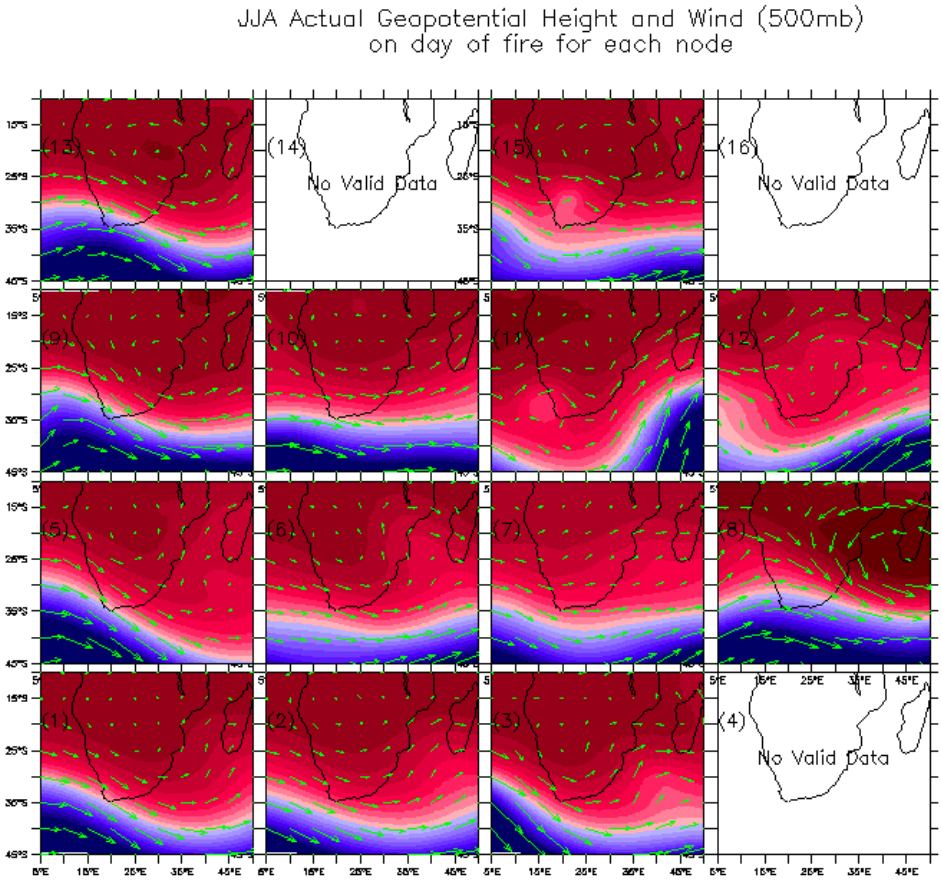

Appendix 23: JJA season Actual Geopotential Height (m) and Wind Vectors at 500mb level, on the day of fire for each node. The number in round brackets represents the node identification number.

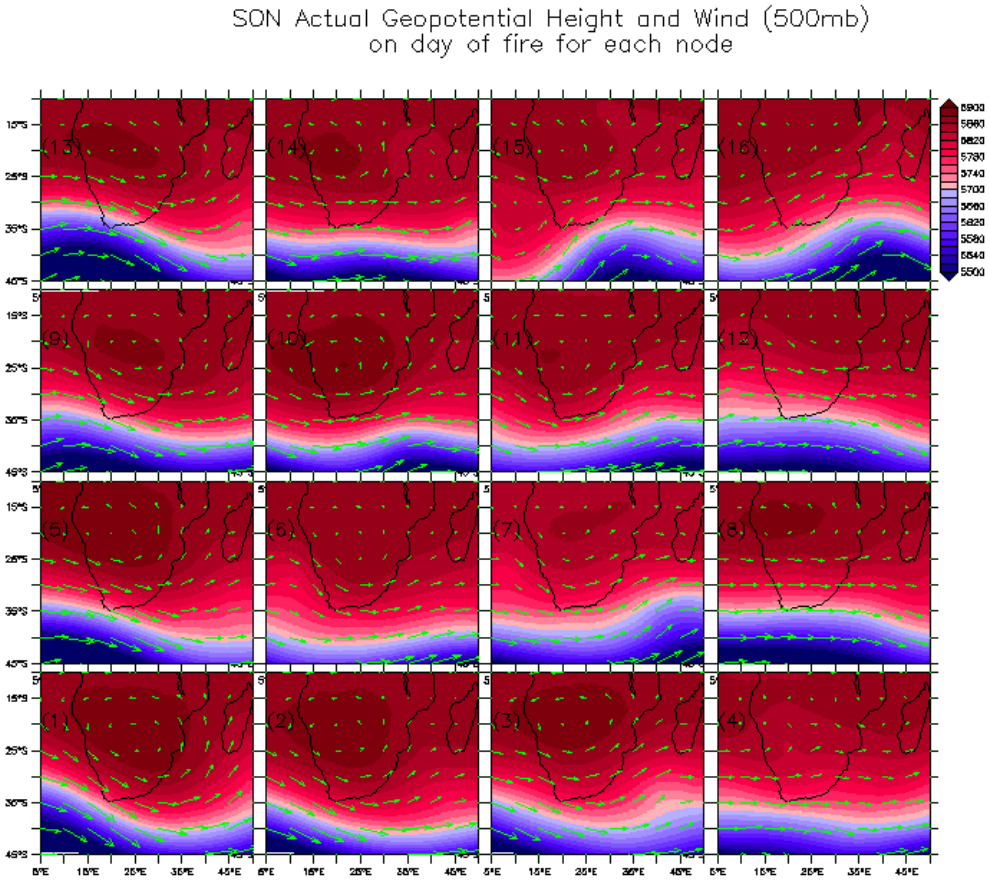

Appendix 24: SON season Actual Geopotential Height (m) and Wind Vectors at 500mb level, on the day of fire for each node. The number in round brackets represents the node identification number.